DIRECTION OF ARRIVAL ESTIMATION OF WIMEDIA UWB MULTIPATH SIGNALS IN THE PRESENCE OF INBAND INTERFERERS

ASHOK KUMAR MARATH

(*M.Sc., NUS, Singapore*)

A THESIS SUBMITTED

FOR THE DEGREE OF DOCTOR OF PHILOSOPHY

DEPARTMENT OF ELECTRICAL AND COMPUTER ENGINEERING

NATIONAL UNIVERSITY OF SINGAPORE

2009

Acknowledgements

It is a pleasure to thank the people who contributed in some way to this thesis.

First, I would like to express my sincere gratitude to my supervisors, Dr. Abdul Rahim Leyman and A/Prof. Hari Krishna Garg for their active encouragement, support and guidance through out this work. They provided me useful insights which helped me to carry forward. I am especially grateful to Dr. Leyman, whom I approached more frequently due to proximity, for his constant encouragement, sound advices, and lots of good ideas to pursue on. At times, when I felt lost and met potential show stoppers, he provided me lot of encouragement and the support to pursue with determination to overcome the challenges. I would probably have been lost without him and his style of guidance.

I would like to express my gratitude to my employers Institute for Infocomm Research (I^2R) for supporting me during this part-time study. I am grateful to Dr. Michael Chia, who encouraged me to pursue Ph.D. degree, Prof. Wong Wai Choong Lawrence, Prof. Lye Kin Mun for their continuous encouragement and support during this pursuit. I also express

my gratitude to my colleagues Santhosh Kumar Pilakkat and Sivakumar Viswanathan for their encouragement and support.

I would like to thank Ponnatath Govindan Master and K Kunhiraman Master for encouraging me to dream big beyond the tiny village of Chemancheri and to reach where I am today.

I would like to thank Dr. Francois Chin for allowing me to use the Mathlab code of UWB transmitter used in this work and Mr. Png Khiam Boon for the excellent discussions I had with him to understand UWB system. I also acknowledge the help from my colleague Dr. Zeng Yonghong in clarifying my doubts. I also acknowledge the help I got from my fellow student Dr. Chen Xi in using Latex.

Finally, I would like to thank my parents, Balan Nair and Jayalakshmi Amma, in-laws, Sankaran Nair and Komalam for their support and encouragement all through these years; my wife Smitha and daughters Swathi and Shruthi, for their understanding, support, patience, and sacrifices, which gave me the width required to make this possible. It is to them, I dedicate this thesis.

Contents

Summary

The increasing popularity of wireless communications is making usable frequency spectrum crowded. We will have to optimally share the spectrum between multiple users to meet this increasing demand. Restricting the transmission to desired direction is one way of optimizing the spectrum usage. By doing this, the power for the desired user is increased while reducing the interfering power for other users of the spectrum. The estimation of direction of arrival of multipath signals would help to decide the optimal transmission directions.

Both shorter range wideband and longer range narrowband systems will have to co-exist in the wireless environment. OFDM based systems are popular for wideband communications. WiMedia Ultra Wide Band (UWB) is a typical example of such a system. These systems will be operating along with narrowband systems like Wimax. This research work looks at estimation of direction of arrival of UWB multipath signals in typical propagation environments in the presence of interferers. The known pilot signals of UWB signals are exploited to develop a new scheme for achieving this. Focussing is used to combine the energy of different frequency com-

ponents to enhance the threshold of estimation. A new focussing scheme not requiring coarse estimation of the direction of arrival is developed to eliminate the asymptotic bias seen in conventional focussing schemes. The superior performance of the new algorithm is demonstrated through simulation. A new receiver architecture which provides significant savings in required hardware is proposed in the thesis to facilitate economical implementation of the system. The thesis presents a new source enumeration technique suitable for estimating the number of multipaths while using the new algorithm.

Extensive computer simulations are conducted to validate the strength of the proposed algorithms in the thesis. A glimpse of future work that can be extended from this thesis is provided at the end.

List of Tables

List of Figures

List of Symbols

ω_c	Carrier frequency of the source signal.
ω_j	j^{th} Pilot subcarrier frequency of the source signal.
λ	Wavelength of the source signal.
τ_m	Delay from reference element to the m^{th} element.
q	Number of array elements.
d	Spacing between array elements.
l	Number of elements in subarray.
p	Number of sources
k_1	Number of desired multipaths.
θ_i	direction of arrival of i^{th} source.
M	Number of subarrays.
$\mathbf{x}(k)$	$q \times 1$ column vector whose i^{th} element is the time domain output of the i^{th} array element at k^{th} instant.
$\mathbf{x}_i(k)$	$l \times 1$ column vector representing the time domain output of i^{th} subarray .
$\mathbf{X}_i$	$l \times N$ matrix representing the frequency domain output of the i^{th} subarray for N symbol duration.

$\mathbf{Z}_i$	$l \times N$ matrix representing the frequency domain noise output of the i^{th} subarray for N symbol duration.
$\mathbf{S}$	$p \times N$ matrix representing the frequency domain output of sources for N symbol duration.
$\mathbf{A}$	$q \times p$ matrix representing the Array steering vectors. Each column of $\mathbf{A}$ represents the steering vector of a source.
$\mathbf{a}(\theta_i)$	Steering vector from direction θ_i at a carrier frequency of ω_c and subcarrier frequency of ω_j and is defined by the relation $\mathbf{a}(\theta_i) \triangleq [1 \; e^{-j(\omega_c+\omega_j)d\sin\theta_i} \; \ldots \; e^{-j(\omega_c+\omega_j)(q-1)\sin\theta_i}]^T$.
$\mathbf{A}_1$	$l \times p$ matrix representing the first l rows of $\mathbf{A}$.
$\bar{\mathbf{A}}_1$	$l \times k_1$ matrix representing the first k_1 columns of $\mathbf{A}_1$.
$\mathbf{D}$	$p \times p$ diagonal matrix whose m^{th} diagonal element is $e^{-j2\pi\frac{d}{\lambda}\sin\theta_m}$.
$\mathbf{r}_1$	$1 \times N$ row vector representing the known frequency domain data of desired source for N symbol duration.
α_m	Expected value of correlation between m^{th} source and desired known waveform.
$\mathbf{D}_\alpha$	$p \times p$ diagonal matrix whose m^{th} diagonal element is α_m.
$\mathbf{T}(\omega_{c,j})$	Focussing matrix at carrier frequency ω_c - subcarrier frequency ω_j combination.
$\mathbf{g}_i$	$l \times 1$ column vector representing the expected value of correlation between i^{th} subarray output and known waveform and is defined by the relation $\mathbf{g}_i \triangleq \mathbf{E}[\mathbf{X}_i\mathbf{r}_1^H]$.
$\mathbf{G}$	Matrix defined by the relation $\mathbf{G} = [\mathbf{g}_1 \cdots \mathbf{g}_M]$.

$\mathbf{G}(\omega_{c,j})$	Matrix $\mathbf{G}$ at carrier frequency ω_c - subcarrier frequency ω_j combination.
u_m	An element of matrix $\mathbf{G}$ given by $u_m = E[\mathbf{x}_m \mathbf{r}_1^H]$, where $\mathbf{x}_m$ is the output of the m^{th} element of the array.
$\hat{u}_m$	Estimated value of u_m
$\breve{e}_i$	Perturbations in $\hat{u}_m$
$\hat{\mathbf{G}}$	Estimated value of $\mathbf{G}$
$\hat{\mathbf{A}}_{mk_1}$	m^{th} row of the first k_1 columns of $\mathbf{A}$
$\hat{\mathbf{A}}_m$	m^{th} row of $\mathbf{A}$

Chapter 1

Introduction

1.1 Wireless Communication Environment

Increasing popularity of wireless communications is making the usable spectrum crowded. Some of these devices are short range, while others are long range. Different schemes like TDMA, FDMA and CDMA facilitates sharing of spectrum between different users. The increasing demands have resulted in existing approaches reaching its capacity limits and researchers have started exploring newer approaches to enhance the utilization efficiency of precious radio spectrum. The reuse of the frequency spectrum in geographically separated areas has been utilized in cellular systems to enhance spectrum efficiency (bits/second/m^2). This approach is further enhanced in spatial division multiple access scheme (SDMA). In this case, instead of using omnidirectional antenna, one would employ directional antennas to restrict the transmission to the desired direction. This would allow the use of same spectrum in other directions for some other applications. This

way, one can enhance the spectrum utilization efficiency.

The wireless signals encounter reflections, refractions and scattering in its propagation environment. These results in multipath propagation, in which multiple replicas of the transmit signal reaches the receiver. These may be coming from different directions and with different delays. In a dense environment, the signals encounter multiple reflections and associated phase shifts making these multipaths non-coherent. By employing antenna arrays on both sides, one would be able to exploit these uncorrelated multipaths between antennas to enhance spectral efficiency. This is used in Multiple Input Multiple Output (MIMO) systems to enhance the throughput. On the other hand, the multipaths are highly correlated in less dense environments.

The requirements on various wireless communication technologies are different. There are many systems requiring large range transmission with low to medium data rates. Cellular systems and Wimax systems address this needs. The typical characteristics of these systems are its high transmit power and narrower bandwidth.

With increasing demand for wireless connectivity, there would be more short range systems working in combination with wired infrastructure. These short range wireless systems are expected to coexist with other narrowband systems.

1.2 UWB Systems

There are many wireless applications like video streaming and wireless USB, which requires very high data rates with short range. Regulatory authorities have allowed very low power transmission with very high bandwidth for these type of applications. They are expected to operate in mainly indoor environments. These systems are expected to coexist with other narrowband systems with higher power, making use of these bands.

There are different types of UWB systems currently available [7]. One type makes use of very narrow pulses (ultra wide in frequency domain) for sending information. In this case, the system occupies the whole allocated spectrum at any instant of time. This throws in lot of challenges in processing of information, as the system has to handle the entire bandwidth at any instant. The system fractional bandwidth can exceed unity and most of the conventional processing algorithms would fail in handling this type of systems. This resulted in another type of UWB systems where the occupied fractional bandwidth is less than 0.2 at any particular instant. The entire allocated spectrum is utilized by employing fast frequency hopping. The multi-carrier OFDM based systems falls into this category. These systems achieve the large bandwidth through multiple hopping of carrier frequency of the OFDM systems in the allocated frequency range. Salient features of the two systems are summarized in the following paragraphs.

1.2.1 Pulse Based Systems

In pulse based UWB systems, the information is conveyed through transmission of very narrow pulses. This system is also called impulse radio. One of the main challenges involved in pulse transmission is the presence of significant lower frequency components and the associated distortion during transmission. Suitable selection of pulse waveform is critical to reduce the low frequency content. Data bits are grouped to form symbols and each symbol is conveyed through one or more pulses transmitted in each symbol interval. In simple systems, each bit is taken as a symbol and information in the bit is conveyed through either pulse position modulation (PPM) or pulse amplitude modulation (PAM). A simple PPM based UWB System is shown in figure 1.1. In more complicated systems, each symbol carry more than one bit of information and these would be communicated through multilevel PAM or multi-slot PPM. System robustness can be improved by repeating the same bit over multiple symbol slots and combining the energy in multiple slots for reliable detection. This would also allow multiple access as the pulse position in multiple symbol periods can be allocated based on an overlay Code Division Multiple Access scheme.

1.2.2 OFDM Based Systems

The UWB definition, released by Federal Communications Commission (FCC), classified any system having bandwidth more than 500 MHz bandwidth in the 3.1 GHz -10.6 GHz frequency range as UWB. This would allow

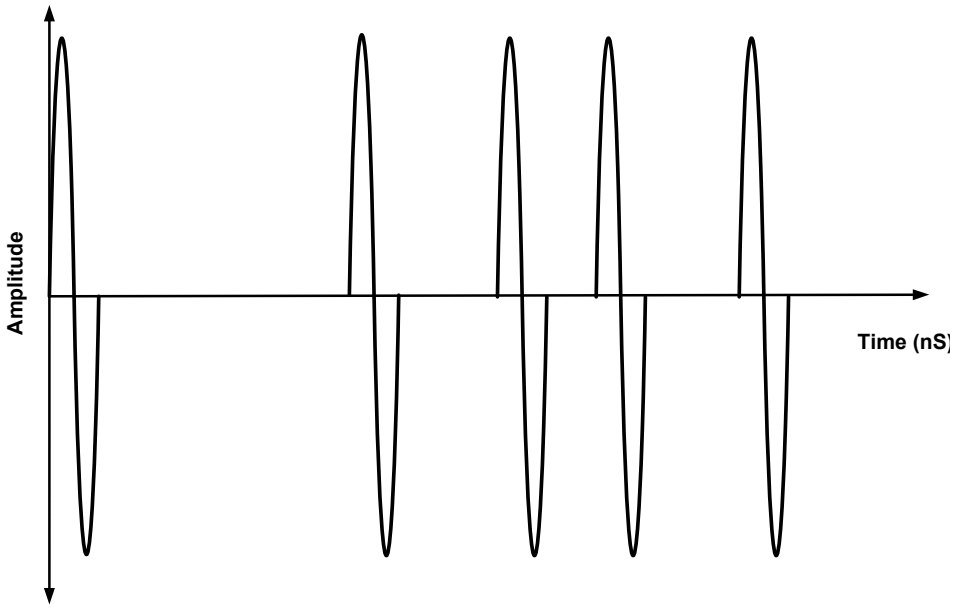

Figure 1.1: Pulse based UWB waveform

any system, irrespective of the waveform used, to be classified as UWB as long as its bandwidth exceeds 500 MHz. Conventional single carrier systems require complex equalization schemes to recover information. On the other hand, OFDM based systems can function with such high bandwidth using frequency domain processing for short range applications without major performance loss. In this case, the bandwidth is decided by the data rate, where as the waveform decides the bandwidth in the case of pulse based systems. These types of systems would make use of the frequency hopping principles to effectively utilize the total available bandwidth. Typical baseband spectrum of OFDM based UWB is shown in figure 1.2. This baseband spectrum would be converted to RF band by multiplying it with an RF car-

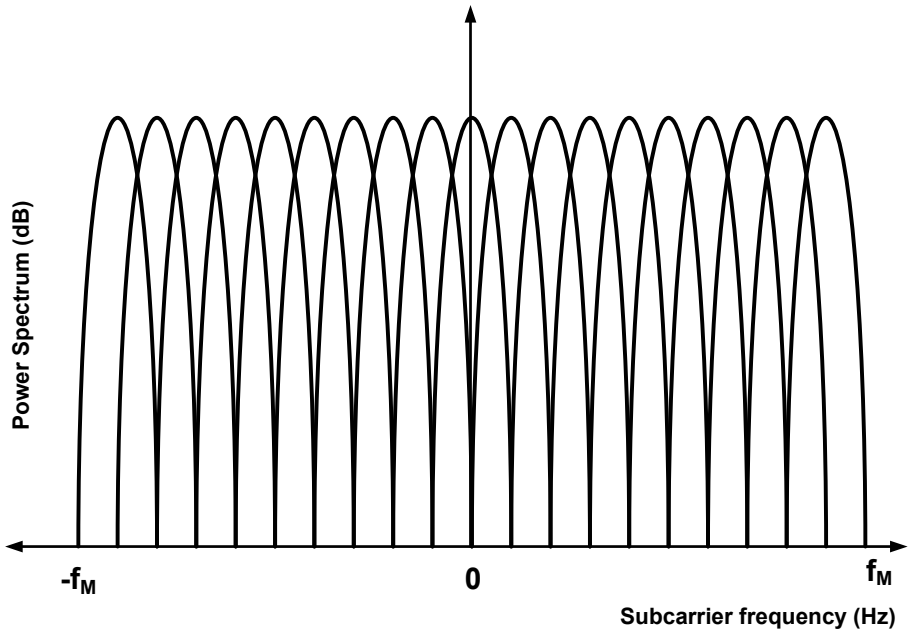

Figure 1.2: Baseband spectrum of OFDM based UWB

rier frequency. In typical implementations, these carrier frequencies would be hopping from symbol to symbol as defined in the standard [88]

One of the proposed techniques making use of multiband OFDM, has generated significant industry interest and is gradually becoming popular. These systems, commonly known by the consortium name WiMedia, are expected to play a significant role in the future short range wireless communications. The main features of the system based on [88] are summarized in the next section.

1.2.2.1 WiMedia UWB systems

Federal Communications Commission (FCC) has allowed an average transmission power of -41.3dBM/ MHz in the frequency range 3.1- 10.6GHz. The minimum instantaneous bandwidth of the system is 500 MHz. WiMedia consortium split this frequency range into smaller bands of 528 MHz around predefined carrier frequencies. They defined a system [88] based on OFDM targeted for very high data rate short range applications. The features of the system relevant to this research are summarized in the following paragraphs. The system was specified with instantaneous adjustable bandwidth of around 500 MHz and a flexible hopping pattern. The defined frequency bands were further combined to smaller groups consisting of 2 or more carrier frequencies. The system is expected to hop among the carrier frequencies in the group in a specified pattern. Different hopping patterns are specified. In one of the most popular implementations, the frequency group consists of 3 carrier frequencies 3432MHz, 3960MHz and 4488MHz. The defined hopping patterns include hopping among the carrier frequencies from symbol to symbol, during alternate symbol or no hopping in a defined sequence. The system supports different data rates from 53.3 Mbits/sec to 480 Mbits/sec.

The system operate with sampling frequency of 528 MHz and 128 subcarriers. The carrier separation is 4.125 MHz. Out of the 128 subcarriers, 100 carriers are used for data, 12 carriers are used as pilot carriers and 10 carriers are used as guard carriers. The data transmitted on the guard car-

riers can be adjusted to achieve the desired bandwidth as specified by the national regulators. The different data rates are supported by changing the modulation format used for each carrier. In the standard, same modulation is used for all carriers in one symbol. QPSK and Dual Carrier Modulation (DCM) are used in the standard. Since the allowed transmission power is very low, one will have to combine the signals from different carriers to achieve the required E_b/N_0 for demodulation. The lower data rates are used for longer ranges and hence made more robust by transmitting the same data in different carriers in the same symbol and in two adjacent symbols in the case of time domain spreading. The data is transmitted in two carriers in the same symbol in DCM used for higher data rates. The data transmitted in all carriers are scrambled to reduce the narrowband interference to the other systems.

The system is based on packet transmission. Each transmit frame starts with a preamble consisting of either 24 or 12 symbols. These preambles are 128 samples of wideband time domain signals defined in the standard. All the symbols would be carrying the same data. This data would be multiplied a cover sequence bit for each symbol to scramble the discrete spectrum. This preamble is used for time and frequency synchronization. This involves the estimation of the frame boundary, symbol boundary and the frequency offset between transmitter and receiver. In the receiver side, one will correlate with this known pattern or use autocorrelation to estimate the frame boundary.

The preamble is followed by 6 symbols for channel estimation purposes. They will also carry same predefined information in all symbols scrambled at symbol level. This is followed by 12 header symbols which will carry system information and the user data symbols. The maximum size of the packet would depend on the packet size and chosen data rate. the maximum allocated user data payload size is 4K bytes. Header symbols are transmitted at 53.3 Mbits/sec data rate. User data rate can be any one of the specified rate.

The basic transmission scheme is based on a block of 6 continuous symbols. The user data is rate adapted by adding pad bits such that the total coded bits will fit into an integer multiple of 6 symbol blocks at the chosen data rate. The coded data is interleaved and split into blocks of size equal to the number of bits/ carried by 6 symbol block at the chosen data rate. These are mapped to 100 data subcarriers for each OFDM symbol. This is done based on the data rate.

The time domain symbol is generated by a 128 point IFFT. The subcarriers are numbered from -64 to 63. The subcarriers -56 to 56 are used for the actual symbol. The subcarriers -61 to -57 and 57 to 61 are used as the data carriers. The guard carriers are assigned values to meet the local regulation or by copying the data of 5 nearest data subcarriers with outermost subacrrier data going to the outermost guard carrier. In the -56 to -56 carrier range, the zeroth carrier is made zero. The locations -55 + 10 I , where I (pilot index) varies from 0 to 11 are allocated for pilot carriers.

The pilot carriers carries a known data sequence defined in the standard for each data rate. For example, the pilot data for 200Mbits/sec data rate are as given in Eqn.(1.1)

$$\begin{aligned} d_{pilot} &= \frac{1+j}{\sqrt{2}} \quad I = 0, 3, 8, 11 \\ &= \frac{-1-j}{\sqrt{2}} \quad I = 1, 2, 4, 5, 6, 7, 9, 10 \end{aligned} \tag{1.1}$$

This data is scrambled by two scrambling sequences (consisting of 1 and -1) by multiplying the pilot data for each OFDM symbol by a bit from one of the sequence. The sequence is selected alternatively for successive OFDM symbols. This is to avoid discrete tone due to the repetitive nature of symbol.

The data symbols, pilot symbols and guard symbols are mapped to the respective subcarriers and time domain data is calculated using 128 point IFFT. The total duration of this 128 sample data sequence is 242.42 nanoseconds. Each symbol transmission is followed by a null period of 37 samples to address the delay spread encountered by the channel. This gives a total duration of 312.5 nanoseconds.

1.3 Direction of Arrival Estimation

The crowding of radio spectrum makes the interference signals coming into the receiver high and thus degrades the performance of all systems. In the futuristic scenario of large scale wireless penetration, it is very important that the transmission power is confined to the desired direction to minimize

the interference levels to the other systems. By restricting the transmission to the optimum directions, one would be able to restrict the interference caused to the other systems to a minimum level. Since the wireless propagation environment is reciprocal, one would be able to reduce the interfering signals to other systems by forming transmitting beams in the directions of arrival of signals from the desired source. Besides, by eliminating the radiations to unwanted areas, one would be able to reuse those frequencies for some other applications. These interference management techniques would be essential for the success of future cognitive radio systems.

Time Division Duplexing (TDD) has been successfully used in short range systems like cordless phone. In TDD, one uses the same frequency for both uplink and downlink. As a result, The propagation environment for both uplink and downlink are the same. In the case of systems using TDD for duplexing, one can safely assume that the angle of departure from transmitter would be same as angle of arrival. This is also true for multipath propagation. The directions of arrival of these multipaths would be the optimum directions for transmission also. Hence it is very important to accurately estimate the direction of arrival of these multipath components.

1.4 Problem Statement

Future Wireless communication systems would consist of both narrowband long range systems and wideband / ultrawideband low power short range systems. These systems will have to coexist and would make use of dy-

namic spectrum management and interference mitigation techniques for their proper operation. These cognitive radio based systems would be relying on proper interference management for optimizing the spectrum utilization. Another notable emerging trend is the increasing popularity of OFDM for high data rate systems. The relative implementation simplicity of OFDM receiver for high data rate wireless systems made it attractive and the trend is expected to continue. Besides, OFDMA also provides an option to dynamically share the spectrum between different users. This would make OFDM a key technology in future wireless communications. One can easily envisage a scenario where OFDM based short range wide bandwidth systems co-exist with other relatively narrowband systems. These short range systems are expected to dominate the indoor environments like office and home. These systems are expected to have little or no mobility. Besides, they are also expected to operate at higher frequencies. In typical environments, these signals undergo reflections from nearby objects and reach the destination with closely spaced delays from nearby angles. These systems would also encounter interference from other nearby short range low power systems as well as higher power narrowband systems from outdoor.

As mentioned in the earlier paragraphs, the accurate estimation of direction of arrival of multipaths would play a key role in interference management of future wireless communication systems. In the case of these wideband systems, one would have to estimate the direction of arrival of

multipaths in the presence of these interfering signals. We haven't come across any research addressing this scenario in literature.

WiMedia UWB is a typical example of such a OFDM based high data rate systems and hence we would use it as an example of OFDM based wideband system in this study. Hence, this research work explores the direction of arrival estimation of multipath clusters in an OFDM based ultra wideband system in the presence of both low level and high level inband interferers. The work aims at developing algorithms for estimating direction of arrival of UWB multipaths and simulation level evaluation of these algorithms.

1.5 Thesis Outline

In Chapter 2, we look at the state of the art in direction of arrival estimation. This looks at the common narrowband approaches followed by a detailed survey of the various schemes for handling wideband signals. Schemes like Maximum likelihood and subspace based techniques are explored. The approaches for handling the coherent cases are also studied. The schemes using the known waveforms for enhancing the accuracy of DOA estimation is also explored here. Mathematical principles behind different techniques are also looked into in this Chapter.

The study of the existing techniques is followed by building the system level model of the current problem in Chapter 3. A mathematical model of the narrowband multipath scenario is developed first. Two im-

portant characteristics of UWB system are made use of in developing the algorithm. Since UWB is operating at frequencies above 3 GHz, one can easily build linear antenna arrays of reasonable size using a patch antennas on a substrate. This would eliminate the errors normally associated with linear arrays. Besides, OFDM systems transmit known data in pilot subcarriers for aiding channel estimation and other receiver processing algorithms. Narrowband algorithm for the estimation of DOA making use of known waveform is developed and its mathematical basis is explained. This is extended to the UWB case. The newly developed algorithm's performance is evaluated for a typical UWB operating scenario. In this case, closely spaced direction of arrival of the multipath signals with exponentially distributed delay is used. The algorithm's performance is compared with those of the existing algorithms of estimation of arrival of wideband multipath signals. The superior performance of the proposed algorithm in typical ultrawideband propagation environment is established through simulation experiments.

The performance of the algorithm developed in Chapter 3 is studied in detail in Chapter 4. Since the ultrawideband algorithm is an extension of the narrowband case, the narrowband performance is thoroughly analyzed. The performance limit of the algorithm is compared with other known algorithms. Large bias in the estimated DOA was a limitation in the algorithm developed in Chapter 3. This was mainly due to the error introduced in coarse estimation used for focussing. A new focussing scheme

to overcome this bias is developed in Chapter 4. The performance of the algorithm is evaluated through computer simulation. It is also compared with conventional focussing schemes for its performance performance under low wideband as well as higher narrowband interference.

The UWB receiver is very expensive and conventional array processing requires as many receivers as the number of antenna elements. This results in a very expensive complicated receiver for the DOA estimation scheme. By making use of known waveform, the proposed algorithm in Chapter 3 derives a new matrix for estimating the direction of arrival of multipaths. The matrix is formed by the weighted sum of the steering vectors of the array corresponding to the different sources. Instead of the instantaneous value of source signals, their expected value is used for weighing the steering vectors. This property is made use in Chapter 5 for simplifying the receiver structure. A new multiplexed receiver architecture making use of fewer receivers is proposed in Chapter 5. The performance of the new architecture is compared with the conventional architecture employing independent receivers for all sensors.

Conventional schemes making use of the eigenvalues for estimating the number of signals fails in estimating the number of multipaths while using the proposed algorithm due to the extremely low values of noise subspace eigenvalues. A new threshold based scheme is proposed to overcome this limitation in Chapter 6. The proposed threshold based method is evaluated under low or no inband interference through computer simulations for new

focussing scheme. The proposed threshold based scheme is also extended to conventional focussing case and its performance is also studied.

Chapter 7 summarizes the contributions of this work and highlights some of the topics requiring further exploration.

Chapter 2

Background- Mathematical Preliminaries

As explained in the previous chapter, the direction of arrival estimation would provide major benefits in wireless communication. Besides, it also plays a major role in radar systems and other localization applications. Some of the localization schemes make use of direction of arrival estimation for finding the location of objects. The underlying phenomenon behind all these direction of arrival estimation schemes is the propagation of electromagnetic waves through homogeneous media. The electromagnetic wave propagation is guided by Maxwell's equations. By intercepting these electromagnetic waves, one would be able to recover the information about the source. We will look into Maxwell's equation for electromagnetic wave propagation in next section.

2.1 Electromagnetic Propagation

Maxwell derived the relation between time varying electric and magnetic fields. He proved that they are interrelated and derived the relations linking them. The equations expressed in terms of total charge are

$$\nabla . \mathbf{E} = \frac{\rho}{\epsilon_0} \tag{2.1}$$

$$\nabla . \mathbf{B} = 0 \tag{2.2}$$

$$\nabla \times \mathbf{E} = -\frac{\partial \mathbf{B}}{\partial t} \tag{2.3}$$

$$\nabla \times \mathbf{B} = \mu_0 \epsilon_0 \frac{\partial \mathbf{E}}{\partial t} + \mu_0 \mathbf{J} \tag{2.4}$$

$\mathbf{E}$ and $\mathbf{B}$ represent the electric field and magnetic field respectively at a point. ρ and $\mathbf{J}$ are the total charge density and current density respectively. ϵ_0 and μ_0 are the permittivity and permeability of free space. He also proved the existence of a time varying electric field associated with a time varying magnetic field. The above equations led to the electromagnetic wave equation

$$\nabla^2 \mathbf{E} = \frac{1}{c^2} \frac{\partial^2 \mathbf{E}}{\partial t^2} \tag{2.5}$$

$$\nabla^2 \mathbf{B} = \frac{1}{c^2} \frac{\partial^2 \mathbf{B}}{\partial t^2} \tag{2.6}$$

The wave equation relates the time rate of change of electric / magnetic field with its variation in space. c is defined as the propagation velocity of electromagnetic field in free space. This predicted a spatially varying electric field around a time varying electric field. The same holds true for magnetic field as well. we would be using electric field for all explanation

in this study. The solution to the wave equation Eqn.(2.5) is

$$\mathbf{E} = \mathbf{E}_0 s(t - \frac{\mathbf{k}.\mathbf{d}}{c}) \tag{2.7}$$

$\mathbf{E}_0$ is the electric field at the reference point and s is a differentiable function of $\frac{\mathbf{k}.\mathbf{d}}{c}$ and t and represents the source waveform in time domain. This reference point is taken as the origin for all measurements. $\mathbf{k}$ is a unit vector in the direction of the source and $\mathbf{d}$ is the position vector of the point at which electric field is measured. Without loss of generality, one can assume that $\mathbf{E}_0$ is equal to one.

These fields are measured using sensors or antennas. They respond to either magnetic or electric field of the incoming electromagnetic wave. These sensors, when exposed to the electric / magnetic field convert the electric / magnetic field to voltage or current, suitable for further processing.

With a single element, one can capture the signal for identifying its characteristics. The resolution in direction of arrival estimation in this case would be limited by the beamwidth of the antenna. One can improve this resolution by increasing the gain of the antenna and thus decreasing its beamwidth. But this necessitates the steering of the antenna to cover the required field of view. Still the achievable resolution using this method is limited. Antenna arrays consisting of multiple antenna elements can be used for enhancing the resolution. There are different techniques for the estimation of Direction of Arrival (DOA) [57] using array of antennas.

2.2 Antenna array

Antenna array consists of a set of antennas arranged in arbitrary locations in three dimensional space as shown in figure 3.1. E0 is the reference element. E1- E4 represent the other antenna elements and **d1-d4**, their respective position vectors with respect to the reference. The antenna array sample the incoming electromagnetic field in different locations in space. The extra information provided by the multidimensional spatially sampled data can be exploited to improve the resolution of DOA estimation. The computational complexity of the algorithms making use of arrays can be significantly reduced by positioning the elements at locations offering simple relationship between signals received by different antenna elements. Linear and circular arrays are examples of such array geometries. In circular array, the elements are placed along the perimeter of a circle. Linear array consists of elements placed along a line. This work makes use of linear array. Linear array with uniform inter-element spacing is known as uniform linear array.

Figure 2.2 illustrates a uniform linear antenna array consisting of M omnidirectional sensor elements with inter-element spacing d. The elements are placed along X axis. The response of the array to incoming signal would depend on its bandwidth. The signals are classified as narrowband or wideband based on the bandwidth of the signal with respect to the inverse of the propagation time across the array. When the bandwidth of the signal is much less than inverse propagation delay, it is generally classified as narrowband. We will look into narrowband modeling before

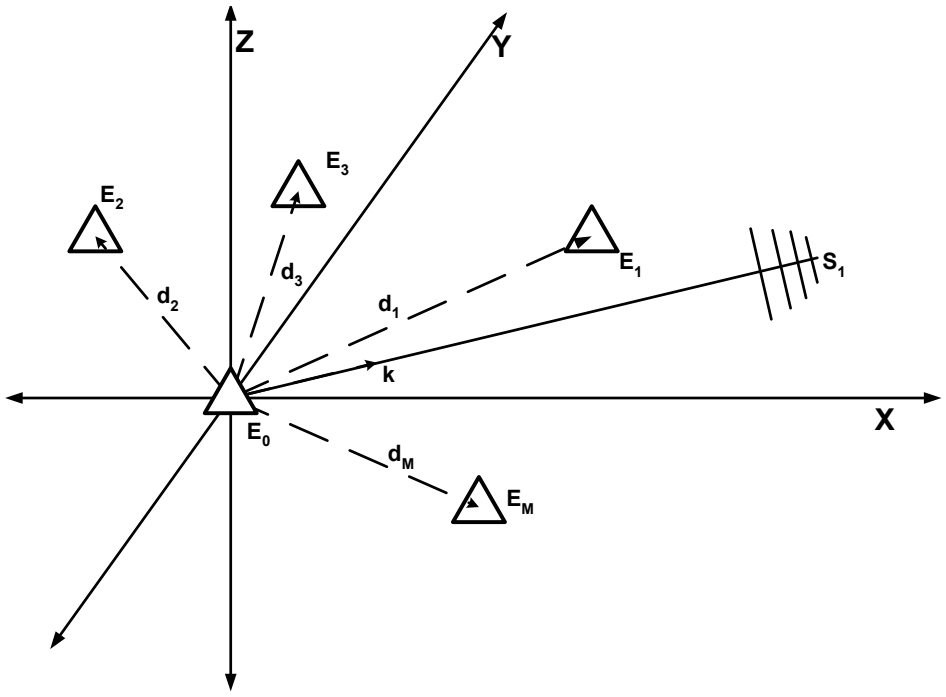

Figure 2.1: Antenna Array

considering the wideband case.

2.3 Narrowband signals

The m^{th} antenna element converts the electric field at its location to a corresponding signal $x_m(t)$. This can be a voltage or current. The narrowband signal can be approximated as a single discrete frequency signal. The signal received by m^{th} antenna element due to a single frequency source is

$$x_m(t) = Asin(\omega_c(t - \frac{\mathbf{k}.\mathbf{d}}{c})) \tag{2.8}$$

Here, ω_c is the carrier frequency of the source signal.

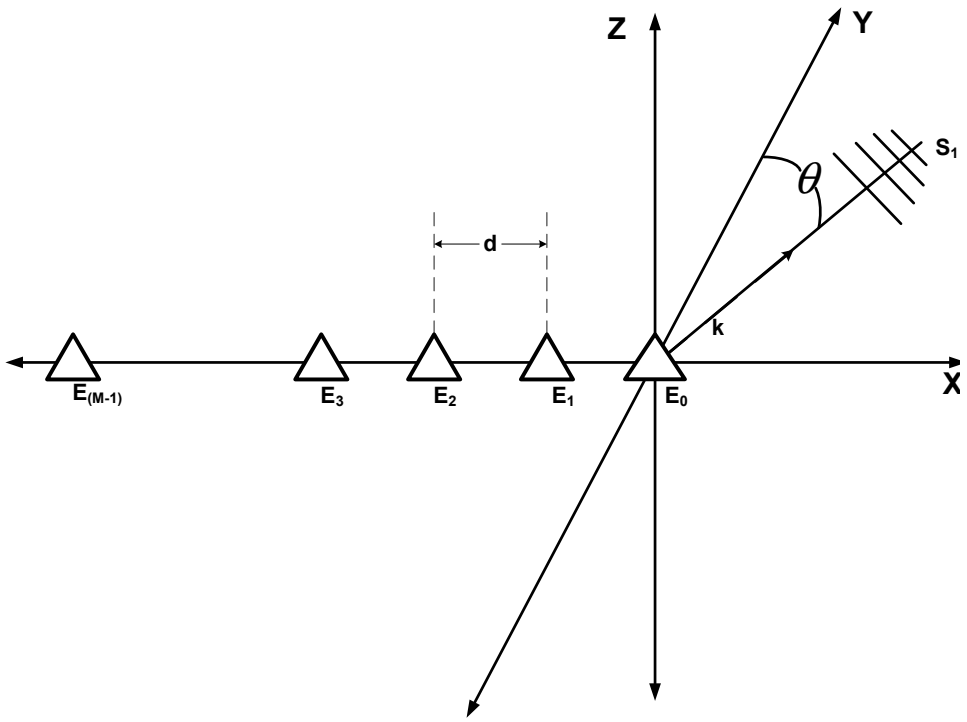

Figure 2.2: Uniform Linear Array

One can write this as

$$x_m(t) = Ae^{-j\omega_c\tau_m} sin\omega_c(t) \tag{2.9}$$

τ_m is the delay from reference element to the m^{th} element and is equal to $\frac{\mathbf{k.d}}{c}$. The delay between the elements are modeled as a phase shift. If we assume uniform linear array and impinging sources in the plane of the array, the path difference between the signals reaching the adjacent antenna elements r can be depicted as shown in figure 2.3. Here, θ is the direction of the arrival of the source with respect to the broadside of the array and the path difference between the two paths reaching the adjacent elements r is equal to $d\sin(\theta)$.

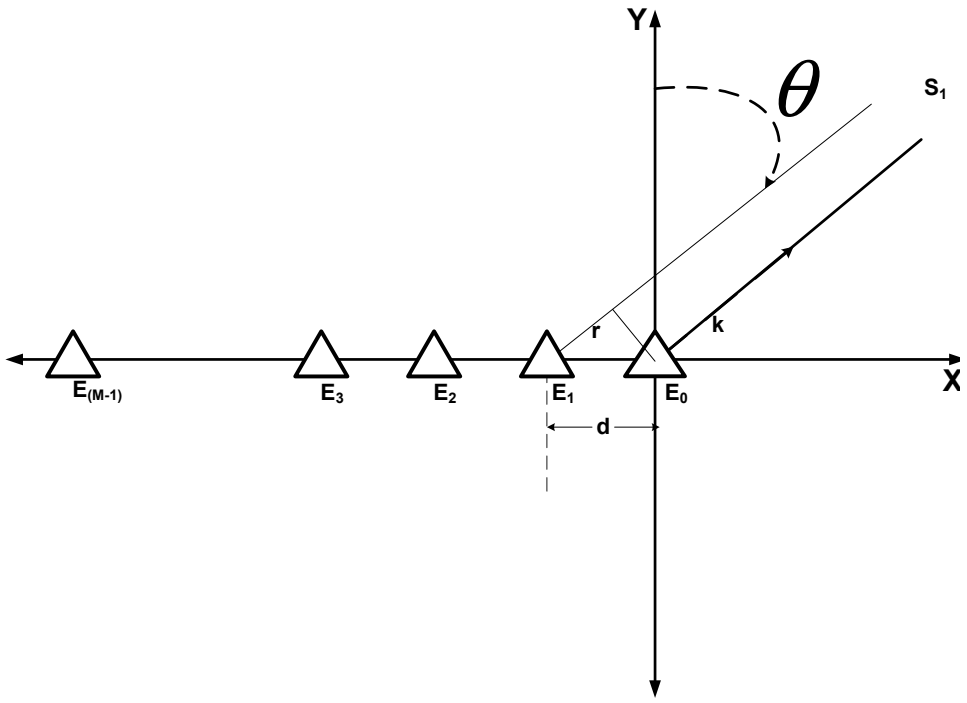

Figure 2.3: Diagram illustrating the path difference between elements

If the antenna array consists of M elements, one can form an array output signal vector $\mathbf{x}$(k) consisting of the outputs of the array elements at discrete time instants k and is

$$\mathbf{x}(k) \triangleq [x_1(k), x_2(k), \cdots, x_M(k)]^T \tag{2.10}$$

$x_m(k)$ represents the signal received by the m^{th} sensor at the k^{th} instant. All the DOA estimation schemes are based on the processing of this array output vector. This array output vector can be expressed as

$$\mathbf{x}(k) = \mathbf{A}\mathbf{s}(k) + \mathbf{z}(k) \tag{2.11}$$

In Eqn.(2.11), each element $a_{m,n}$ of $\mathbf{A}$ represents the phase shift encountered by the n^{th} source at the m^{th} element at frequency ω_0. $\mathbf{s}$(k) and

$\mathbf{z}$(k) represent the input signal and array noise vector respectively at the k^{th} instant.

If one calculates the covariance matrix of this array vector defined by E[$\mathbf{x}\mathbf{x}^H$], it would be a matrix with rank equal to one in the case of a single source. This approximation is valid as long as the bandwidth of the signal is much less than the inverse of the maximum propagation delay across the antenna array. The model of assuming a phase shift to account for the delay between the array elements start to fail at this point. As the bandwidth of the signal increases, the system will start deviating from the conventional rank 1 model of ideal single frequency signal. The wideband signal would look like an extended source. In fact, the covariance matrix of a nonzero bandwidth signal would be a full rank matrix. The problem with nonzero bandwidth is studied in [106]. Even though the matrix is of full rank, the eigenvalues would be generally very small. As the bandwidth increases, additional significant eigenvalues appear in covariance matrix even for single source with wide bandwidth and rank 1 model will no longer be valid. One will have to look into wideband methods to estimate the DOA under such conditions.

Far field sources at angles $[\theta_1, \theta_2, \cdots, \theta_p]$ are impinging the antenna array. In the coming two sections, we would look at the main schemes for estimation of narrowband and wideband signals.

2.4 Direction of Arrival Estimation - Narrowband

As mentioned in the earlier paragraphs, narrowband direction of arrival schemes model the signal source as a single frequency source. This model results in rank 1 approximation for the source and all narrowband algorithms make use of this property to estimate the number of sources and the direction of arrival. The main schemes exploited multidimensional nature of the data and these included beamforming, Subspace methods and maximum likelihood estimation. We will look into details of various schemes in next few sections.

2.4.1 Beamforming

Beamforming was used for estimation of DOA. One would form beams in different look directions by combining suitably weighted incoming signals from different elements. The weighing coefficients depends on the look direction. The received powers from different spatial directions are compared to decide the signal directions.

Fig.(2.4) shows a typical block diagram of beamforming method. Mathematically, this is done by pre multiplying the input data vector by the conjugate transpose of the steering vector of the desired direction and finding the expected value of the square of this product. In the case of an M-element linear array, the steering vector for direction θ_m is given by

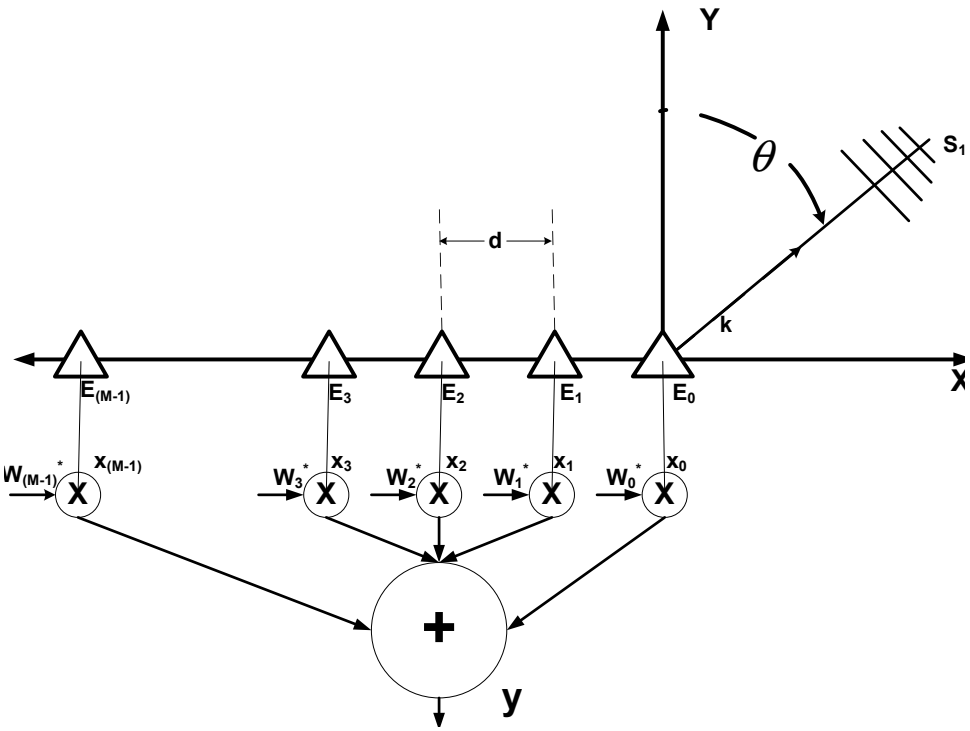

Figure 2.4: Beamforming

Eqn.(2.12), where $a_m(\theta)$ is given by Eqn.(2.13)

$$\mathbf{a}(\theta) \triangleq [a_1(\theta), a_2(\theta), \cdots, a_M(\theta)]^T \tag{2.12}$$

$$a_m(\theta) = e^{\frac{-j2\pi(m-1)dsin(\theta)}{\lambda}} \tag{2.13}$$

Here λ represent the wavelength of incoming signal. The total signal at the output of the array is given by Eqn. (2.14)

$$y(k) = \mathbf{w}^H \mathbf{x}(k) \tag{2.14}$$

Here y(k) is the array output at time instant k and $\mathbf{w}$ is the array weight vector used for summing. $\mathbf{w}^H$ stands for Hermitian transpose of $\mathbf{w}$ and is equal to the conjugate transpose of the steering vector $\mathbf{a}(\theta)$ for forming

beam in a direction θ . The total power in the given direction is calculated. This is repeated for angles spanning from -90 to 90 degree. The spatial power spectrum is calculated and peaks are located for potential sources.

$$\begin{aligned} P(\theta) &= E(|y(k)|^2) && (2.15)\\ &= E(|\mathbf{w}^H)\mathbf{x}(k)|^2 && (2.16)\\ &= \mathbf{w}^H\mathbf{R}_x\mathbf{w} && (2.17)\\ &= \mathbf{a}^H(\theta)\mathbf{R}_x\mathbf{a}(\theta) && (2.18) \end{aligned}$$

Here $\mathbf{R}_x = E[\mathbf{x}\mathbf{x}^H]$ and E[.] is the mathematical expectation operator. The resolution of the scheme is limited by the number of antenna elements. The performance of the bemforming was severely effected by the presence of other signals in the sidelobes of the desired directions. Capon [57] proposed new method to overcome this problem.

2.4.1.1 Capon's Method

In conventional beamforming, the strongest beam is pointed in the look direction. The sidelobes of the array response pick signals which are not in the direction of main lobe. It works well when there is only one source. In general, the received power in any direction is the sum of the desired signal in that particular direction and the other interfering signals picked from other directions by the array. This results in poor resolution. All the degrees of freedom available in selecting the weighing coefficients are used for forming the beam in a particular look direction. Capon's minimum variance method tries to overcome this problem by simultaneously forming

beam in a particular direction and forming nulls in the directions of the interfering signals. The available degree of freedom is split between these two requirements. This technique works on the principle of minimizing the total power while maintaining unity gain in the chosen look direction. It is shown that the optimum weight vector is given by Eqn.(2.19) [57]

$$\mathbf{w} = \frac{\mathbf{R}_x^{-1}\mathbf{a}(\theta)}{\mathbf{a}^H(\theta)\mathbf{R}_x^{-1}\mathbf{a}(\theta)} \tag{2.19}$$

$\mathbf{R}_x$ and $\mathbf{a}(\theta)$ are the auto covariance of input vector and array steering vector respectively. By computing Capon's spatial spectrum over the whole range of angle and locating peaks, one would be able to estimate the DOA's of sources. Capon's method fails when the interfering signals are correlated due to the destructive combining of correlated signals. Besides, this method requires the computation of matrix inversion in the real time. The beamforming performance degrades in low SNR conditions. The multidimensional nature of array vector could be exploited to find the directions by looking at directions that maximizes the likelihood functions of the multivariable input data. The key points of maximum likelihood approach is summarized below.

2.4.2 Maximum Likelihood Estimation

This was based on maximizing the likelihood function. By assuming deterministic [48] unknown source signals with known frequency and white Gaussian random sensor noise, one could calculate the likelihood function of N samples of array vectors. The probability density function of the ob-

servations when all the parameters are known is called likelihood function. Under the above assumption, one could model the array output vector as a white Gaussian random vector with mean $\mathbf{As}$(k) and covariance matrix $\sigma^2\mathbf{I}$. Here $\mathbf{A}$ and $\mathbf{s}$ are as defined in Eqn.(2.30) and (2.32).

Under the assumption of independent measurements, the likelihood function is given by Eqn.(2.20) [48].

$$L_{DML}(\mathbf{\Theta}, \mathbf{s}(k), \sigma^2) = \Pi_{k=1}^{N}(\pi\sigma^2)^{-M} e^{-\|\mathbf{x}(k)-\mathbf{As}(k)\|^2/\sigma^2} \tag{2.20}$$

This could be translated to the minimization of log likelihood function given by Eqn.(2.21) [48] to determine the parameters.

$$l_{DML}(\mathbf{\Theta}, \mathbf{s}(k), \sigma^2) = Mlog(\sigma^2) + \frac{1}{\sigma^2 N}\sum_{k=1}^{N}\|\mathbf{x}(k) - \mathbf{As}(k)\|^2 \tag{2.21}$$

The solutions for this minimization was given in [48]

One could solve this by first calculating the sample auto-covariance of the observed data $\hat{\mathbf{R}}$ and Moore- Penrose pseudo inverse $\mathbf{A}^\dagger$ of array matrix as shown in Eqn.(2.22) and Eqn.(2.23)

$$\hat{\mathbf{R}} = \frac{1}{N}\sum_{k=1}^{N}\mathbf{x}(k)\mathbf{x}^H(k) \tag{2.22}$$

$$\mathbf{A}^\dagger = (\mathbf{A}^H\mathbf{A})^{-1}\mathbf{A}^H \tag{2.23}$$

Using the above results, one could calculate the following quantities

$$\mathbf{\Pi}_A = \mathbf{A}\mathbf{A}^\dagger \tag{2.24}$$

$$\mathbf{\Pi}_A^\perp = \mathbf{I} - \mathbf{\Pi}_A \tag{2.25}$$

Using the above results one can calculate $\hat{\sigma}^2$ and $\hat{\mathbf{s}}(k)$ corresponding to the minimum value of ML function as follows.

$$\hat{\sigma}^2 = \frac{1}{M} Tr(\Pi_A^{\perp} \mathbf{R}) \tag{2.26}$$

$$\hat{\mathbf{s}}(k) = \mathbf{A}^{\dagger} \mathbf{x}(k) \tag{2.27}$$

From the above results, one could obtain the parameter $\mathbf{\Theta}_{DML}$ by solving the following minimization problem [48] to estimate directions of arrival.

$$\mathbf{\Theta}_{DML} = arg\{\min_{\mathbf{\Theta}} \ Tr\{\Pi_A^{\perp} \hat{\mathbf{R}}\}\} \tag{2.28}$$

This minimization was a multidimensional one with significant computational complexity. Even though it could provide the most accurate solution when it converges, the computational complexity was a big disadvantage for ML methods. Subspace method makes use of the structure in the array data to provide a high resolution scheme with much reduced complexity. The multidimensional search is reduced to a single dimensional search. The basic principle of subspace based algorithms and some of the previous works are summarized in the following paragraphs.

2.4.3 Subspace Based Methods

The subspace based techniques are based on the partition of M dimensional complex subspace spanned by the received signal vectors into two orthogonal subspaces, namely signal and noise subspaces. If there are p uncorrelated sources, the direction vectors of the sources would span a p dimensional subspace of this M dimensional complex vector space. This is

called signal subspace. The (M-p) dimensional space orthogonal to the signal subspace is called the noise subspace. The noise in the different sensor elements are assumed to be uncorrelated among themselves as well as with the source signals. Johnson [43] gives an introduction to the basic methods using eigenstructure methods.

The orthogonality between source directional vectors and noise subspace was the basis for MUSIC [74] and ESPRIT [73] algorithms for estimation of the DOA. Bienvenu [10, 11] proved the mathematical basis of the subspace based approach and provided solution for handling correlation between sensor noise. He also proved [9] that eigenvectors corresponding to the largest eigenvalues of the covariance matrix of the array output would span the same subspace as the directional vectors of the sources contributing to the array output. Barabell [6] proposed some polynomial based enhancements to enhance resolution performance. Bronez and Cadzow [15] also looked into the algebraic approach to direction finding by finding a vector orthogonal to noise free data vector. Since it was not possible to determine noise free data, they developed constrained optimizations based on statistics of the data and proved that roots of the z transform of this vector would give the directions of arrival. Cadzow [18] also analyzed the mathematical basis for orthogonality of different subspaces. Wax [97] provided a detailed analysis of the principle of eigenstructure methods.

The following paragraphs briefly explain the main subspace based direction of arrival estimation techniques.

We assume that p ($p < M$) statistically independent far field sources at frequency ω_0 at angles $[\theta_1, \theta_2, \cdots, \theta_p]$ are impinging a linear antenna array. Then,

$$\mathbf{x}(k) = \mathbf{A}\mathbf{s}(k) + \mathbf{z}(k) \tag{2.29}$$

$$\mathbf{s}(k) \triangleq [s_1(k), s_2(k), \cdots, s_p(k)]^T \tag{2.30}$$

$$\mathbf{z}(k) \triangleq [z_1(k), z_2(k), \cdots, z_M(k)]^T \tag{2.31}$$

Here $\mathbf{x}$(k), $\mathbf{s}$(k) and $\mathbf{z}$(k) are defined in Eqns.(2.14), (2.30) and (2.31) respectively. $\mathbf{z}$(k)is the sensor noise vector. $\mathbf{A}$ is a $M \times P$ array matrix and is given by Eqn.(2.32).

$$\mathbf{A} = [\mathbf{a}(\theta_1), \mathbf{a}(\theta_2), \cdots, \mathbf{a}(\theta_M)]^T \tag{2.32}$$

$\mathbf{a}(\theta_m)$ is the array steering vector as defined in Eqn.(2.12) for frequency ω_0

The input covariance matrix is given by

$$\mathbf{R}_x \triangleq E[\mathbf{x}(k)\mathbf{x}(k)^H] \tag{2.33}$$

$$= \mathbf{A}\mathbf{R}_s\mathbf{A}^H + \mathbf{R}_z \tag{2.34}$$

Where signal correlation matrix $\mathbf{R}_s$, and noise correlation matrix $\mathbf{R}_z$ are defined as $E[\mathbf{s}(k)\mathbf{s}^H(k)]$ and $E[\mathbf{z}(k)\mathbf{z}^H(k)]$ respectively.

For p uncorrelated sources, the covariance matrix $\mathbf{R}_s$ would be of rank p. If $\lambda_1, \cdots, \lambda_p$ represent the p largest eigenvalues of $\mathbf{R}_s$, the remaining eigenvalues of $\mathbf{R}_s$ would be zero. This implies that (M-p) smaller eigenvalues of $\mathbf{R}_x$ and $\mathbf{R}_z$ would be equal.

As a result, it can be proved that

$$(\mathbf{R}_x - \mathbf{R}_z)\mathbf{e}_i \quad = \quad \mathbf{A}\mathbf{R}_s\mathbf{A}^H\mathbf{e}_i = 0 \tag{2.35}$$

$\mathbf{e}_i$ represents the eigenvector corresponding to smaller eigenvalues of $\mathbf{R}_x$. If $\mathbf{A}$ is of full rank, the Eqn.(2.35) implies that $\mathbf{A}^H\mathbf{e}_i = 0$. This is true for all eigenvectors corresponding to smaller eigenvalues.

Hence eigenvectors of $\mathbf{R}_x$ can be split into two groups. If the number of sources are known, p eigenvectors corresponding to the largest eigenvalues can be grouped as columns to form signal subspace matrix $\mathbf{E}_s$. Similarly, noise subspace matrix $\mathbf{E}_n$ can be formed with the remaining eigenvectors as columns.

In MUSIC, spatial spectrum [74] defined by Eqn. (2.36) was calculated.

$$P_{Music}(\theta) = \frac{\mathbf{a}^H(\theta)\mathbf{a}(\theta)}{\mathbf{a}^H(\theta)\mathbf{E}_n\mathbf{E}_n^H\mathbf{a}(\theta)} \tag{2.36}$$

The p steering vectors corresponding to the direction of arrival of the p sources would generate peaks in the MUSIC spectrum due to the orthogonality between the direction vectors and noise subspace. Array steering vectors could either be calculated from the geometrical structure of the array or it could be measured and stored. Peaks were located in the spatial spectrum as potential angles of arrival.

ESPRIT algorithm made use of the shift invariance property of linear arrays. Two arrays shifted by unit inter-element distances were formed by picking the first M-1 elements for the first array and last M-1 elements for the second array. The array matrix of the two arrays $\mathbf{A}_1$ and $\mathbf{A}_2$ would be

connected by the relation $\mathbf{A}_2 = \mathbf{A}_1\mathbf{\Phi}$. $\mathbf{\Phi}$ was a $p \times p$ diagonal matrix whose m^{th} diagonal element was $e^{\frac{-j2\pi dsin(\theta_m)}{\lambda}}$. ESPRIT tried to find the $\mathbf{\Phi}$ matrix using subspace approach. This did not require exhaustive search through all possible steering vectors. The peak search was eliminated. Main advantage of ESPRIT was its lower computational and storage requirements. The calibration requirements were also not stringent.

Kumaresan [50] and Reddi [71] proposed polynomial based approach to eliminate the search in the DOA space. The basic principle was to identify a polynomial whose roots would be corresponding to the direction of arrival. The polynomial was identified from the noise subspace eigenvectors.

Sharman and Durrani [81] enhanced the algorithm by merging ML and subspace methods. Here, the product of the noise subspace space eigenvectors and direction vectors were treated like a random variable with given distribution and the likelihood function of these random variables are calculated. The DOAs are estimated by maximizing the likelihood function.

The subspace based schemes provides satisfactory performance as long as signal bandwidth is narrow. The computational complexity is also much less compared to the maximum likelihood methods. The basic principle of subspace methods was the partition of M dimensional complex space to two distinct subspaces called signal and noise subspaces. As the signal bandwidth increases, it becomes increasingly difficult to do this partition with a single frequency model. The next section looks into methods for handling sources with increasing bandwidth.

2.5 Direction of Arrival Estimation - Wideband

The time delay between sensor elements was modeled as a phase shift in narrow band analysis. This is applicable when the source signal consists of a discrete frequency impulse. In the zero bandwidth case, the covariance matrix of the m^{th} signal is given by

$$\mathbf{R}_m = s_m \mathbf{a}(\theta_m)\mathbf{a}^H(\theta_m) \tag{2.37}$$

The $(k,l)^{th}$ element of this matrix is given by

$$r_{kl} = s_m e^{j2\pi f_0 \tau_{kl}} \tag{2.38}$$

Here, τ_{kl} represents the propagation delay between k^{th}element and l^{th} element. As the signal bandwidth increases, the rank one representation of the source is no more valid. One will have to calculate the covariance matrix of the wideband signal by integrating each element of the covariance matrix over the desired range of frequency. The wideband covariance matrix is given by [106]

$$\mathbf{R}_m = \int_{f_0-\frac{b}{2}}^{f_0+\frac{b}{2}} s_m(f)\mathbf{a}(\theta_m, f)\mathbf{a}^H(\theta_m, f)df \tag{2.39}$$

Here b is the bandwidth of the signal. As can be seen from Eqn.(2.39), the signal covariance matrix is full rank for nonzero bandwidth signal. But most of the eigen values are very small. The cut off point is the bandwidth at which the second eigenvalue of noise free covariance matrix is larger

than the noise level [106]. Sorelius [83] and Delmas [25] analyze the error in MUSIC estimates due to nonzero bandwidth. These papers provide a quantitative analysis of the performance degradation in wideband systems.

The phase shift is calculated at the discrete frequency of the spectrum. As the bandwidth increases, the phase shift encountered by different frequency components is different and the narrowband model fails. The first approach was to convert the wideband signal into frequency domain [97]. One can approximate the time delay by corresponding phase shift for individual frequency components.

$$\mathbf{X}(\omega_n) = \mathbf{A}(\omega_n)\mathbf{S}(\omega_n) + \mathbf{Z}(\omega_n) \tag{2.40}$$

In the above Eqn.(2.40), $\mathbf{X}$, $\mathbf{S}$, $\mathbf{Z}$ represents the fourier coefficient of array output, source signal and noise at frequency ω_n respectively. $\mathbf{A}$ represents array matrix at frequency ω_n. The covariance matrix of the fourier coefficients of the array output is calculated. The eigendecomposition of the covariance matrix was done to estimate the signal and noise subspace. The MUSIC spectrum was calculated for each angle at all the frequencies. The direction of arrival is estimated by calculating either the geometric mean or arithmetic mean of the spectrum across all the frequencies. For example, the following metric was defined in the case of arithmetic mean.

$$J(\theta) = \frac{|\mathbf{A}_\theta^\dagger(\omega_n)\mathbf{A}_\theta(\omega_n)|}{\frac{1}{M}\sum_{n=1}^{J}\frac{1}{m-\hat{d}}\sum_{k=\hat{d}+1}^{M}|\mathbf{A}_\theta^\dagger(\omega_n)\hat{\boldsymbol{V}}_k(\omega_n)|^2} \tag{2.41}$$

Here J, $\hat{d}$, m represent the number of frequency components , the assumed number of sources and the number of antenna elements respectively.

The peaks in the combined spectrum was located to determine the direction of arrival. This technique suffered in low SNR due to the error in eigendecomposition of the covariance matrix of the individual frequency components.

Wang and Kaveh [92] proposed coherent combining of the subspaces to enhance the performance. Since the signal subspaces at different frequencies are different, they proposed focussing to translate the different subspaces to one subspace at a common frequency. If the array matrix at frequency ω_0 and ω_j for the source arrival problem are given by $\mathbf{A}_0$ and $\mathbf{A}_j$, the column space of these matrices represent the signal subspaces at the respective frequencies. The focussing operation is to find a matrix $\mathbf{T}_j$ such that $\mathbf{T}_j\mathbf{A}_j = \mathbf{A}_0$. But array matrices are not known as it is dependent on the angle of arrival. To estimate array matrices, a coarse estimation of the angle of arrival is done using conventional beamforming like methods. Based on this estimated coarse DOA, the array matrices at different frequencies are calculated. The focussing matrix is calculated based on this estimated matrices. The coherently combined covariance matrix $\mathbf{R}$ and noise matrix $\mathbf{R}_n$ are given by Eqn.(2.42) [92].

$$\begin{aligned} \mathbf{R} &= \sum_{j=1}^{J} \mathbf{T}_j\mathbf{A}_j\mathbf{R}_{sj}\mathbf{A}_j^H\mathbf{T}_j^H \\ \mathbf{R}_n &= \sum_{j=1}^{J} \mathbf{T}_j\mathbf{R}_{nj}\mathbf{T}_j^H \end{aligned} \tag{2.42}$$

$\mathbf{R}_{sj}$ refers to the source covariance matrix at frequency ω_j. The DOA is estimated by generalized eigendecomposition of the matrix pencil $(\mathbf{R}, \mathbf{R}_n)$. Direction of arrival is estimated using conventional MUSIC like methods.

Since the summing of the covariance matrices at different frequencies are equivalent to integration of the power spectral density, the $(kl)^{th}$ element of the covariance matrix would be equal to the autocorrelation of the signal for delay of τ_{kl}. Hence the final matrix would be a full rank matrix unless the multipaths arrive with equal delay. Hence the coherent subspace method is able to handle multipaths in some cases depending on the autocorrelation properties of the source signal. One of the main drawback of the focussing scheme is the need to estimate the coarse DOA. The error in coarse DOA is translated to final estimation error. This situation will worsen in the presence of stronger interferers.

The later methods tried to address the problems due to the errors in coarse estimation. Bienvenu [12] and Friedlander [32] proposed interpolation of arrays to align the signal subspace at different frequencies. The basic principle is to align the signal space by varying the spacing between the array elements so as to make the directional vectors at different frequencies the same. Instead of actually changing the array, virtual array is calculated for each sector through interpolation. This is also similar to the focussing scheme and usefulness of this scheme in the presence of interferer is limited.

Chen et al. [21] studied the performance of broadband interpolation based methods and improved its performance at larger arrival angles. The larger estimation error encountered in large arrival angles was reduced by first shifting the larger angles to smaller angles. The mean of the coarse

estimated DOA angles θ_m is calculated. The phase of the signal received by the p^{th} sensor is shifted by multiplying it with $e^{\frac{j2\pi f_i(p-1)\sin\theta_m}{c}}$. This is equivalent to compressing the angle of arrival to smaller range around small DOAs. The interpolation like in Bienvenu's [12] method is used to combine subspaces. The angles are shifted back after interpolation. Conventional algorithms are used for estimation of the DOA. This scheme reduces the error in larger angles of arrival. The interpolation error in low SNR effects the performance.

Buckley and Griffiths [16] proposed BASS-ALE estimation scheme by employing broadband models instead of the narrowband focussed model of Wang. This scheme is mostly suitable for high SNR environments. In many array configurations like linear array, broadband sources result in ambiguity in (ω, θ) pairs. This is due to the presence of $(\omega sin(\theta))$ product in the elements of array direction vectors. Their proposed scheme eliminates this by adding L -1 delay elements to each of M sensor outputs. A new array output vector is constructed by by concatenating outputs of each sensors at different delays one below the other in a sequential order. This is given by

$$\mathbf{a}_\theta(\omega) = [1 \; e^{-j\omega T_d} \; \ldots \; e^{-j\omega(L-1)T_d}]^T \bigotimes \mathbf{a}(\theta, \omega) \tag{2.43}$$

In the above Eqn.(2.43), $\mathbf{a}(\theta, \omega)$ is the conventional array vector as defined in Eqn.(2.12) and T_d is the temporal sample delay added at the sensor outputs. The new ML array direction vector removes the ambiguity as long as $L > 1$ and $[\omega T_d] mod 2\pi$ is unambiguous over the frequency band of the

source. The technique is based on a new low rank model of the broadband source. If one calculates the span of the newly defined ML dimensional array vector for the source for all frequencies, it would be spanning a much smaller dimensional subspace. The dimension of the subspace is of the order of the product of the total bandwidth of signal and the total observation time (The observation time is equal to the sum of $(L-1)T_d$ and the maximum propagation delay across the array τ_m). If the maximum propagation delay is made less than MT_d, this product would be less than $M+L$ in the case of Nyquist sampling. This would be much less than ML even with small values of L. One would be able to determine the direction of the sources if the number of sources is less than $\frac{ML}{M+L}$.

By eigendecomposition of the covariance matrix of the new observation vector one can identify the broadband source representation space in terms of the eigenvectors in the ML dimensional complex subspace. Separately, a source covariance matrix for each potential angle of arrival of the broadband source would be calculated. By eigendecomposition of this matrix, one will be able to identify the broadband subspace corresponding to each angle of arrival. By comparing the distance between calculated broadband representation space and the broadband subspace for each angle of arrival, one will pick those angles which gives minimum distance. The computational complexity of the algorithm is very high due to the eigenvalue decomposition of ML order matrix and hence it is of limited practical value.

Krolik and Swingler [49] proposed steered covariance approach for broadband location. Here, the covariance matrix is calculated after introducing delays to sensor outputs to form beams in chosen directions.

The delay $\tau_m(\theta)$ added at the m^{th} sensor output is equal to $\frac{(m-1)d}{c}sin(\theta)$. Covariance matrix of the new array output vector formed by the delayed sensor outputs are calculated. This output vector is given by

$$\mathbf{y}(k) = [x_1(k-\tau_1), x_2(k-\tau_2), \ldots, x_M(k-\tau_M)]^T \tag{2.44}$$

The covariance matrix of $\mathbf{y}$(k) is calculated and is given by

$$\mathbf{R}_y(\theta) = E[\mathbf{y}(k)\mathbf{y}(k)^H] \tag{2.45}$$

$$= \sum_{k=l}^{h} \mathbf{T}_k(\theta)\mathbf{K}(\omega_k)\mathbf{T}_k(\theta)^H \tag{2.46}$$

Here, $\mathbf{K}(\omega_k) = E[\mathbf{Y}(k)\mathbf{Y}^H(k)]$, where $\mathbf{Y}$(k) is the Fourier transform of the sensor output vector before delay at frequency ω_k. The signal is assumed to be extending from ω_l to ω_h. $\mathbf{T}_k(\theta)$ is a diagonal matrix whose m^{th} element is equal to $e^{-j\omega_k\tau_m(\theta)}$. It can be seen that this is similar to the focussing matrix in the single group case proposed by Wang and Kaveh [92]. The spatial spectrum is estimated based on the steered minimum variance method and the power in given direction is given by

$$P_{STMV}(\theta) = \frac{1}{[\mathbf{1}^H\mathbf{R}_y(\theta)^{-1}\mathbf{1}]} \tag{2.47}$$

Here $\mathbf{1}$ is a $M \times 1$ vector of ones. One will have to estimate $\mathbf{R}_y(\theta)$ for each angle of arrival and then calculate the spatial spectrum for that angle. The basic principle is to split the observation space to look directions and do focussing like combining and estimate the power in the chosen look

direction. Even though, this does not require any estimation of coarse DOA, the scheme suffers due to the computational complexity. The accuracy of focussing would be largely depending on the size of the sector and for best accuracy, one will have to make the sector size much less than the beamwidth of the array.

Valaee and Kabal proposed [91] a new two sided correlation transformation for aligning the subspaces. This method is similar to focussing. In focussing, the authors propose pre-multiplying with a unitary matrix so as to minimize the error between the array matrices at frequency ω_j and focussing frequency ω_0. In their approach, Valaee and Kabal proposed to pre-multiply by one unitary matrix and to post-multiply by another unitary matrix to minimize the error between the noise free correlation matrices of array output at two frequencies. If $\mathbf{P}_0$ and $\mathbf{P}_j$ are noise free correlation matrices at reference frequency f_0 and frequency f_j, Two sided Correlation Transformation (TCT) focussing matrices are found by minimizing

$$\min_{\mathbf{U}_j} \|\mathbf{P}_0 - \mathbf{U}_j \mathbf{P}_j \mathbf{U}_j^H\| \tag{2.48}$$

such that $\mathbf{U}_j^H \mathbf{U}_j = \mathbf{I}$.

The solution for this optimization problem is given by

$$\mathbf{U}_j = \mathbf{X}_0 \mathbf{X}_j^H \tag{2.49}$$

Here $\mathbf{X}_0$ and $\mathbf{X}_j$ are eigenvector matrices of $\mathbf{P}_0$ and $\mathbf{P}_j$ respectively. They proved that this would minimize the approximation error.

The algorithm depends on the coarse estimation of the direction of arrival using conventional methods like beamforming. This information is

used to calculate the source power spectral density using the formula

$$\hat{\mathbf{S}}_j = (\mathbf{A}_j^H \mathbf{A}_j)^{-1} \mathbf{A}_j^H [\hat{\mathbf{R}}_j - \hat{\sigma}_j^2 \mathbf{I}] \mathbf{A}_j (\mathbf{A}_j^H \mathbf{A}_j)^{-1} \tag{2.50}$$

The average of $\mathbf{S}_j$ is taken as $\mathbf{S}_0$. From this estimate of $\mathbf{S}_0$, $\mathbf{P}_0$ is calculated and is given by

$$\mathbf{P}_0 = \mathbf{A}_0 \mathbf{S}_0 \mathbf{A}_0^H \tag{2.51}$$

$$\mathbf{P}_j = \hat{\mathbf{R}}_j - \hat{\sigma}_j^2 \mathbf{I} \tag{2.52}$$

Though the method provides asymptotically unbiased estimate, the computational complexity is relatively high. Besides, the unitary matrix is calculated based on the estimated noise free power spectral density and the quality of the estimated DOA is highly dependent on this estimate. Frikel [33] extended this further by trying to align the signal eigenspace at different frequencies.

Lee proposed [54] another modification aimed at focussing the different subspaces using beamforming invariance technique to reduce the error arising from the coarse estimation errors. The beamforming is aimed at achieving the same result as focussing. This is achieved by minimizing the difference between beamspace patterns in field of view of the array in the frequency band of interest. Let $\Psi(\theta, f_j) \triangleq \mathbf{w}_j^H \mathbf{a}(\theta, f_j)$ is the beam pattern at frequency f_j. The objective is to find beamforming coefficients at different frequencies so as to minimize the error between beam patterns in the field of view at different frequencies. In practice, one frequency would be chosen as the reference frequency and beamforming weighing vector at that

frequency would be fixed to get a desired beam pattern. Optimization is aimed at calculating the weighing vector at other frequencies. Mathematically, this can be stated as

$$\min_{\mathbf{w}_j} \int_{\Omega} \rho(\theta) |\mathbf{w}_0^H \mathbf{a}(\theta, f_0) - \mathbf{w}_j^H \mathbf{a}(\theta, f_j)|^2 d\theta \tag{2.53}$$

for all frequencies $j = 1, \ldots, J$.

Multiple beams are formed in the area of interest. This is achieved by converting the $M \times 1$ element space data snapshot vector to $K \times 1$ beamspace data snapshot vector by premultiplying it with beamforming matrix $\mathbf{W}_j^H$ at frequency f_j. K should be made larger than the number of sources and less than the number of sensors. The columns of $\mathbf{W}$ are the $M \times 1$ beamforming vectors determined using Eqn.(2.53) at frequency for the beams in the sector of interest. This new beamspace data vector is defined as $\mathbf{X}_B(n, f_j) \triangleq \mathbf{W}_j^H \mathbf{X}(n, f_j)$. It can be shown that

$$\mathbf{X}_B(n, f_j) = \mathbf{W}_j^H \mathbf{A}(f_j) \mathbf{S}(n, f_j) + \mathbf{W}_j^H \mathbf{Z}(n, f_j) \tag{2.54}$$

In the beamforming invariance method, $\mathbf{W}_j^H \mathbf{A}(f_j)$ at different frequencies are made equal to $\mathbf{B}(f_0)$. This would result in $\mathbf{X}_B(n, f_j) = \mathbf{B}(f_0)\mathbf{S}(n, f_j) + \mathbf{W}_j^H \mathbf{Z}(n, f_j)$. This is similar to the focussing and similar approaches can be used to determine DOA. The performance is highly dependent on the bandwidth and the beamforming error increases significantly with increasing bandwidth. Ward etc. [96] proposed a similar approach using time domain frequency invariant beamforming. It is essentially the same as Lee's approach.

Yoon et al. [104, 105] proposed a scheme by making use of algebraic calculation of new subspace at frequency ω_2 and DOA θ_2 from the known subspace at ω_1 and θ_1. The algorithm is based on the fact that even when frequency changes, the DOA won't change. They derived a diagonal matrix for providing this linear transformation. The k^{th} diagonal element of this transformation matrix $[\Phi(\omega_i, \theta_i)]_{(k,k)}$ is given by

$$[\Phi(\omega_i, \theta_i)]_{(k,k)} = e^{-j\omega_i \frac{(k-1)d}{c} \sin\theta_i} \tag{2.55}$$

It can be shown that the array vector $\mathbf{a}(\omega_j, \theta_j)$ at frequency ω_j and DOA θ_j can be translated to $\mathbf{a}(\omega_k, \theta_k)$ by pre-multiplying it with $[\Phi(\omega_i, \theta_i)]_{(k,k)}$. Here, the frequencies and DOAs are related by the equation

$$\omega_k = \omega_i + \omega_j \tag{2.56}$$

$$\sin\theta_k = \frac{\omega_i}{\omega_k} \sin\theta_i + \frac{\omega_j}{\omega_k} \sin\theta_j \tag{2.57}$$

If $\theta_i = \theta_j$, $\theta_k = \theta_i$ and this is the basic principle of TOPS algorithm. Through the transformation matrix, one is able to transform array vector at one frequency to another frequency.

The received signal would be converted to frequency domain and signal and noise subspaces at each frequency would be calculated. Let columns of $\mathbf{F}_i$ and $\mathbf{W}_i$ represent the orthogonal basis vectors of signal and noise subspaces respectively. Let $\Delta\omega_i = \omega_i - \omega_0$. New matrix $\mathbf{U}_i(\phi) = \mathbf{\Phi}(\Delta\omega_i, \phi)\mathbf{F}_0$ is calculated. Here ϕ is an arbitrary angle. Another new matrix $\mathbf{D}(\phi) = [\mathbf{U}_1^H\mathbf{W}_1|\mathbf{U}_2^H\mathbf{W}_2|\cdots|\mathbf{U}_{K-1}^H\mathbf{W}_{K-1}]$ is defined.

It was proven that whenever this arbitrary angle coincides with one of the actual angles of arrival,the matrix $\mathbf{D}(\phi)$ becomes rank deficient.

Basically, the new matrix is a test of the orthogonality of the translated subspace with the noise subspace at the frequency. When the arbitrary angle is equal to one of the angles of arrival, the signal space for that angle of arrival does not change after translation. Thus retains its orthogonality with the noise subspace at all frequencies. This results in zero element row $\mathbf{D}(\phi)$. This was used to estimate DOA. The main weakness of the algorithm is that it is similar to the non-coherent methods as the signal subspaces at each individual frequencies are calculated based on the signal covariance matrix at that frequency and hence the algorithm suffers at low SNR conditions. The algorithm doesn't make use of the wide bandwidth of the signal. Its provides better performance at medium SNR. It also suffers in coherent environment.

As can be seen in above paragraphs, most of the approach in wideband signal processing is aimed at combining the signal subspaces at different frequencies to improve the signal to noise ratio.

Wireless signals reaches the antenna through multiple paths due to reflection and diffraction from surrounding objects. These result in correlated signals reaching the antenna array from different directions. The challenges posed by these correlated signals are discussed in the next section.

2.6 DOA estimation of Coherent / Multi-paths

One of the basic assumptions used in subspace methods was that the source covariance matrix is uncorrelated/ partially correlated. This ensures full rank for the $\mathbf{R}_s$ matrix in Eqn. (2.34). If the sources are correlated, the rank of the $\mathbf{R}_s$ would be less than p, and as a result, the signal subspace eigenvectors spans the subspace defined by directional vectors only partially. As a result, noise space eigenvectors span the orthogonal subspace of direction vector subspace as well as part of the direction vector subspace. This results in the failure of subspace based algorithms like MUSIC.

Shan et al. [79] proposed spatial smoothing for direction of arrival estimation of coherent signals. The spatial smoothing is applied in arrays , which can be split into group of subarrays of equal elements having translational invariance among them. This is generally applicable for uniform linear arrays. Let the number of elements in subarray be L_1. The first L_1 elements forms the forms the first subarray and elements j to $j + L_1 - 1$ forms the j^{th} subarray and so on. The received signal of j^{th} subarray, $\mathbf{r}_j(k)$, can be written as

$$\mathbf{r}_j(k) = \mathbf{A}\mathbf{D}^{(j-1)}\mathbf{s}(k) + \mathbf{n}_j(k) \tag{2.58}$$

In the above equation, $\mathbf{D}$ is given by

$$\mathbf{D} = diag(e^{(-j\omega\frac{d}{c}\sin\theta_1)}, \cdots, e^{(-j\omega\frac{d}{c}\sin\theta_p)}) \tag{2.59}$$

The covariance matrix of each of the subarray is calculated and the

mean of the covariance matrices of subarrays is calculated. This average covariance matrix can be made full column rank if the number of subarrays exceeds that of multipaths. Conventional MUSIC algorithm can be applied on this averaged covariance matrix to find the DOA. One of the drawback of this scheme was that the number of array elements required for estimating k direction of arrival is $2k$. Pillai and Kwon [68] proposed Forward/ backward smoothing for reducing the number of sensor elements required for identification. Basically, the scheme used backward and forward subarrays to increase the number of translationally invariant subarrays used in the averaging of covariance matrix. Pillai [69] analyzed the performance in the limited case of 3 symmetrical sources.

When the sources are closely spaced, the performance of spatial smoothing degrades at low SNR. Moghaddamjoo [61] proposed the removal of the effect of noise before doing spatial smoothing. In this case, one calculate the covariance matrix of the array data and subtract the sum of the outer product of noise space eigenvectors weighted by its noise variance. This will eliminate the effect of noise vectors in noise subspace. The covariance matrix of the subarray is calculated by pre-multiplying and post-multiplying noise free covariance matrix by the respective subarray selection matrix and its Hermitian respectively. Spatial smoothing is applied by calculating the mean of the covariance matrices of the subarrays. Madurasinghe [58] proposed an iterative approach to remove the effect of noise before smoothing. It improved the resolution capability of the closely spaced signals in the

narrowband case when the rank of the source covariance matrix is much less than the one third of the total number of sources.

Zoltowski and Haber [107] proposed using linear combination of direction vectors instead of direction vectors in computing the MUSIC spectrum to handle the coherent case. This was based on the principle that the noise subspace is orthogonal to the linear combination of direction vectors. The main disadvantage of the algorithm was the increasing computational complexity with increasing number of multipaths due to the multidimensional search. Totarong and El-Jaroudi [87] used the fact that signal eigenvectors are linear combination of direction vectors. They treated the elements of signal space eigenvectors as time series representing spatial frequencies and retrieved direction of arrival using harmonic retrieval methods. This is quite effective in high SNR as the noise element in signal space eigenvectors would be small. They used the square root of difference between the corresponding eigenvalue and noise variance as the weighing coefficients for combining signal eigenvectors. To handle coherent case, they applied spatial smoothing before calculating signal space eigenvectors.

Cadzow analyzed the failure of subspace methods in coherent cases. It is known that the signal space eigenvectors are contained in the range space of direction vectors. When there is no coherent sources among the incident sources, the signal space eigenvectors form the basis vectors for the range space of direction vectors. In [17], he proposed a coherency test to determine the presence of coherent sources. For this, a distance metric

of a potential direction vectors with signal subspace is taken. This metric is given by

$$d(\theta) = 1 - \frac{\mathbf{a}^H(\theta)\mathbf{Q}\mathbf{E}_s[\mathbf{E}_s^H\mathbf{Q}\mathbf{E}_s]^{-1}\mathbf{E}_s^H\mathbf{Q}\mathbf{a}(\theta)}{\mathbf{a}^H(\theta)\mathbf{Q}\mathbf{a}(\theta)} \tag{2.60}$$

In the above equation $\mathbf{Q}$ is a user selected positive definite matrix. This metric should ideally be zero for direction vectors if they span the same subspace as eigenvectors. In the case of coherent sources, this won't be generally true and the number of directions in which the distance metric would be close to zero would be fewer than rank of the signal subspace. On detecting the presence of coherent sources, he proposed a nonlinear search to estimate the potential DOA estimation.

He also proposed a translational/ transrotational subarray based schemes to increase the rank of the source covariance matrix. In this case, array elements are positioned such a way that there would be many subarrays with p elements formed from the main array with s elements with position vectors $[\boldsymbol{\kappa}_1^n, \boldsymbol{\kappa}_2^n, \cdots, \boldsymbol{\kappa}_p^n]$. Here $\boldsymbol{\kappa}_m^n$ represents a 3 dimensional vector representing the position of the m^{th} sensor of n^{th} subarray. The position vectors of the m^{th} elements of subarrays 1 and 2 are related by the Eqn.(2.61), where $\boldsymbol{\kappa}_0$ is a reference vector and $\mathbf{T}$, a unitory transformation vector.

$$\boldsymbol{\kappa}_m^1 = \mathbf{T}\boldsymbol{\kappa}_m^2 + \boldsymbol{\kappa}_0 \tag{2.61}$$

In the case of translational subarrays, the subarray i is formed by $p \times s$ subarray selection matrix $\mathbf{P}^i$. The subarray steering vector is formed by premultiplying the main array steering vector by the respective subarray selection matrix. Let $\mathbf{E}_s$ be the matrix formed by the eigen vectors corre-

sponding to larger eigen values as column vectors. He proved that if one can have p and the number of subarrays greater than the number of incident signals, the matrix $\mathbf{E}_{zs}$ formed by concatenating the matrix product $\mathbf{P}^i\mathbf{E}_s$ for all subarrays would be having rank greater than the number of incident sources. One can calculate the direction of arrival by locating the subarray direction vectors whose distance metric defined Eqn.(2.62) is zero.

$$d_1(\theta) = 1 - \frac{\mathbf{a}^1(\theta)^H\mathbf{Q}\mathbf{E}_{zs}[\mathbf{E}_{zs}^H\mathbf{Q}\mathbf{E}_{zs}]^{-1}\mathbf{E}_{zs}^H\mathbf{Q}\mathbf{a}^1(\theta)}{\mathbf{a}^1(\theta)^H\mathbf{Q}\mathbf{a}^1(\theta)} \tag{2.62}$$

The main disadvantage of the scheme was its computational complexity.

Moghaddamjoo [62] proposed technique based on subarrays to overcome the limitation of spatial smoothing in resolving closely spaced sources. He proposed the introduction of a new transformation to the subarray outputs to make the effective source covariance matrix diagonal. This is achieved by calculating new subarray vectors by weighing the original subarray vectors. The number of new subarray vectors would be equal the number of subarrays. The weighing coefficients are calculated so as to make the new effective source covariance matrix diagonal. This algorithm is computationally complex when more than one independent sources are there. The complexity increases with bandwidth.

Pal [66] proposed a new scheme based on the assumption of distinct path delays and distinct DOA for multipaths from a single source. The basic principle is the fact that the signal observed at any instant is influenced by finite number (r) of symbols. The scheme assumes antenna arrays of M elements and p multipaths coming from different directions. The received

signal vector $\mathbf{x}$ is oversampled (at Δ intervals) and the covariance of the oversampled array vector is calculated. The received oversampled signal vector is given by

$$\mathbf{Y}(t_0 + i\Delta) = \mathbf{A}(\boldsymbol{\theta})\mathbf{D}_\alpha\mathbf{P}(t_0 + i\Delta, \boldsymbol{\tau})\mathbf{S}(t_0 + i\Delta) + \mathbf{N}(t_0 + i\Delta) \quad (2.63)$$

In the above equation,

$$\mathbf{Y}(t_0 + i\Delta) = [y_1(t_0 + i\Delta), \cdots, y_M(t_0 + i\Delta)]^T \quad (2.64)$$

$$\mathbf{S}(t_0 + i\Delta) = [s_{k0}, \cdots, s_{k0+r-1}]^T \quad (2.65)$$

$$\mathbf{N}(t_0 + i\Delta) = [n_1(t_0 + i\Delta), \cdots, n_M(t_0 + i\Delta)]^T \quad (2.66)$$

$\mathbf{A}(\boldsymbol{\theta})$ represents the $M \times N$ array matrix for the M element array receiving signal from N different directions and $\mathbf{D}_\alpha$ is N element diagonal matrix representing the amplitude of the multipaths. $\mathbf{P}(t_0 + i\Delta, \boldsymbol{\tau})$ is a $N \times r$ matrix capturing the impulse response of the pulse shaping and receiver filters combined. When one finds the mean of the covariance of the oversampled array output, the mean of the product $\mathbf{P}(t_0 + i\Delta, \boldsymbol{\tau})\mathbf{P}(t_0 + i\Delta, \boldsymbol{\tau})^H$ is calculated. This would result in a full rank matrix if the signal is oversampled sufficiently and the length of channel impulse response in terms of number of symbols is more than that of the number of multipaths. The direction of arrival is estimated by solving the polynomial equations derived from the left singular vectors corresponding to the zero singular values. The scheme is having limited application.

Jeng etc. [42] proposed subspace smoothing approach for finding the DOA of multipath of a single source. The approach is suitable for the

time varying environment, where channel coefficients vary. An antenna array with M elements is used. They defined a spatial signature associated with the emitter. The spatial signature at instant i is defined as $\mathbf{a}^i = \Sigma_{l=1}^{N} \alpha_l^i \mathbf{a}^i(\theta_l)$. If one estimates the spatial signature at $p$different instance and forms a matrix $\mathbf{A}$ with spatial signature at each instant as columns, it can be seen that this would span the subspace corresponding to the direction of arrivals. One can use singular value decomposition of $\mathbf{A}$ and MUSIC to estimate the direction of arrival. This scheme is mostly applicable for time varying environment.

Jeng and Tseng [41] proposed a new scheme for finding the direction of arrival for single OFDM source in multipath case. In this case, they are deriving a new matrix $\mathbf{A}$ whose A_{ij} is equal to the combined channel effect (sum of phaseshifted signals weighted by the magnitudes of respective paths) encountered by the source in reaching antenna element i at subcarrier frequency ω_j. Basically, each column represent the spatial signature at frequency ω_j. It was proven that, this will span the whole signal space if there are sufficient number of subcarriers. Two translationally equivalent subarrays are picked and the $\mathbf{A}$ matrix is calculated for both. TLS ESPRIT was used for finding DOA. Main drawback is that the scheme is applicable in single source case and would require high SNR.

Ballance [5] proposed ML approach for DOA estimation of 2 multipaths. He derives closed form estimation for the amplitude and use this information to simplify the search for angle parameters. Method is suitable only

for 2 path scenario and will not be useful when the number of correlated paths are more.

Most of the spatial smoothing based techniques rely on the reduction in correlation between the sources produced by spatial smoothing. Ermolaev and Gershman [29] analyzes the decorrelation brought by the spatial smoothing. The following Eqn.(2.67) gives the spatial smoothing efficiency for two correlated sources. It is defined as the ratio of $\Delta = \lambda_2 - \sigma^2$ and $\tilde{\Delta} = \tilde{\lambda}_2 - \sigma^2$ corresponding to the difference between the second eigenvalue and noisespace eigenvalue of full array covariance matrix and smoothed covariance matrix respectively. Here M and L represents the number of elements in the main array and subarray respectively. $K$is the number of subarrays and $|\rho|$ and φ are the magnitude and phase of the correlation coefficient between the two sources impinging from angles θ_1 and θ_2 respectively. ψ is given by the relation $\psi = \varphi + (\pi d/2)(K-1)(\sin\theta_1 - \sin\theta_2)$.

$$\frac{\Delta}{\tilde{\Delta}} = \left[\frac{L(1-g^2(L))}{M(1-g^2(M))}\right]\left[\frac{(1-g^2(K)|\rho|^2)}{(1-|\rho|^2)}\right]\left[\frac{1+g(M)|\rho|\cos\varphi}{1+g(L)g(K)|\rho|\cos\psi}\right] \quad (2.67)$$

The function g(N) is defined as

$$g(N) = \frac{\sin[(\pi d/\lambda)N(\sin\theta_1 - \sin\theta_2)]}{N\sin[(\pi d/\lambda)(\sin\theta_1 - \sin\theta_2)]} \quad (2.68)$$

The equation proves the dependence of spatial smoothing on the phase relation between the signals and angle of arrivals.

Doron [28] proposed array manifold interpolation for coherent source estimation. Array manifold at one frequency is calculated after knowing the array manifold at another frequency and this is used for combining the

subspace at different frequencies. They have separated the direction vectors to product of two matrices one related to frequency and sensor position and the second one a function of the direction of arrival. This partition is used to calculate new focussing matrix. Basically, the scheme is also similar to coherent signal subspace processing and rely on the ability of CSSP to handle coherent path.

Many communication systems as well as positioning systems make use of known waveforms for enhancing the performance or simplifying the implementation of processing schemes. For example, communication systems transmit known symbols for aiding receivers in synchronization and channel estimation. Similarly positioning systems also uses known waveforms. The algorithms discussed so far did not make use of the possibilities provided by the known received data in aiding the direction of arrival estimation. Nest section looks into the benefits of using known waveforms.

2.7 DOA estimation Using Known Waveforms

Most of the algorithms for DOA estimation doesn't make use of the knowledge of the input signal. Messer [59] studied the benefits of using source spectral information in the estimation of direction of arrival. She studied the performance of DOA estimation of a source in the presence of interferer. She proposed a generalized likelihood ratio test using an antenna array with M elements. Let H_0 and H_1 represent the cases when signal is absent and present respectively. Let $p(\mathbf{Z}/H_0, \boldsymbol{\gamma}_0)$,$p(\mathbf{Z}/H_1, \boldsymbol{\gamma}_1)$ represent

probability density functions of $\mathbf{Z}$ under the two hypothesis and its corresponding parameter vectors. The decision is made on either of these hypothesis based on the test given by Eqn.(2.69). Here $\hat{\gamma}_i$ is the estimate of corresponding quantity.

$$\frac{p(\mathbf{Z}/H_1, \hat{\gamma}_1)}{p(\mathbf{Z}/H_0, \hat{\gamma}_0)} \underset{H_0}{\overset{H_1}{\gtrless}} \lambda \tag{2.69}$$

Let $\mathbf{X}(\omega_j)$ represents the array output vector at frequency ω_j. Let $\boldsymbol{\mu}_0$ and $\mathbf{K}_0$ represent the mean and covariance of array output vector when the desired signal is absent (condition H_0) and $\boldsymbol{\mu}_1$ and $\mathbf{K}_1$ represent those quantities when desired signal is present (condition H_1) respectively. Then the log likelihood ratio at ω_j is given by

$$L(\mathbf{X}, \omega_j) = -ln\frac{det\ \mathbf{K}_1}{det\ \mathbf{K}_0} - (\mathbf{Z} - \boldsymbol{\mu}_1)^H \mathbf{K}_1^{-1}(\mathbf{Z} - \boldsymbol{\mu}_1) + (\mathbf{Z} - \boldsymbol{\mu}_0)^H \mathbf{K}_0^{-1}(\mathbf{Z} - \boldsymbol{\mu}_0) \tag{2.70}$$

Since the first term of Eqn.(2.70) is not depended on data,one can drop that term from GLRT. In the case of zero mean gaussian processes $\mu_0 = \mu_1 = 0$, $\mathbf{K}_0(\omega) = \eta(\omega)\mathbf{I}_M$ and $\mathbf{K}_1(\omega) = \mathbf{P}_s(\omega)\mathbf{a}(\theta_s, \omega)\mathbf{a}^H(\theta_s, \omega) + \eta(\omega)\mathbf{I}_M$ when there is no interference. This relation holds good for all frequency component. Messer incorporated the spectral information into covariance function $\mathbf{K}_1$ whenever it is known and assumed $\mu_1 = 0$. When the spectral information is unknown,the conditional pdf of the data which has a nonzero mean is used. Under these assumptions, the ML estimate of the mean is calculated. Using these results, he proved that the detection performance is improved when the signal spectrum is known. This performance improvement is achieved in the presence of interferer as well.

She provides further results [60] on the resolution capability of arrays when source frequency spectrums are known. He has proven that the number of sources which can be detected can be made more than the number of sensors if source spectral density is known and fourier coefficients are uncorrelated.

Let $\mathbf{R}_x(f_k)$ is the covariance matrix array output at frequency f_j and $\boldsymbol{\theta}_1$, $\boldsymbol{\theta}_2$ represents all spatial parameters and spectral parameters respectively. She proved [60] that $CRB(\boldsymbol{\theta}_1)$ is given by

$$CRB(\boldsymbol{\theta}_1) = \left\{ \sum_{k=1}^{J} \mathbf{J}_1(f_k) - \sum_{k=1}^{J} \mathbf{J}_{12}(f_k)\mathbf{J}_2^{-1}(f_k)\mathbf{J}_{21}(f_k) \right\}^{-1} \quad (2.71)$$

$$= \{\mathbf{J}_{\boldsymbol{\theta}_1} - \Delta\mathbf{J}\}^{-1} \quad (2.72)$$

Where

$$J_1(f_k)_{ij} = trace\left\{ \frac{\partial R_x(f_k)}{\partial \theta_{1_i}} R_x^{-1}(f_k) \frac{\partial R_x(f_k)}{\partial \theta_{1_j}} R_x^{-1}(f_k) \right\} \quad (2.73)$$

$$J_{12}(f_k)_{ij} = J_{21}(f_k)_{ij} \quad (2.74)$$

$$= trace\left\{ \frac{\partial R_x(f_k)}{\partial \theta_{1_i}} R_x^{-1}(f_k) \frac{\partial R_x(f_k)}{\partial \theta_{2_j}} R_x^{-1}(f_k) \right\} \quad (2.75)$$

$$J_1(f_k)_{ij} = trace\left\{ \frac{\partial R_x(f_k)}{\partial \theta_{2_i}} R_x^{-1}(f_k) \frac{\partial R_x(f_k)}{\partial \theta_{2_j}} R_x^{-1}(f_k) \right\} \quad (2.76)$$

In Eqn.(2.72), ΔJ is the contribution of the spectral parameters on the achievable estimation error. If the spectral parameters are known, this would be equal to zero. Otherwise, it would be nonzero positive matrix and hence causing higher estimation error.

Li and Compton [55] proposed making maximum likelihood estimation of the DOA when source signal waveforms are known. They assume zero correlation between desired signal and undesired waveform and noise. Let

P signals are impinging on an antenna array with M elements from angles $[\theta_1, \theta_2, \cdots, \theta_P]$. Let $\mathbf{x}$(k),$\mathbf{s}$(k) and $\mathbf{z}$(k) represents the array output, source signal and array noise vector respectively. The array output can be modeled as a product of a diagonal matrix $\mathbf{P}$(k) representing the known value of the source signal at k^{th} instant and a column vector $\boldsymbol{\alpha}$ representing propagation channel coefficients of source signals. This can be expressed as

$$\mathbf{x}(k) = \mathbf{A}(\theta)\mathbf{P}(k)\boldsymbol{\alpha} + \mathbf{z}(k) \tag{2.77}$$

They proposed maximum likelihood based estimation of DOA. In one of the case, they proposed IQML based DOA estimation followed by correlation with known waveform to identify the correspondence between the DOA and the source. They also proposed iterative search technique based on ML principle to minimize the error between the observed sensor signals and estimated sensor signals under the condition of assumed parameters. This involved minimization of a cost function q defined in Eqn.(2.78)

$$q = \frac{1}{N}\sum_{k=1}^{N}[\mathbf{x}(k) - \mathbf{A}(\theta)\mathbf{P}(k)\boldsymbol{\alpha}]^H[\mathbf{x}(k) - \mathbf{A}(\theta)\mathbf{P}(k)\boldsymbol{\alpha}] \tag{2.78}$$

The seed value of DOA is estimated from other methods like MUSIC. The seed value for $\boldsymbol{\alpha}$ is given by Eqn.(2.79).

$$\gamma = \left[\sum_{k=1}^{N}\mathbf{P}^H(k)\mathbf{A}^H(\theta^0)\mathbf{A}(\theta^0)\mathbf{P}(k)\right]^{-1}\left[\sum_{k=1}^{N}\mathbf{P}^H(k)\mathbf{A}^H(\theta^0)\mathbf{x}(k)\right] \tag{2.79}$$

The algorithm iteratively determine the angle of arrival and channel coefficient. In each iteration, minimization is performed with respect to θ_1 first and then with respect to α_1 and so on. The main drawback of the algorithm was its computational complexity.

Li and others [56] proposed sample decoupled maximum likelihood estimator for uncorrelated narrowband sources with known waveforms to reduce implementation complexity. Here, the same array model as the previous case was used. $\mathbf{s}$(k) was defined as a product of a diagonal matrix $\mathbf{\Gamma}$ representing the channel coefficient and a column vector $\mathbf{y}$(k) representing the instantaneous value of the source signal.

$$\mathbf{x}(k) = \mathbf{A}(\theta)\mathbf{\Gamma}\mathbf{y}(k) + \mathbf{z}(k) \tag{2.80}$$

$$\mathbf{x}(k) = \mathbf{B}\mathbf{y}(k) + \mathbf{z}(k) \tag{2.81}$$

Let E$[\mathbf{z}(k)\mathbf{z}^H(k)]$ =$\mathbf{Q}$.

Let

$$\mathbf{Q} = E[\mathbf{z}(k)\mathbf{z}^H(k)] \tag{2.82}$$

$$\hat{\mathbf{R}}_{yx} = \frac{1}{N}\sum_{k=1}^{N}\mathbf{y}(k)\mathbf{x}^H(k) \tag{2.83}$$

$$\hat{\mathbf{R}}_{yy} = \frac{1}{N}\sum_{k=1}^{N}\mathbf{y}(k)\mathbf{y}^H(k) \tag{2.84}$$

$$\hat{\mathbf{R}}_{xx} = \frac{1}{N}\sum_{k=1}^{N}\mathbf{x}(k)\mathbf{x}^H(k) \tag{2.85}$$

$$F = \left|\frac{1}{N}\sum_{k=1}^{N}[\mathbf{x}(k) - \mathbf{B}\mathbf{y}(k)][\mathbf{x}(k) - \mathbf{B}\mathbf{y}(k)]^H\right| \tag{2.86}$$

By minimizing the cost function defined in Eqn.(2.86), one can estimate $\mathbf{B}$ and $\mathbf{Q}$. In the above equation, |.| stands for the determinant of a matrix. Estimates of $\mathbf{B}$ and $\mathbf{Q}$ are given by

$$\hat{\mathbf{B}} = \hat{\mathbf{R}}_{yx}^H\hat{\mathbf{R}}_{yy}^{-1} \tag{2.87}$$

$$\hat{\mathbf{Q}} = \hat{\mathbf{R}}_{xx} - \hat{\mathbf{R}}_{yx}^H\hat{\mathbf{R}}_{yy}^{-1}\hat{\mathbf{R}}_{yx} \tag{2.88}$$

If the sources are uncorrelated, the matrix $\hat{\mathbf{R}}_{yy}$ would become diagonal in the case of large number of samples. This was used to decouple the different source contributions. The direction of arrival is estimated by maximizing the function

$$\theta_k = \max_{\theta_k} \frac{|\mathbf{a}^H(\theta_k)\hat{\mathbf{Q}}^{-1}\hat{\mathbf{b}}_k|^2}{\mathbf{a}^H(\theta_k)\hat{\mathbf{Q}}^{-1}\mathbf{a}(\theta_k)} \tag{2.89}$$

In the above Eqn.(2.89), $\hat{\mathbf{b}}_k$ refers to the k^{th} column of $\hat{\mathbf{B}}$. Thus the proposed algorithm allows one dimensional search to find the DOA of multiple sources. The main weakness is its unsuitability for coherent cases.

Cedervall and Moses [19] extended it to multipath cases. They proposed function given by Eqn.(2.90) as a metric to estimate the initial value of $\boldsymbol{\theta_k}$ corresponding to d_k directions of arrival of k^{th} source. Here the number of multipaths are assumed to be known.

$$f(\theta) = \hat{\mathbf{b}}_k^H \left[\hat{\mathbf{Q}}^{-1} - \frac{\hat{\mathbf{Q}}^{-1}\mathbf{a}(\theta)\mathbf{a}^H(\theta)\hat{\mathbf{Q}}^{-1}}{\mathbf{a}^H(\theta)\hat{\mathbf{Q}}^{-1}\mathbf{a}(\theta)}\right]\hat{\mathbf{b}}_k \tag{2.90}$$

This initial value would be applied in the cost function given by Eqn.(2.91) to estimate the final angle of arrival.

$$\hat{\boldsymbol{\theta}}_k = \arg\min_{\boldsymbol{\theta}_k} \left\{\hat{\mathbf{b}}_k^H[\hat{\mathbf{Q}}^{-1} - \hat{\mathbf{Q}}^{-1}\mathbf{A}(\boldsymbol{\theta}_k)(\mathbf{A}^H(\boldsymbol{\theta}_k)\hat{\mathbf{Q}}^{-1}\mathbf{A}(\boldsymbol{\theta}_k))^{-1}\mathbf{A}^H(\boldsymbol{\theta}_k)\hat{\mathbf{Q}}^{-1}]\hat{\mathbf{b}}_k\right\} \tag{2.91}$$

But this extension results in multidimensional multipath search where the dimension of search is equal to the number of multipaths of the desired signal.

Wang et al. [93] proposed a technique based on subarray beamforming. The DOA estimation is done after beamforming thus providing the possibility of eliminating the error introduced by the interfering signals. The

scheme makes use of two arrays like ESPRIT. One subarray is a translational equivalent of the other. If one picks the first M-1 elements for the subarray A and the last M-1 elements for subarray B, one can express subarray output vectors as

$$\mathbf{x}_A(k) = \sum_{p=1}^{P} s_p(k)\mathbf{a}(\theta_k) + \mathbf{n}_A(k) \tag{2.92}$$

$$\mathbf{x}_B(k) = \sum_{p=1}^{P} e^{-j2\pi d \sin\theta_p/\lambda} s_p(k)\mathbf{a}(\theta_k) + \mathbf{n}_B(k) \tag{2.93}$$

From the above equations, it is clear that the phaseshift between k^{th} signal components of two arrays is a function of the DOA θ_k of k^{th} source. Beamforming weight for one subarray is selected by minimizing the error between the known signal and recovered reference signal. Then the same weight vector is used in the second array also. By doing this, one will be able to reject all the components from sources other than the desired source.

This is achieved by solving the Eqn.(2.94)

$$\min_{\mathbf{w}_p^B} E\left[|(\mathbf{w}_p^B)^H \mathbf{x}_B(k) - e^{-j2\pi d \sin\theta_p/\lambda} r_p(k)|^2\right] \tag{2.94}$$

The solution for this optimization problem is

$$\mathbf{w}_p^B = \mathbf{w}_p^A \tag{2.95}$$

$$= \mathbf{R}_A^{-1}\mathbf{h}_p^A \tag{2.96}$$

Where

$$\mathbf{R}_A = E[\mathbf{x}_A(k)\mathbf{x}_A^H(k)] \tag{2.97}$$

$$\mathbf{h}_k^A = E\{[r_p(k)]^*\mathbf{x}_A(k)\} \tag{2.98}$$

The recovered reference signal would be a phase shifted version of the known waveform and this phase shift is a function of DOA. By measuring this phase shift, one can estimate DOA. This is achieved by solving the Eqn.(2.99)

$$\min_{\hat{\theta}_p} \|\hat{\boldsymbol{r}}_p - e^{-j2\pi d \sin\hat{\theta}_p/\lambda}\mathbf{r}_p\|_2 \tag{2.99}$$

The main drawback of the scheme is that the scheme is applicable only for uncorrelated sources.

Independent of the research work in this thesis, Atallah and Marcoss [4] proposed time domain version of the algorithm similar to the one proposed in this thesis for narrowband systems. The main difference is that this work has independently developed it in frequency domain for ultrawideband systems using the known pilot waveform.

2.8 Multi-antenna methods for UWB systems

Kaiser and Sieskul [44] studied the state of the art in the applications of multi-antennas for UWB and its benefits. The main focus is on using multi-antenna for exploiting MIMO techniques for UWB systems. The paper highlights the benefits of cluster beamforming. In this case, instead of forming beams in all potential directions of multipath, the beams would be formed only in directions of main clusters. As described in [34], UWB multipath model proposed by 802.15 group consists of multipath clusters

consisting of individual paths with exponentially decaying power. This allows forming beams in the direction of the main clusters. This thesis would be focusing on the estimation of direction of arrival of these clusters. Bharadwaj and Buehrer [8] introduced a simple narrowband interference mitigation scheme using array antennas. This is based on the fact that the UWB signal show greater immunity to fading compared to narrowband signals across the antenna array. Hence, by using array based scheme. one would be able to achieve better output signal to interference ratio.

Hashemi et al. [36] analyzed the benefits of array based systems for UWB applications. They studied the main characteristics of both MIMO type and spatial combining type arrays for ultra wideband. The paper [36] studied the selection of inter element spacing for various types of arrays. It is suggested to use half wavelength of highest frequency component as inter element spacing. This paper also looked into the issues of array systems for pulse based UWB with large instantaneous bandwidth. Seyedi et al. [77] presented an array based OFDM UWB system. Their focuss was on utilizing the diversity techniques to enhance the performance of the system. The paper described different approaches for combining the antenna outputs. Yang et al. [102] proposed MIMO based array scheme for enhancing the data rate

2.9 Summary

As seen in earlier paragraphs, subspace based methods offers the best possible resolution with reasonable computational complexity. The subspace methods have been extended to wideband case using focussing to combine the subspaces at different frequency bands. Focussing combines the translated subspaces to form a single subspace. Wang and Kaveh's classic focussing scheme has been the main theme running through most of the proposals with major effort focussing on improving the focussing scheme so as to minimize the bias. The main drawback of the existing methods was the need for coarse estimation of direction of arrival to estimate the focussing matrix. Existing methods not requiring coarse estimation are either iterative methods with significant computational complexity or working in high SNR environments. Besides, they also perform badly in the presence of inband interfering signals.

Similarly spatial smoothing or some variant of it is used for removing the singularity of the source covariance matrix. Use of known waveforms for estimating the DOA is very limited. Most of these schemes are computationally intensive. The method proposed by Atallah and Marcos [4] is quite efficient in terms of computational complexity. But it is addressing narrowband case only.

In the following chapters, we will be looking at methods for estimating the direction of arrival of multipath signals of ultra wideband signals. The key challenges are the loss of rank due to coherent multipaths and the failure

of rank 1 model due to ultra wide bandwidth of the incoming waveform. We will explore techniques for increasing the rank of the source correlation matrix. We will be making use of the known pilot subcarrier waveform to enhance the performance in the presence of interferers as well as to develop focussing schemes not requiring coarse estimation. We will also explore making use of known waveforms to reduce the implementation complexity of the processing system.

Chapter 3

Direction of Arrival of UWB Multipaths

3.1 Introduction

The wireless signals encounter multipath propagation environment while traveling from from its source to destination. These multipath signals reach the receiver with different propagation delays. This delay spread would result in inter-symbol interference and thus effect the performance of the system. This would become more challenging as data rate increase due to increasing demand from newer applications as well as newer users. Orthogonal frequency division multiplexing (OFDM) with a suitable cyclic prefix has become one of the most popular method to alleviate this problem arising from the multipath propagation. Because of this reason, OFDM based technologies are expected to play a major role in future wireless communication systems including both outdoor and indoor applications.

Many applications require knowledge of the location of the source. This can be achieved by attaching wireless transceiver to it. By estimating the direction of arrival, one would be able to localize the item. OFDM based transceiver would be better choice for these applications as well.

The crowding of frequency spectrum due to increasing demand calls for better spectrum management techniques. Spatial reuse of spectrum improve the spectrum utilization efficiency. If one can restrict the transmission to the location of the intended receiver, one can improve the spectrum utilization. In a typical communication scenario, one will have a central access point and many terminals accessing this access point. The wireless signal get reflected in the propagation path and reaches the access point from different directions. In a time division duplex system, the propagation channels are symmetric and one can transmit in the direction of received signals to ensure efficient transmission. This would also reduce the interference caused by the system to other users. At the same time, the increasing density of transmitting devices would increase the interfering signals encountered by various receivers. As a result, the future wireless systems would have to develop schemes to operate in an increasingly interference dominated environment. This is true for direction of arrival estimation algorithms as well. Hence, this work looks at the direction of arrival estimation of OFDM based ultra wideband signals in the presence of interferers. WiMedia UWB is a typical, well defined, OFDM based high data rate system for short range applications [88]. Hence it is chosen for

this study.

The IEEE channel model [34] specify many multipath components consisting of clusters and rays within these clusters. It does not explicitly talk about direction of arrival of these multipaths components. The arrival rates of these clusters and rays are Poisson distributed and inter arrival times are exponentially distributed. The amplitude of individual clusters / rays are exponentially decaying with time. Depending on the sampling rate used, many rays combine to form a dominant multipath component from the cluster/ direction. Because of the exponential nature of the amplitudes, these dominant component would be largely determined by the first few rays of the cluster. In short range environments, one will encounter few such clusters. In general, it can be assumed that these clusters represent different directions of arrival at the access point. Hence one need to transmit only in the direction of clusters.

Since the number of multipaths are too large, it will not be practical to estimate the directions of arrival. Kaiser and Sieskul [44] highlights the benefits of cluster beamforming. Here, one will form beams in the direction of the dominant clusters. Hence, this work focus on estimating the direction of arrival of dominant clusters as specified in the IEEE model. The direction of arrival information is added to each cluster. The initial delay between the cluster follows the exponentially distributed inter arrival times of IEEE channel model [34]. Since the system is using the same frequencies in a coordinated manner for both uplink and downlink, one can

reasonably assume that angle of departure from the transmit side would be same as the DOA of uplink. By determining the direction of dominant clusters, one would be able to focus the transmit energy in the direction of them. This would also be able to improve the system performance as many other multipath components would be eliminated.

In real operation, these systems will have to coexist with other UWB systems at a distance as well as other narrowband systems operating at higher power level. We need to estimate the direction of arrival of these multipath components in the presence of these inband uncorrelated interferers. Conventional schemes doesn't differentiate between desired signals and undesired ones. As a result, the total number of signals including both desired and undesired will have to be less than the number of antenna elements. Atallah et al. [4] has developed algorithm for DOA estimation of narrowband multipath signals in time domain by exploiting known waveforms for impinging narrowband sources independently. In their work, they have developed an algorithm similar to the one described here for estimating the direction of arrival of narrowband multipath signals in the presence of narrowband interferers. They correlated the array output with known time domain training sequence to differentiate the desired and undesired sources. They also used the subarray based scheme to handle the rank reduction due to multipath. Their scheme is not applicable for UWB systems in the presence of interferers and the author hasn't come across any schemes for achieving this.

In this work, the known data transmitted by pilot carriers in each OFDM symbol is exploited to enhance accuracy and improve the resolution capacity of the DOA estimation in the presence of interferes. A new algorithm exploiting these known pilot signal waveforms for detecting the DOA of multipath clusters in WiMedia UWB system in the presence of uncorrelated interferers is developed. Its performance is compared with other known schemes for estimating the direction of multipaths in wideband systems.

3.2 Data Model

In normal operation, UWB systems operate in their own nets using different hopping sequences so as to avoid spectral overlapping. Spatially separated nets uses same hopping sequences. At present, all the UWB modes use the same pilot carrier locations and pilot data. It would be better to change the pilot locations for better performance.

Besides, as mentioned previously, UWB systems encounter narrowband interferers in operation. These interfering signals overlapping with the known pilot locations of the desired signals will constitute an inband interference. In a typical operational scenario, the system may encounter few interfering signals at some of the subcarrier locations of the desired UWB signal. To study these scenarios, the interfering signals are modeled as another UWB waveform with uncorrelated data at its pilot locations. The different scenarios can be evaluated by changing the parameters suitably.

The system consists of multiple UWB sources conforming to the WiMedia UWB standard [88]. Consider p UWB signals $\{s_1(n), s_2(n), \cdots, s_p(n)\}$ impinging on a q element uniform linear array (ULA) from different directions $\{\theta_1, \theta_2, \cdots, \theta_p\}$. The angle θ_i is measured with respect to the broadside of the array. The signal received at the m^{th} element of array is given by Eqn.(3.1)

$$x_m(k)e^{j\omega_c(k)} = \sum_{i=1}^{p} s_i(k - \tau_{m,i})e^{j\omega_c(k-\tau_{m,i})} \tag{3.1}$$

Here, $x_m(k)$ represents the complex envelope of the signal in the m^{th} element, $s_i(k)$ represents the complex envelope of the i^{th} source and $\tau_{m,i}$ represents the differential delay of i^{th} source to the m^{th} element with respect to the reference element. In baseband notation, this can be written as

$$x_m(k) = \sum_{i=1}^{p} s_i(k - \tau_{m,i})e^{-j\omega_c\tau_{m,i}} \tag{3.2}$$

In frequency domain, this can be written as

$$X_m(\omega) = \sum_{i=1}^{p} S_i(\omega)e^{-j(\omega_c+\omega)\tau_{m,i}} \tag{3.3}$$

The array output spectrum can be split into multiple frequency components.

In a multipath environment, impinging signals are associated with L different sources $\{\tilde{s}_1, \cdots, \tilde{s}_L\}$, where $L \leq p$. That is, there may be more than one impinging signals (DOA) corresponding to the same source. The signals associated with one common source are highly correlated with each other. The signals from different sources are assumed to be uncorrelated or

having negligible correlation. This is an assumption adopted by previous works using known waveforms for DOA estimation [55], [93]. The estimation of the DOA of multipaths belonging to a particular target source $\tilde{s}_1$ is the objective of this study.

Perfect synchronization is assumed in this study before calculating the direction of arrival. The synchronization basically involves the estimation of frame boundary, symbol boundary and frequency offset. This is necessary to extract the known pilot subcarrier frequency domain data. Besides, the system timing should not change during the period of data capture. As explained in Chapter 1, the WiMedia UWB transmitter would start its transmission by sending a preamble at the beginning. This preamble is used for estimating the frame and symbol boundaries and frequency offset. Standard synchronization schemes like autocorrelation based ones are adequate to estimate the frame and symbol boundaries within few samples error. It can also detect frequency offsets to within very small error limit. The system can make use of the output of the reference element to estimate the synchronization parameters by employing these standard algorithms. The proposed algorithms should work satisfactorily under the achieved synchronization parameters.

r1 is the frequency domain data carried by the pilot subcarriers of the OFDM based systems. These are QPSK based symbols as defined in Chapter 1. They are used for finer channel estimation and frequency correction. They are multiplied by a spreading sequence to ensure the average value of

this wave form would be zero. This waveform would be used as the known waveform in this study. These waveforms are pseudo-random with low correlation with other signals and noise. This is a key assumption in this thesis. Other assumption is related to negligible inter-element coupling. This assumption is quite reasonable for inter element separation of more than $\lambda/2$. This becomes more accurate in the multiplexed receiver where every fourth element is sampled at the same time. Third assumption is related to the property of linear array. Ideal characteristic is assumed in this work. This also can be considered reasonable in the frequency range employed by UWB systems as one can fabricate highly accurate patch antenna based arrays using modern lithographic techniques.

3.3 Narrowband Algorithm

Since the analysis of UWB signals is an extension of the narrowband case, the narrow band algorithm is developed first. Consider p narrowband signals instead of the UWB signals impinging on the array. The objective is to estimate all the directions of arrivals associated with target source $\tilde{s}_1$ by utilizing the known signal $r_1(n)$ of source $\tilde{s}_1$. Without loss of generality, the first k_1 impinging signals $\{s_1(n), s_2(n), \cdots, s_{k_1}(n)\}$ are assumed to be corresponding to the target source $\tilde{s}_1$, where $k_1 > 1$. The remaining signals are assumed to be inband interferers uncorrelated with the desired source. Hence the goal is to estimate the directions of arrival $\{\theta_1, \theta_2, \cdots, \theta_{k_1}\}$ from this source.

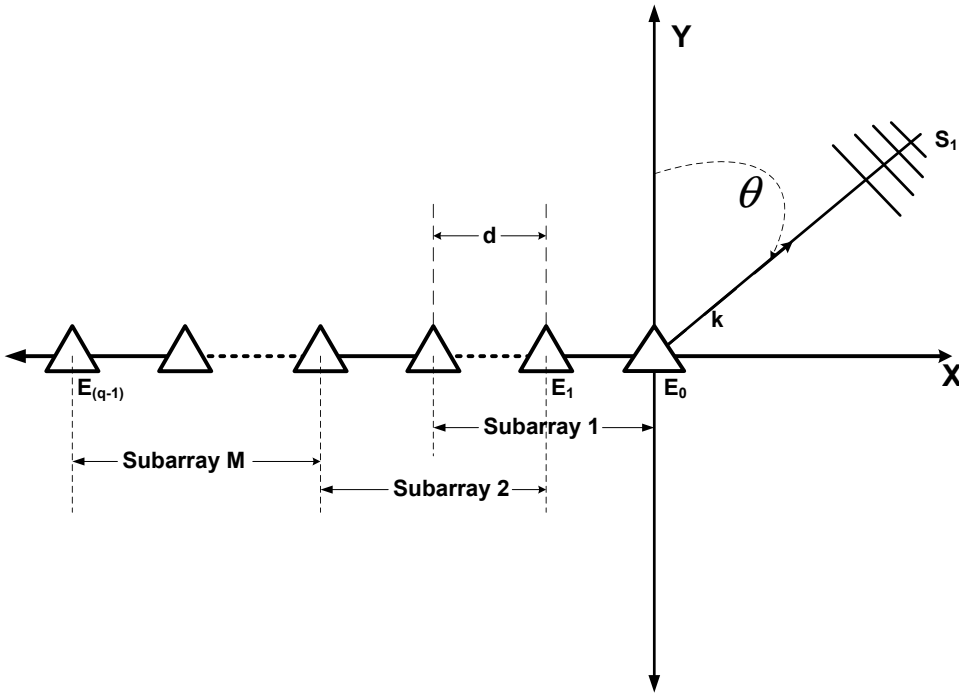

Figure 3.1: Antenna Array

In the proposed scheme, the q elements of uniform linear array are divided into M overlapping subarrays of size $l \triangleq (q - M + 1)$ with sensors $\{1, \cdots, l\}$ forming the first subarray, sensors $\{2, \cdots, l+1\}$ forming the second subarray and so on. The i^{th} subarray output is an $l \times 1$ vector obtained by taking the i^{th} to $(i + l - 1)^{th}$ entries out of $\mathbf{x}$(n). It can be easily verified that

$$\mathbf{x}_i(n) \triangleq \mathbf{A}_1 \mathbf{D}^{i-1} \mathbf{s}(n) + \mathbf{z}_i(n) \quad i = 1, \cdots, M \tag{3.4}$$

where $\mathbf{A}_1$ is a matrix consisting of first l rows of $\mathbf{A}$ and $\mathbf{z}_i(n)$ is a $l \times 1$ column vector whose elements are the noise output of the sensor elements constituting i^{th} subarray. $\mathbf{D}$ is defined as

$$\mathbf{D} = diag(e^{-j2\pi \frac{d}{\lambda} \sin\theta_1} \; e^{-j2\pi \frac{d}{\lambda} \sin\theta_2} \; \cdots \; e^{-j2\pi \frac{d}{\lambda} \sin\theta_p}]^T \tag{3.5}$$

where d and λ are the inter-element spacing and wavelength of the incoming

signal respectively.

Let $\mathbf{X}_i \triangleq [\mathbf{x}_i(n)\ \mathbf{x}_i(n+1) \cdots \mathbf{x}_i(n+N)]$, $\mathbf{Z}_i \triangleq [\mathbf{z}_i(n)\ \mathbf{z}_i(n+1) \cdots \mathbf{z}_i(n+N)]$ be the matrices formed by concatenating the i^{th} subarray output vectors and noise vectors respectively at different time lags . It can be shown that

$$\mathbf{X}_i \triangleq \mathbf{A}_1 \mathbf{D}^{i-1} \mathbf{S} + \mathbf{Z}_i \quad i = 1, \cdots, M \tag{3.6}$$

where

$$\mathbf{S} \triangleq \begin{bmatrix} s_1(n) & s_1(n+1) & \cdots & s_1(n+N) \\ s_2(n) & s_2(n+1) & \cdots & s_2(n+N) \\ \vdots & \vdots & \ddots & \vdots \\ s_p(n) & s_p(n+1) & \cdots & s_p(n+N) \end{bmatrix} \tag{3.7}$$

One can define $\mathbf{r}_1$ as $\mathbf{r}_1 \triangleq [r_1(n)\ r_1(n+1)\ \cdots\ r_1(n+N)]$.

Since the signal $r_1(n)$ is only correlated with first k_1 impinging signals $\{s_1(n), s_2(n), \cdots, s_{k_1}(n)\}$ associated with target source $\tilde{s}_1$, we can have $E[\mathbf{S}\mathbf{r}_1^H] = [\alpha_1\ \cdots\ \alpha_{k_1}\ 0\ \cdots\ 0]^T$, where $\alpha_1 \cdots \alpha_{k_1}$ are nonzero. Consequently,

$$\begin{aligned} E[\mathbf{X}_i \mathbf{r}_1] &= \mathbf{A}_1 \mathbf{D}^{i-1} E[\mathbf{S}\mathbf{r}_1] \\ &= \bar{\mathbf{A}}_1 \mathbf{D}_\alpha \begin{bmatrix} e^{-j2\pi \frac{d}{\lambda}(i-1)\sin\theta_1} \\ \vdots \\ e^{-j2\pi \frac{d}{\lambda}(i-1)\sin\theta_{k_1}} \end{bmatrix} \end{aligned} \tag{3.8}$$

for $i = 1, \cdots, M$ and $\bar{\mathbf{A}}_1$ denotes the submatrix consisting of the first k_1 columns of $\mathbf{A}_1$, $\mathbf{D}_\alpha \triangleq diag(\alpha_1\ \cdots\ \alpha_{k_1})$ is a diagonal matrix with nonzero diagonal elements. Let $\mathbf{g}_i \triangleq \mathbf{E}[\mathbf{X}_i \mathbf{r}_1^H]$. Hence we can express the following

$$\mathbf{G} = [\mathbf{g}_1 \cdots \mathbf{g}_M] \tag{3.9}$$

$$\mathbf{G} = \bar{\mathbf{A}}_1 \mathbf{D}_\alpha \begin{bmatrix} 1 & e^{-j2\pi\frac{d}{\lambda}\sin\theta_1} & \cdots & e^{-j2\pi\frac{d}{\lambda}(M-1)\sin\theta_1} \\ \vdots & \vdots & \ddots & \vdots \\ 1 & e^{-j2\pi\frac{d}{\lambda}\sin\theta_{k_1}} & \cdots & e^{-j2\pi\frac{d}{\lambda}(M-1)\sin\theta_{k_1}} \end{bmatrix}$$
$$= \bar{\mathbf{A}}_1 \mathbf{D}_\alpha \mathbf{B} \tag{3.10}$$

Theorem 3.3.1. *The Matrix* $\mathbf{G}$ *as defined in Eqn.(3.9) spans the column space of matrix* $\bar{\mathbf{A}}_1$ *and the null space of* $\mathbf{G}\mathbf{G}^H$ *would be perpendicular to directional vectors of the sources.*

Proof. Due to the special structure , for $M \geq k_1$, $\mathbf{B}$ is a full row rank matrix. Also for $l > k_1, \bar{A}_1$ is a full column rank matrix. $\mathbf{D}_\alpha$ is of rank k_1. The lower limit of the rank of the product of two matrices $\mathbf{A}$ and $\mathbf{B}$ are stated in theorem in page 96 of [82]. According to the theorem, if $\mathbf{A}$ is a m X n matrix of rank r_A and $\mathbf{B}$ is a n X p matrix of rank r_B, the lower bound of the rank of the matrix product $\mathbf{AB}$ is equal to $r_A + r_B - n$. Therefore, given the condition $M \geq k_1$, $\mathbf{B}$ would be of rank k_1 and $\mathbf{D}_\alpha\mathbf{B}$ would be of rank k_1. With $l > k_1$ satisfied, the matrix G would be of rank k_1. We also have $\mathcal{R}(\mathbf{G}) = \mathcal{R}(\bar{\mathbf{A}}_1)$, where $\mathcal{R}(.)$ denotes the range (column) space. It means $\mathbf{G}^H$ would be having null space of order $l - k_1$. $\mathbf{G}\mathbf{G}^H$would be of rank k_1 and hence would be having $l - k_1$ eigenvalues equal to zero. Hence the eigenvectors corresponding to zero eigenvalues of $\mathbf{G}\mathbf{G}^H$ would be spanning the same space as the null space of $\mathbf{G}^H$. This null space of $\mathbf{G}^H$ is perpendicular to the column space of G. Hence they would be perpendicular to the directional vectors of the source. □

Hence, by locating the directional vectors perpendicular to the non signal eigenvectors of $\mathbf{G}\mathbf{G}^H$, one would be able to estimate the DOA. Note that the above conditions $M \geq k_1$ and $l > k_1$ require that we have $q \geq 2k_1$ sensors irrespective of the number of sources p. This would allow us to detect more multipaths than under spatial smoothing scheme for the same size array in the presence of interferers.

3.4 UWB Extension

The same concept can be extended to UWB case by using frequency domain approach. The time domain data is divided into blocks of data and is translated into frequency domain. The block size is chosen as one OFDM symbol. The UWB system starts the transmission with a preamble consisting of 24 OFDM symbols. These symbols with sharp autocorrelation properties are used for achieving synchronization of the OFDM symbol boundary. In a typical operating scenario, this scheme can achieve synchronization within few sample error from the starting point. This is adequate for proper operation of OFDM receiver. Assuming synchronized operation, one can easily calculate the frequency components for each symbol. Conventional OFDM processing will translate the time delay into an equivalent phase shift in the frequency domain for the subcarriers. If one picks the frequency domain data at one subcarrier frequency, this can be treated as the narrow band case with the symbol index replacing the time index. Multiple OFDM symbols would be used for calculating the correlation between known frequency

domain data and the received frequency domain data. Here, only pilot information is known in advance. Hence, only pilot subcarrier frequencies are used for estimation of DOA.

The array output vector at any pilot subcarrier frequency ω_j and main carrier frequency ω_c is given by Eqn.(3.11).

$$\begin{aligned}\mathbf{X}(\omega_c+\omega_j) &\triangleq [X_1(\omega_c+\omega_j)\ X_2(\omega_c+\omega_j)\ \cdots\ X_q(\omega_c+\omega_j)]^T \\ &= \mathbf{A}(\omega_c+\omega_j)\mathbf{S}(\omega_c+\omega_j)+\mathbf{Z}(\omega_c+\omega_j) \qquad (3.11)\end{aligned}$$

Here $\mathbf{A}(\omega_c+\omega_j) \triangleq [\mathbf{a}(\theta_1)\ \cdots\ \mathbf{a}(\theta_p)]$ is a $q \times p$ steering matrix consisting of p steering vectors $\mathbf{a}(\theta_i)$ defined by

$$\mathbf{a}(\theta_i) \triangleq [1\ e^{-j(\omega_c+\omega_j)d\sin\theta_i}\ \cdots\ e^{-j(\omega_c+\omega_j)(q-1)\sin\theta_i}]^T$$

$\mathbf{Z}(\omega_c+\omega_j)$ denotes $q \times 1$ additive noise vector and $\mathbf{S}(\omega_c+\omega_j)$ is the $p \times 1$ signal vector.

$$\mathbf{Z}(\omega_c+\omega_j) \triangleq [Z_1(\omega_c+\omega_j)\ Z_2(\omega_c+\omega_j)\ \cdots\ Z_q(\omega_c+\omega_j)]^T$$

$$\mathbf{S}(\omega_c+\omega_j) \triangleq [S_1(\omega_c+\omega_j)\ S_2(\omega_c+\omega_j)\ \cdots\ S_p(\omega_c+\omega_j)]^T$$

The subspaces at different frequencies are different. Wang and Kaveh [92], proposed focussing to align the signal subspaces at different frequency. Most of the proposed algorithms for wideband processing has been enhancements to this basic concept. If one can perfectly align N_f signal subspaces, that would be equivalent to multiplying the number of samples used for narrowband processing of one of the frequency components by the same amount. The improvement in performance will be significant for low

SNR case. At higher SNR, one can achieve fairly accurate estimate with fewer samples using narrowband approach. Since this investigation would be considering both lower and higher SNR, the proposed algorithm also makes use of focussing to effectively utilize the information available at other frequency components. The matrix $\mathbf{G}$ at any frequency ω_j is given by

$$\begin{aligned}\mathbf{G} &= [\mathbf{g}_1 \cdots \mathbf{g}_M] \\ &= \begin{bmatrix} u_1 & u_2 & \cdots & u_M \\ u_2 & u_3 & \cdots & u_{M+1} \\ \vdots & \vdots & \ddots & \vdots \\ u_{q-M+1} & u_{q-M+2} & \cdots & u_q \end{bmatrix}\end{aligned} \tag{3.12}$$

Here, $u_i = E(\mathbf{X}_i \mathbf{r}_1^H)$ is the correlation of the i^{th}array output at frequency ω_j with the known waveform r_1. As seen from Eqn.(3.12), each column of $\mathbf{G}$ is obtained by upward shifting of the previous column and dropping the first element and adding the correlation of the next element at the bottom.

The focusing matrix $\mathbf{T}(\omega_j)$ defined in [38] is a unitary matrix which translates the subspace at one frequency to another one at the focussing frequency. Mathematically, if $\mathbf{A}(\omega_j, \boldsymbol{\theta})$ represents the matrix formed by direction vectors at frequency ω_j and $\mathbf{A}(\omega_0, \boldsymbol{\theta})$ at frequency ω_0, the focussing matrix is defined by the relation $\mathbf{A}(\omega_0, \boldsymbol{\theta}) = \mathbf{T}(\omega_j)\mathbf{A}(\omega_j, \boldsymbol{\theta})$. The focussing matrix is found by minimizing the Frobenius norm of the difference between the focussed array vector corresponding to the selected frequency and the array vector at the focussing frequency. The focussing matrix is equal to

$\mathbf{VU}^H$, where $\mathbf{U}$ and $\mathbf{V}$ are the left and right singular matrices of the matrix product $\mathbf{A}(\omega_j, \boldsymbol{\theta})\mathbf{A}(\omega_0, \boldsymbol{\theta})^H$. This generates a deterministic error in each array vector element depending on the frequencies and the group of angles related to coarse DOA estimates $\boldsymbol{\theta}$ used in estimating the focussing matrix. If focussing is done after subarray formation, this would result in avoidable error in the terms of $\mathbf{G}$. For example, u_2 in the first column and u_2 in the second column would be different. Hence the proposed algorithm does the focussing before the subarray formation.

In the proposed algorithm, the array data at different pilot frequencies for each carrier frequency is to be translated to an equivalent narrowband component at the focussing frequency by pre-multiplying it with the focussing matrix. This new data would be processed like the narrowband case to calculate $\mathbf{G}$. $\mathbf{GG}^H$ should be calculated for each translated frequency and average of the $\mathbf{GG}^H$ at the focussed frequency is used for calculating DOA by using conventional MUSIC.

Algorithm 3.1

1. Sample the outputs from array elements at the defined sampling rate. The samples corresponding to the selected carrier frequencies are grouped (based on the hopping sequences).

2. Estimate coarse DOA using conventional beamforming.

3. $\mathbf{X}(\omega_j)$ at each subcarrier ω_j and carrier ω_c is translated to a common focussing frequency ω_0 by pre-multiplying it with corresponding

focussing matrix $\mathbf{T}(\omega_{c,j})$.

4. $\mathbf{T}(\omega_{c,j}) \triangleq \mathbf{V}\mathbf{U}^H$, where $\mathbf{U}$ and $\mathbf{V}$ are left and right singular vectors of the matrix product $\mathbf{A}(\omega_{c,j}, \boldsymbol{\gamma})\mathbf{A}^H(\omega_0, \boldsymbol{\gamma})$.

5. $\mathbf{A}(\omega_{c,j}, \boldsymbol{\gamma})$= Steering matrix corresponding to subcarrier frequency ω_j - carrier frequency ω_c combination at preselected angles $\boldsymbol{\gamma}$. $\boldsymbol{\gamma}$ is a set of angles including the estimated coarse DOA. For example, if coarse DOA's are β_1, β_2 and ϕ the beamwidth of subarray, then $\boldsymbol{\gamma}$= $[\beta_1,\ \beta_1-0.25\phi,\ \beta_1+0.25\phi,\ \beta_1-0.5\phi,\ \beta_1+0.5\phi,\ \beta_2,\ \beta_2-0.25\phi,\ \beta_2+0.25\phi, \beta_2-0.5\phi,\ \beta_2+0.5\phi]$

6. Focus the correlated data matrix corresponding to each pilot subcarrier - carrier frequency combination to a common focussing frequency.

7. Form subarray 1 data $\mathbf{X}_1$ by picking the focused output of first l array elements for each subcarrier - carrier frequency combination, subarray 2 data $\mathbf{X}_2$ by picking the focused output of 2^{nd} to l+1 array elements for each subcarrier - carrier frequency combination and so on...The i^{th} subarray data is the focused output of the i^{th} to $(i+l-1)^{th}$ array elements.

8. Calculate $\mathbf{g}_i = E(\mathbf{X}_i\mathbf{r}_1^H)$ for each subcarrier - carrier frequency combination. Here, $\mathbf{r}_1^H$ is column vector consisting of the conjugate of known frequency domain pilot data of source 1 for the selected subcarrier- carrier frequency combination. In practice, one would be estimating expected value based on finite data set. The estimated

value $\hat{\mathbf{g}}_i$ given by the expression $\hat{\mathbf{g}}_i = \frac{1}{N}[\mathbf{X}_i \mathbf{r}_1^H]$ would be used in place of $\mathbf{g}_i$

9. Calculate matrix $\mathbf{G} = [\mathbf{g}_1 \cdots \mathbf{g}_M]$ for each subcarrier - carrier frequency combination.

10. Find the average of the $\mathbf{G}\mathbf{G}^H$ corresponding all frequency components. Find noise subspace of this average value

11. If columns of matrix $\mathbf{E}_N$ are the eigen vectors spanning the noise subspace of $\mathbf{G}\mathbf{G}^H$ and $\mathbf{a}(\theta)$ is the array steering vector of the subarray, then the MUSIC spectrum is given by $P(\theta) = \frac{1}{\mathbf{a}^H(\theta)\mathbf{E}_N\mathbf{E}_N^H\mathbf{a}(\theta)}$

12. Direction of arrival is determined by locating peaks in MUSIC spectrum.

3.5 Computer Experiments

In this experiment, UWB system operating at 200 Mbits/sec is chosen. This consists of 100 data subcarriers modulated with random QPSK symbols representing the coded data and 12 pilot subcarriers modulated with known data as defined in the standard [88]. The guard carriers were also included as defined in the standard. The positions of data subcarriers, pilot subcarriers and guard subcarriers are positioned at defined locations. The remaining points in the 128 point set was set to zero. The mapped subcarrier data was converted to time domain data using 128 point IFFT. This was appended with 37 zero padding bits as defined in the standard

for each symbol to make 165 sample symbol. This data is modulated to a set of hopping carrier frequencies. The set consists of 3.432GHz, 3.96GHz and 4.488GHz respectively. The system changed frequency from symbol to symbol in a cyclical fashion starting from 3.432GHz.

An antenna array with 10 elements was chosen for the experiment. The subarray size was fixed at 6 and thus giving a total of 5 subarrays. Array element spacing was chosen based on the highest frequency component. In this experiment, it was fixed at 4.8GHz. Packet size was chosen as 12000 bytes (equal to around 1500 OFDM symbols)

Four multipath signals arriving from $-40°$, $-30°$, $10°$, $20°$ was generated with equal amplitude and phase, thus creating the scenario of highly correlated multipaths. The multipath components are assumed to be reaching the antenna array through different angles of arrival with different propagation delays. This propagation delays were defined with respect to OFDM symbol boundary and is equal to the time the signal takes in reaching the reference element. The propagation delays were set to be exponentially distributed with maximum delay of 55ns. This would ensure that the encountered delay would be within the guard interval used. The propagation delay was expressed as multiples of sampling period. The baseband data was subjected to a delay corresponding to the propagation delay of the path. This was done by delaying the output baseband data by integer number of samples corresponding to the integer part of propagation delay. Sample values at these delayed sample points were made zero. The base-

band data was interpolated to calculate the signal values at new sampling instants arising because of the fractional propagation delay in reaching the elements. This newly interpolated values were appended to the initial zero valued samples. For example, if the initial delay to the reference element is 10.52 sample period for a particular path, the output baseband data would be delayed by 10 samples. This is done by making the first 10 samples of the output data equal to zero. New signal values delayed by 0.52 sample period would be calculated for all sampling instants. This new interpolated values would be appended to the zero valued samples corresponding to the integer part of the delay. The total number of samples would be limited to the original 165 samples. Additional delay with respect to the reference element was calculated for each source and this delay was added to the fractional part of the fixed delay in calculating the interpolated values of output signal samples at the remaining antenna elements.

The SNR is defined as the ratio of the path power to the noise power in each sensor element. The sensor noise power was assumed to be 1. The signal power was chosen so as to meet the desired SNR for the particular multipath. Because of the propagation delay, the output baseband signal would encounter an additional phase shift due to the phase shift of the main carrier. This is accounted by multiplying the baseband signal by an exponential term equal to $e^{-j\omega_c\tau}$. Here ω_c is the carrier frequency and τ is the propagation delay to the element. Similarly, values for other multipath signals would be calculated and added to the corresponding sensor output

values.

Three uncorrelated UWB signals arriving from $-10°$, $0°$, $40°$ were added as interferers. Each UWB interfering signal may be coming from a single source or may be the combined effect of few narrowband interferers. In this study, they are modeled as uncorrelated UWB sources. The interfering signal power was kept 10dB above the desired multipath power. The initial propagation delay of these signals were made random. The signal values for different antenna element was calculated as in the case of the desired signal.

In the receiver side, perfect synchronization was assumed. This is quite realistic scenario as the system can pick the output of the reference sensor and use conventional synchronization approaches like autocorrelation based schemes to detect the start of packet frame and the OFDM symbol boundary. Otherwise, it can have stable system reference clock. This experiment made use of the succeeding data symbols to estimate the DOA. The first 128 samples from the OFDM symbol boundary were picked and the next 32 samples were added to the first 32 samples. Remaining 5 samples were discarded. This process was repeated for each symbol. The picked 128 samples were converted to frequency domain using a 128 point FFT for each antenna element. The initial angle was estimated with conventional beamforming. Beams were formed for each direction for each of the frequencies and power of all the frequency components were summed up to get the spatial power in the direction. It is shown in Fig.3.2. It failed to

resolve the multipaths. The coarse estimated angles were $-33°$, $-2.25°$, $18.5°$, $40°$.

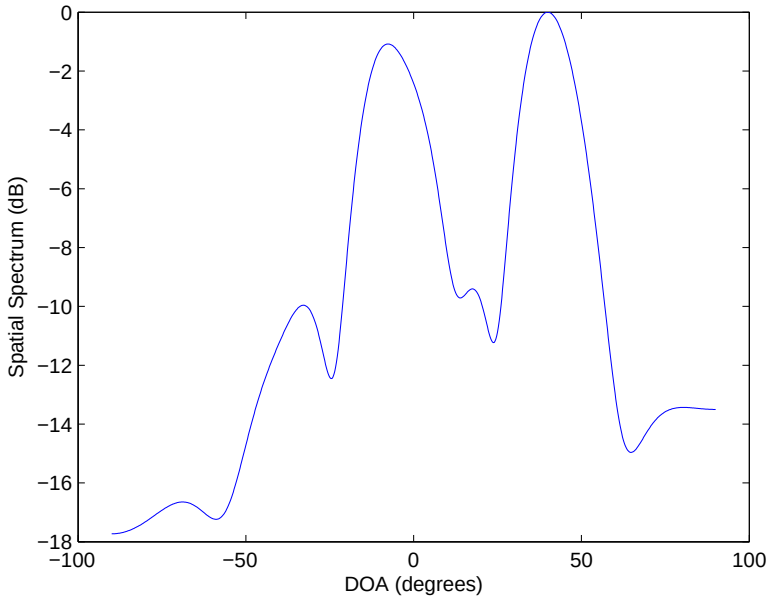

Figure 3.2: Spatial spectrum using beamforming for desired multipath at DOA of $-40°$, $-30°$, $10°$, $20°$ and interferers at DOA of $-10°$, $0°$, $40°$.

The pilot carrier location data for each symbol was separated and shifted to a common focusing frequency. Three frequencies were used in the experiment. These were 4.714875 GHz (the frequency of the pilot frequency at the upper end), 4.508625 GHz (the pilot frequency nearer to the midband of highest carrier frequency) and 3.980625 GHz (the pilot frequency nearer to the midband total bandwidth).

The array data was focussed to focussing frequency using focussing matrices defined in [38]. Focussing matrix was calculated with $\boldsymbol{\theta}$ equal to combined set of estimated angles, estimated angles $+/-0.25$ *beamwidth*

and estimated angle $+/-0.5$ *beamwidth* for each estimated direction. Beamwidth refers to the beamwidth of the subarray which is equal to 23^0. This would give an equivalent signal for each pilot frequency. The subarrays were formed as in the narrowband case for each of the translated pilot frequencies. This was correlated with the pilot signal defined in the standard for the respective pilot frequency and the associated hopping carrier frequency separately. The vector $\mathbf{g}_i$ defined in the narrowband case was calculated for each subarray and the matrix $\mathbf{G}$ was formed for each of the pilot frequency and corresponding hopping carrier frequency. The $\mathbf{GG}^H$ matrix was calculated for each frequency and the average of all $\mathbf{GG}^H$ was taken to form the total correlation matrix. The direction of arrival was determined using the conventional MUSIC analysis at the focussing frequency for the correlation matrix. The system was evaluated for 5dB to 25dB SNR at 5dB increments. The interference power was maintained at 10dB higher at all SNR. 100 Monte Carlo runs were carried out for each SNR and focussing frequency.

The computer experiments were designed to compare the performance of the new algorithm with two previous methods used for DOA estimation of wideband signals. Coherent signal subspace method (CSSM) is generally expected to handle the multipath signals. The earlier experiment was repeated with the coherent signal subspace method. The same model of data was used. The system performance was evaluated at the three focussing frequencies mentioned earlier. Instead of using only pilot subcarrier data,

the data from all subcarrier frequencies was focussed. DOA was estimated by applying conventional MUSIC algorithm for the final covariance matrix at the focussing frequency.

Spatial smoothing is the most popular subspace based approach for handling coherent signals in the narrowband case. Since spatial smoothing can't handle more than l-1 (l: Number of elements in the subarray) sources, two of the interfering signals 0°, 40° were removed. The input data was focussed to the chosen focussing frequencies. In this experiment, data from all the subcarriers were as in the case of CSSM. Subarrays with 6 elements were formed. Average smoothed covariance matrix was calculated for each focussed subcarrier frequency separately. Final covariance matrix was calculated by averaging the subarray covariance matrices corresponding to each focussed subcarrier. DOA was estimated by applying conventional MUSIC algorithm for the averaged smoothed covariance matrix at the focussing frequency. The performance comparison of these methods are done in the following paragraphs.

3.6 Discussions

The schemes are evaluated for typical operating environmental conditions. Many of the future wireless systems will have to operate in environments with inband interferers. This is especially true in the case of ultra wideband systems. They would have to encounter narrowband interferers at higher power. As shown in Fig.3.3, the proposed scheme was able to resolve the

Table 3.1: Mean DOA

SNR \ DOA	-40	-30	10	20
5	-39.09	-27.08	8.93	21.27
10	-38.89	-26.89	8.81	21.15
15	-39.04	-26.92	8.65	21.16
20	-39.03	-26.91	8.87	21.23
25	-38.98	-27.09	8.92	21.31

Table 3.2: Variance of DOA

SNR \ DOA	-40	-30	10	20
5	0.35	0.74	0.61	0.67
10	0.31	0.56	0.41	0.35
15	0.26	0.62	0.41	0.32
20	0.38	0.87	0.42	0.36
25	0.32	1.15	0.59	0.51

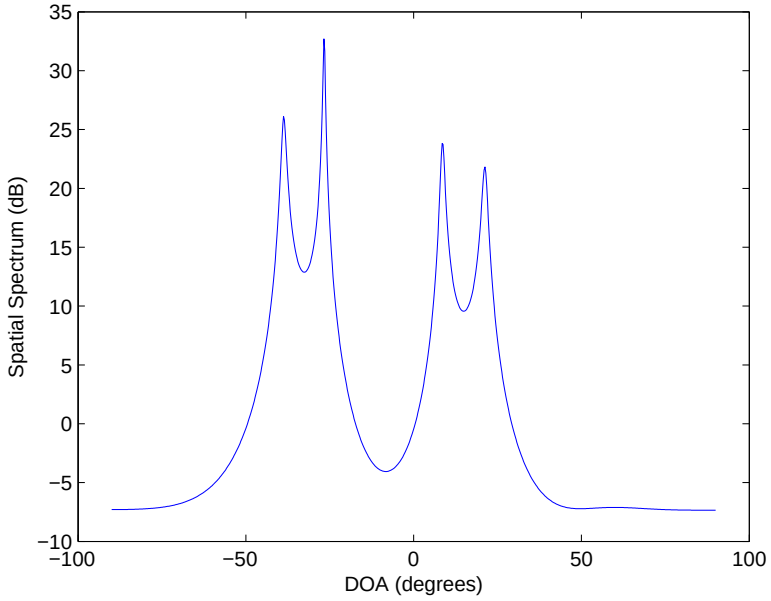

Figure 3.3: Spatial spectrum using the proposed method for desired multipath at DOA of $-40°$, $-30°$, $10°$, $20°$ and interferers at DOA of $-10°$, $0°$, $40°$.

direction of arrival of the desired multipaths with a focussing frequency of 4.714875GHz. The mean and variance of the estimated DOA's focussing frequency of 4.714875GHz are summarized in Table (3.1) and Table (3.2).

As can be seen from the tables, there is no significant variation between the DOA estimated at different SNR values. This insignificant variation in estimated DOA shows that the proposed method is quite insensitive to the input SNR. This was an expected result. Since the algorithm correlates the array output with known waveform, the effect of noise would be largely eliminated. Besides, the interference and focussing error would play the major role in determining the final error. Focussing error introduces an

irreducible bias in the DOA estimation. The presence of larger interfering signal would introduce larger error in coarse estimation and thus effect the performance.

The effect of the initial delay was an additional phase rotation to antenna array vector. Let two multipath components coming from directions θ_1 and θ_2 encounter delays τ_1 and τ_2 respectively while reaching the reference element. Let $a(\theta_i)$ be the direction vector corresponding to θ_i and ω_i be the signal frequency. If the delays are such that $e^{-j\omega_i\tau_1}a(\theta_1)$- $e^{-j\omega_i\tau_2}a(\theta_2)$ is smaller than $a(\theta_1) - a(\theta_2)$, then the scheme may fail to resolve the DOA. This is especially true when the directions of arrival and the corresponding delays are very close. This coupled with the error introduced in focussing resulted in few cases of failure in the algorithm to resolve closely spaced sources. Since the difference between the two direction vectors are larger at higher frequencies, it would be advisable to use larger focussing frequencies. In the computer experiments, the focussing frequency of 4.714875 resulted in around 3% failure. This increased to around 6% at focussing frequency 4.508625GHz. The failure rate reached around 20% at focussing frequency of 3.980625GHz. This shows that a higher frequency would be better choice in real world situations where the closely spaced signals encounter nearly equal delays.

The conventional focussing method proposed by Wang and Kaveh relies on the difference in the delay of multipath signals in resolving multipath components. If the difference in delay is small, the scheme fails to resolve

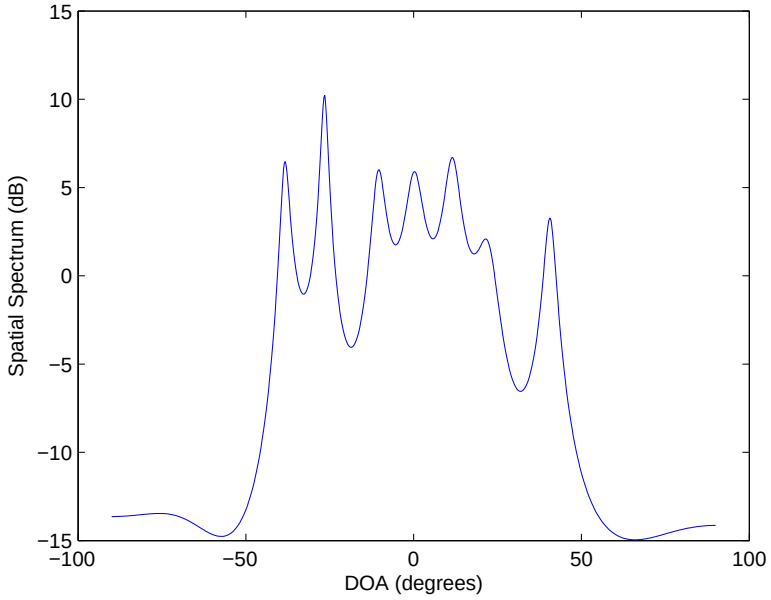

Figure 3.4: Spatial spectrum using the CSSM method for desired multipath at DOA of $-40°$, $-30°$, $10°$, $20°$ and interferers at DOA of $-10°$, $0°$, $40°$.

the multipaths. The system was evaluated for similar conditions using Kaveh's method. The scheme was evaluated at 3 focussing frequencies. The scheme mostly failed at 3.96GHz. It was successful in around 10% cases at focussing frequency of 4.508GHz. It was successful resolving the DOA around 42% cases with focussing frequency of 4.714875GHz. The resulting spatial spectrum is shown in Figure 3.4.

The mean and variance of the successful cases are given in Table (3.3) and Table (3.4). It can be seen that the bias is much higher in Kaveh method. This can be attributed to the effect of larger noise as well as the presence of un-attenuated interfering signals in the correlation matrices. It can also be seen that the bias and the variance of higher power interfering

Table 3.3: Mean DOA of CSSM

SNR \ DOA	-40	-30	-10	0	10	20	40
5	-38	-26.64	-10.34	0.38	11.72	22.86	40.65
10	-37.88	-26.73	-10.32	0.6	11.86	22.83	40.73
15	-37.93	-26.41	-10.68	0.37	11.53	22.23	40.64
20	-37.93	-26.51	-10.33	0.39	11.82	22.79	40.65
25	-38	-26.67	-10.24	0.46	12.2	22.85	40.68

Table 3.4: Variance of DOA of CSSM

SNR \ DOA	-40	-30	-10	0	10	20	40
5	0.88	1.36	0.13	0.22	1.72	2.05	0.07
10	0.6	1.13	0.10	0.14	1.32	1.38	0.05
15	0.45	1.57	0.14	0.22	2.38	0.92	0.06
20	0.56	1.70	0.07	0.10	1.45	1.35	0.4
25	0.39	0.98	0.1	0.2	1.55	2.28	0.06

signals are much smaller than the desired multipaths. This shows that the stronger interfering signal dominates the DOA estimation. Thus the proposed algorithm performs better than the conventional focussing method in two aspects. One, it is able to estimate the DOA better than conventional scheme in cases where closely spaced signals comes with closely spaced delays. Secondly, it provides better estimation of desired multipaths in the presence of stronger interferers.

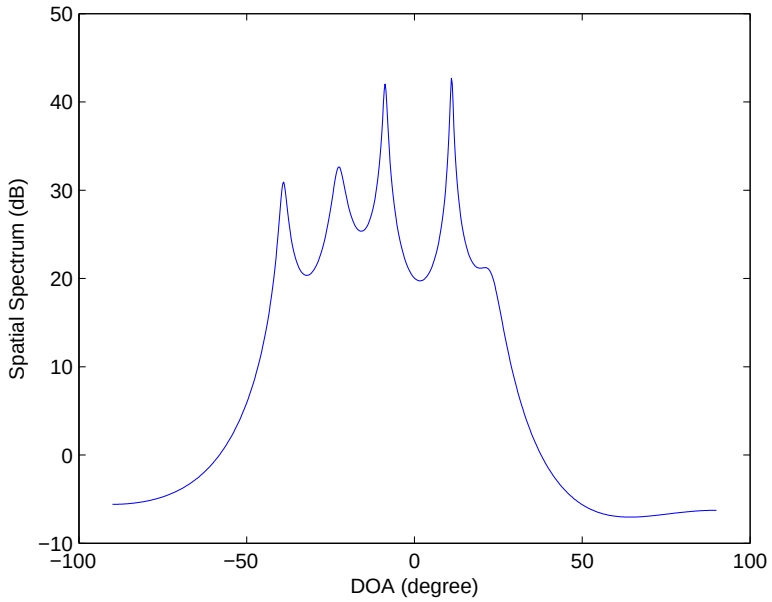

Figure 3.5: Spatial spectrum using the subarray smoothing method for desired multipath at DOA of $-40°$, $-30°$, $10°$, $20°$ and interferers at DOA of $-10°$.

The subspace smoothing was employed to enhance the rank of the source covariance matrix in coherent narrow band case. In the UWB case, the subspace smoothing was applied after focussing the different frequency com-

ponents to the common focussing frequency. Since the subspace smoothing doesn't differentiate between desired and undesired signals, the maximum number of resolvable sources was restricted by the subarray size. In the experiment, this resulted in keeping the number of interferers to just one so that the total number of sources (5) is less than subarray size. As a result, the MUSIC spectrum was calculated using just one noise space eigenvector and this resulted in poor performance. The subspace smoothing failed to resolve the DOA at focussing frequency of 3.980625 GHz. It was successful in around 10% of the cases at 4.508625GHz and 30% of cases at focussing frequency of 4.714875GHz. Thus the simulations proved the ineffectiveness of subspace smoothing in resolving multipaths in UWB case in the presence of interferers. The Figure 3.5 shows one of the successful case. The mean and variance of the successful cases are given in Table (3.5) and Table (3.6). As can be seen from the table, it shows wide fluctuations in variance due to the large number of failures and near failure cases. This is especially true for the signals coming from directions closer to the stronger interfering signal. The bias is also significantly high and hence this scheme is not really suitable. By comparing the results of the experiments using the three different methods, it is clear that the proposed scheme in this thesis performs better than the other 2. The experiments validated the superiority of the proposed scheme in handling the real world scenarios of closely spaced delays. Since it correlates the incoming data with the known reference data, the effect of noise would be less and hence this scheme is

able to handle the closely spaced delays better than other schemes for estimating the direction of arrival of coherent signals. The proposed scheme failed in less than 5% of the cases.

The mean values and variances of the estimated DOAs of the desired multipaths are plotted in Figure 3.6 and Figure 3.7.

As can be seen from the tables and graphs, the proposed algorithm provides the best performance. As mentioned earlier, when the signals coming from closer angles are coming with closely spaced initial delay from the symbol boundary, the algorithm fails. For example, if the multipath coming from -30^0 is delayed by an additional 0.1 sample period, the algorithm fails. This is quite a realistic scenario in the actual environment as closely spaced angles of arrival is likely to be due to reflections from closely spaced objects. In simulated experiments, this was not prominent when few frequency components were used. Hence this failure mechanism could be attributed to the combined effect of focussing error and the small rotation of the array vector due to this incremental arrival delay. This is true for all the algorithms. But the proposed algorithm performs better. Even when the algorithm resolves the two closely spaced signals, the resolved angles varies significantly from the mean value. This phenomenon was observed in all the three schemes. This was not observed when all multipaths reaches the reference sensor with the same delay. The proposed algorithm performed better in all the cases.

Table 3.5: Mean DOA of subarray smoothing

SNR \ DOA	-40	-30	-10	10	20
5	-38.24	-22.6	-8.76	11.53	21.45
10	-38.36	-22.25	-8.69	11.21	21.49
15	-38.62	-22.16	-8.72	11.25	21.11
20	-38.34	-22.05	-8.72	11.23	21.34
25	-38.42	-22.44	-8.70	11.30	21.45

Table 3.6: Variance of DOA of subarray smoothing

SNR \ DOA	-40	-30	-10	10	20
5	0.34	1.08	0.03	0.39	0.35
10	0.17	1.99	0.04	1.89	0.40
15	0.5	1.89	0.06	1.88	0.49
20	0.12	0.93	0.03	0.35	0.20
25	0.13	1.614	0.05	1.62	0.39

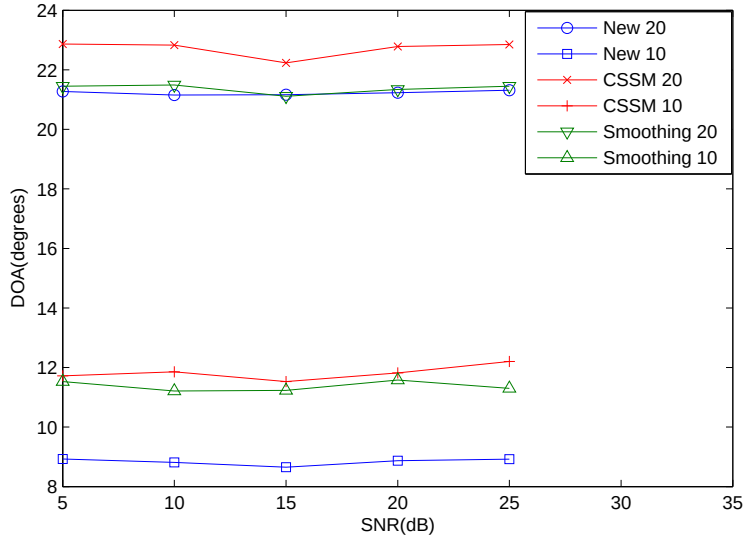

(a) 10°, 20°

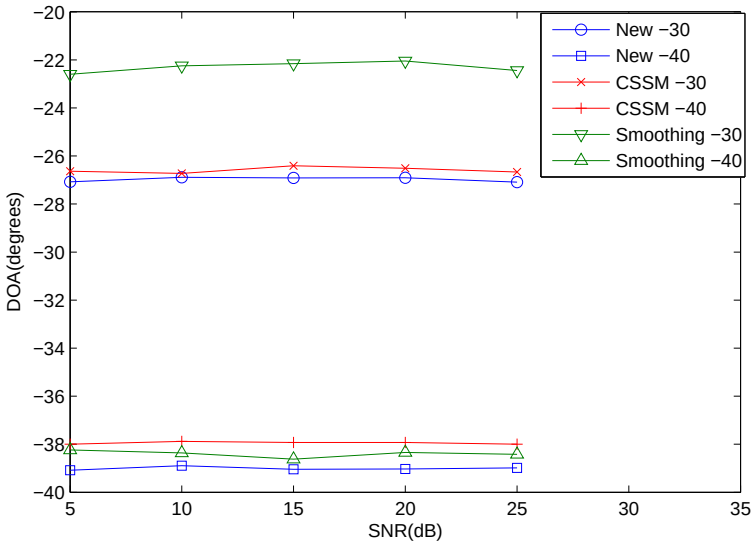

(b) −40°, −30°

Figure 3.6: Mean of estimated direction of arrival of different methods for angles of arrival of −40°, −30°, 10°, 20° and interferers at DOA −10°, 0°, 40°.

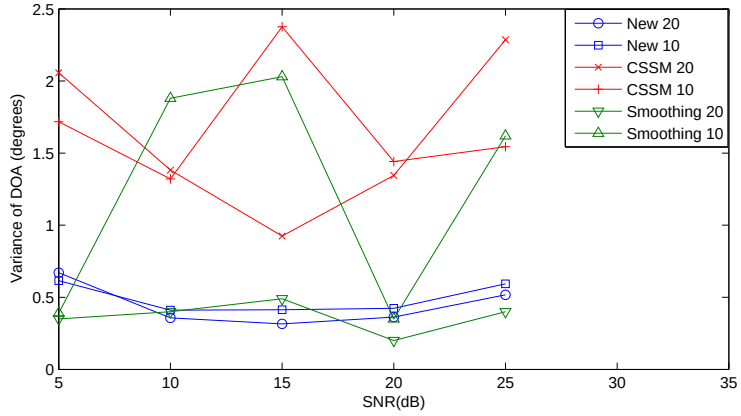

(a) 10°, 20°

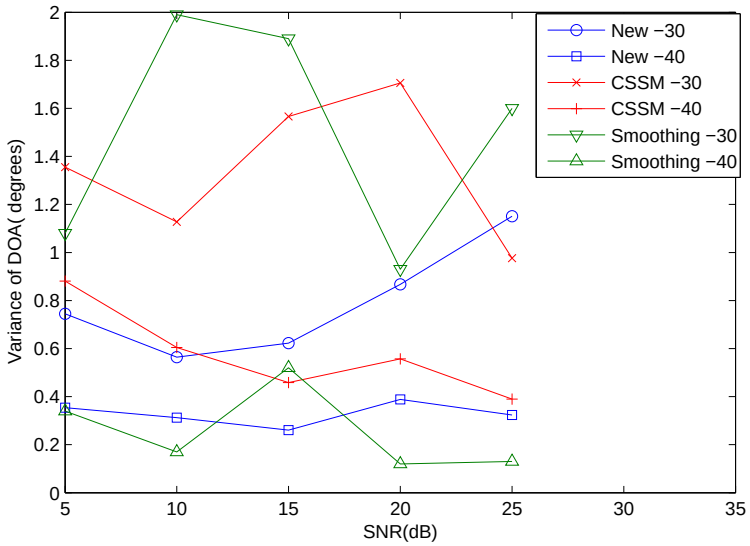

(b) −40°, −30°

Figure 3.7: Variance of estimated direction of arrival of different methods for angles of arrival of −40°, −30°, 10°, 20° and interferers at DOA −10°, 0°, 40°.

3.7 Summary

The strength of proposed method are twofold. Firstly, this method considers multipath propagation environment for UWB sources and estimates

all direction of arrival associated with the target source, in the presence of inband interferers. Secondly, this method has a less restrictive condition on the number of sensors. To estimate all the directions of arrival associated with the target source, this algorithm requires that the number of sensors to be no less than $2k_1$ where k_1 is the number of paths (directions) through which the target source signal impinges on the receiver irrespective of the number of interferers. Spatial smoothing requires the number of sensors to be larger than the total number of sources. Thirdly, the proposed algorithm handles the closely spaced signals with closely spaced delays better than the other algorithms handling coherent signals. The literature does not discuss the performance of the known algorithms in scenarios involving closely spaced signals impinging the array with closely spaced delays.

The performance of the algorithm is heavily dependent on the convergence Eqn.(3.8). One of the basic requirements is the negligible cross correlation between interfering signals and the source. The final residue signal after cross correlation would also depend on the interfering signal power. As the analysis in Chapter 4 shows, the perturbation term in matrix $\mathbf{GG}^H$ is the order of $O(N^{-1})$ compared to the $O(N^{-1/2})$ order found in the covariance matrices estimation used in conventional schemes. This gives an advantage of approximately 5dB while employing N= 100 symbols for the case of no interference. The performance in the presence of interferers would be dependent on both the cross correlation and the power of interfering signal. Hence, it is very difficult to calculate the sample

size required. In the simulated experiments, 512 symbols were used for each subcarrier and the proposed system was able to outperform the other known schemes in successfully resolving the DOA and in the accuracy of final estimated DOA with -10dB SIR. Hence it can be safely assumed that the scheme would be able to perform satisfactorily with a sample size of few hundred samples.

Chapter 4

Performance Analysis and New Focussing Technique for Reducing Bias

4.1 Introduction

This research has proposed a new algorithm for direction of arrival estimation of multipath components of WiMedia UWB signals in Chapter 3. The algorithm was proved to be superior to other known methods using simulation experiments. In this chapter, the theoretical basis for the superior performance is analyzed. The focussing operation is based on minimizing the Frobenius norm of the difference of two matrices. There is no closed form analytical expression for this Frobenius norm of difference. Hence, this analysis would make comparative study with the other known performance

studies of DOA estimation in the literature.

Many authors have analyzed the performance of MUSIC and other subspace methods. Most of these analysis is based on the asymptotic results of eigenvectors and eigenvalues provided by Anderson [3] and the gradient operator by Brandwood [13]. Anderson proved that the asymptotic mean and variance of the perturbation in eigenvectors of sampled covariance matrix is inversely proportional to the sample size N. Kaveh and Barabell [45, 46] analyzed the MUSIC for its resolution power. They provided analytical expression for the finite data performance of MUSIC for narrowband as well as the resolution threshold for two source cases. They calculated the asymptotic mean and variance of the MUSIC spectrum. In the two source case, mean and variance of the MUSIC spectrum are given by [45]

$$\overline{\hat{D}(\omega_k)} \backsimeq \sigma_n^2 \mathbf{V}^H(\omega_k) \left[\frac{\lambda_1(L-2)}{(\lambda_1-\sigma_n^2)^2} \mathbf{S}_1\mathbf{S}_1^H + \frac{\lambda_2(L-2)}{(\lambda_2-\sigma_n^2)^2} \mathbf{S}_2\mathbf{S}_2^H \right] \mathbf{V}(\omega_k)/N \quad (4.1)$$

$$\begin{aligned} var(\hat{D}(\omega_k)) \backsimeq\ & \frac{2(L-2)}{N}\sigma_n^2 \left\{ \sum_{i=1}^{2} \frac{\lambda_i}{(\lambda_i-\sigma_n^2)^2} [|\mathbf{V}^H(\omega_k)\mathbf{S}_i|^2 - |\mathbf{V}^H(\omega_k)\mathbf{S}_i|^4] \right\} \\ & - \frac{2(L-2)}{N}\sigma_n^2 \left\{ \left(\sum_{i=1}^{2} \frac{\lambda_i}{(\lambda_i-\sigma_n^2)^2} \right) |\mathbf{V}^H(\omega_k)\mathbf{S}_1\mathbf{S}_2^H\mathbf{V}(\omega_k)|^2 \right\} \end{aligned} \quad (4.2)$$

In the above equation, $\mathbf{S}_1$ and $\mathbf{S}_2$ represent the signal space eigenvectors corresponding to eigenvalues λ_1 and λ_2 respectively. N, L and σ_n^2 represent the number of samples, the number of antenna elements and noise variance respectively. $\mathbf{V}^H(\omega_k)$ represent the steering vector from direction ω_k. The resolution of the system was highly dependent on the variance of the MUSIC spectrum.

Wang and Kaveh analyzed both narrowband systems and wideband systems. They [94] provided probability of error in the detection of the number of sources and an estimation of the quality of signal subspace estimation with finite data for two source cases for narrowband sources. They introduced a quality measure for the estimated signal subspace. This measure was based on the angle between the correct signal subspace and the estimated subspace. It was defined as the mean square value of the difference between the ideal value(=1) and the cosine of the smallest angle. They derived an expression for this metric in terms of number of samples, SNR and number of elements. This metric is valid only for two sources case as there is no closed form expression for eigenvalues in the presence of multiple sources. In [95], they extended it to the wideband case using coherent signal subspace approach. Here again, the analysis is restricted to case where two closely spaced sources are involved within one beamwidth. The focussing matrix in this scenario is a diagonal matrix and and hence it is easy to analyze. Other focussing matrix are not easy to analyze. Stoica [85] did a detailed study of the behavior of MUSIC in finite data case as well as its asymptotic behavior. He also derived the expressions for the variance of the DOA estimates and studied its performance in comparison with Cramer Rao bound. Farrier et al. [30, 31] extended this analysis to second order to get better predictions in the two source cases as well as the case of correlated noise fields. Jeffries [40] extended this analysis to include the complex case. Analytical expressions are mostly derived for the case

of two sources for conventional MUSIC. Beyond this, the computation of the eigenvectors and eigenvalues are too complex to be done analytically. Lee [53] analyzed the eigenvalues and eigenvectors of covariance matrices. But the analysis is valid only in the case of group of closely spaced sources. Lee [52] and Sharman [80] analyzed the resolution threshold of two source case.

The algorithm proposed in Chapter 3 performs well when the correlation between the array output signals and known reference signals are known. This should be able to provide unbiased estimation of the direction of arrival of the multipath components from the desired source in the narrowband case. In practice, one would not be able to get the exact value of correlation between the received data and the known data. Besides, the assumption of non-correlation between undesired signal and known data also is approximate in the limited data case. The performance of the algorithm proposed in Chapter 3 would be analyzed here for the finite data case. As can be seen from above, there is no real analysis of the focussed data case for more than two sources. This is also restricted to the case where all the sources are in a single beam. The focussing operation is not mathematically tractable for cases other than all sources coming within single beam of array where a diagonal matrix is used for focussing. In all the other cases, the error introduced in focussing operation is a complex function of estimated coarse DOA, actual DOA and the frequencies involved. Hence only a qualitative analysis and simulated evaluation for specific cases would

be carried out for evaluating the performance of focussed UWB case.

4.2 Data Model

The analysis of the narrowband case is done first. p narrowband signals $\{s_1(n), s_2(n), \cdots, s_p(n)\}$ are impinging on a q element uniform linear array (ULA) from different directions $\{\theta_1, \theta_2, \cdots, \theta_p\}$. This can be narrowband signal or signal corresponding to one subcarrier of a WiMedia UWB Signal. The array output at any subcarrier frequency ω_j and carrier frequency ω_c during n^{th} OFDM symbol is a $q \times 1$ vector and is given by

$$\begin{aligned}\mathbf{X}(n, \omega_c + \omega_j) &\triangleq [X_1(n, \omega_c + \omega_j)\ X_2(n, \omega_c + \omega_j)\ \cdots\ X_q(n, \omega_c + \omega_j)]^T \\ &= \mathbf{A}(\omega_c + \omega_j)\mathbf{S}(n, \omega_c + \omega_j) + \mathbf{Z}(n, \omega_c + \omega_j) \qquad (4.3)\end{aligned}$$

Here $\mathbf{A}(\omega_c+\omega_j)$, $\mathbf{S}(n, \omega_c+\omega_j)$ and $\mathbf{Z}(n, \omega_c+\omega_j)$ are as defined in Chapter 3.

In a multipath environment, impinging signals are associated with L different sources $\{\tilde{s}_1, \cdots, \tilde{s}_L\}$, where $L \leq p$. Proposed algorithm tries to estimate the DOA of multipaths belonging to a particular target source $\tilde{s}_1$.

4.3 Proposed Algorithm

In the proposed scheme, we divide the q elements of uniform linear array into M overlapping subarrays of size $l \triangleq (q-M+1)$ with sensors $\{1, \cdots, l\}$ forming the first subarray, sensors $\{2, \cdots, l+1\}$ forming the second subarray and so on. The i^{th} subarray output is an $l \times 1$ vector obtained by

taking the i^{th} to $(i+l-1)^{th}$ entries out of $\mathbf{x}(\mathrm{n})$. For brevity, we will drop ω_j from equations and n refers to the OFDM symbol index. It can be easily verified that

$$\mathbf{x}_i(n) = \mathbf{A}_1\mathbf{D}^{(i-1)}\mathbf{s}(n) + \mathbf{z}_i(n) \quad i = 1, \cdots, M \tag{4.4}$$

where $\mathbf{A}_1$ consisting of first l rows of $\mathbf{A}$, and

$$\mathbf{D} = diag(e^{-j2\pi\frac{d}{\lambda}\sin\theta_1} \; e^{-j2\pi\frac{d}{\lambda}\sin\theta_2} \; \cdots \; e^{-j2\pi\frac{d}{\lambda}\sin\theta_p}) \tag{4.5}$$

In Chapter 3, it was shown that

$$\begin{aligned} E[\mathbf{X}_i\mathbf{r}_1] &= \mathbf{A}_1\mathbf{D}^{i-1}E[\mathbf{S}\mathbf{r}_1] \\ &= \bar{\mathbf{A}}_1\mathbf{D}_\alpha \begin{bmatrix} e^{-j2\pi\frac{d}{\lambda}(i-1)\sin\theta_1} \\ \vdots \\ e^{-j2\pi\frac{d}{\lambda}(i-1)\sin\theta_{k_1}} \end{bmatrix} i = 1, \cdots, M \end{aligned} \tag{4.6}$$

$i = 1, \cdots, M$ and $\bar{\mathbf{A}}_1$ denotes the submatrix consisting of the first k_1 columns of $\mathbf{A}_1$, $\mathbf{D}_\alpha \triangleq diag(\alpha_1 \; \cdots \; \alpha_{k_1})$ is a diagonal matrix with nonzero diagonal elements. According to theorem 3.3.1, the matrix $\mathbf{G}$ defined by the relation $\mathbf{G} \triangleq [\mathbf{g}_1 \cdots \mathbf{g}_M]$ where $\mathbf{g}_i \triangleq \mathbf{E}[\mathbf{X}_i\mathbf{r}_1^H]$, would span the same subspace as the directional vectors of the k_1 multipaths. In practice, one will have to calculate the expected values from observing finite length data. The following paragraphs will analyze the error introduced by the finite observation data.

Theorem 4.3.1. *If $\hat{\mathbf{G}}$ is the estimated value of matrix $\mathbf{G}$ by observing N data samples, the extreme fluctuations in the elements of matrix $\hat{\mathbf{G}}$ would be of the order $O(N^{-1/2})$*

Proof. Let $\mathbf{X}_i \triangleq [\mathbf{x}_i(n)\ \mathbf{x}_i(n+1) \cdots \mathbf{x}_i(n+N)]$ be the matrix formed by concatenating the i^{th} subarray output vectors during the symbols n to $n+N$. It can be shown that

$$\mathbf{X}_i = \mathbf{A}_1 \mathbf{D}^{i-1} \mathbf{S} + \mathbf{Z}_i \quad i = 1, \cdots, M \tag{4.7}$$

where

$$\mathbf{S} \triangleq \begin{bmatrix} s_1(n)\ s_1(n+1)\ \cdots\ s_1(n+N) \\ s_2(n)\ s_2(n+1)\ \cdots\ s_2(n+N) \\ \vdots \qquad \vdots \qquad \ddots \qquad \vdots \\ s_p(n)\ s_p(n+1)\ \cdots\ s_p(n+N) \end{bmatrix} \tag{4.8}$$

As stated in Chapter 3, each pilot subcarrier carries known data for channel estimation. In the proposed algorithm, we make use of this known data for estimating DOA.

One can define $\mathbf{r}_1$ as

$$\mathbf{r}_1 \triangleq [r_1(n)\ r_1(n+1)\ \cdots\ r_1(n+N)] \tag{4.9}$$

as the data carried by the pilot carrier during the selected symbols.

In the proposed algorithm, we correlate the subarray output at the pilot frequencies with this known data.

Consequently, the expectation would be replaced by sample average $\hat{\mathbf{g}}_i$

$$\hat{\mathbf{g}}_i = \frac{1}{N}[\mathbf{X}_i \mathbf{r}_1^H] \tag{4.10}$$

$$= \mathbf{A}_1 \mathbf{D}^{i-1} \frac{1}{N}[\mathbf{S}\mathbf{r}_1^H] + \frac{1}{N}[\mathbf{Z}_i \mathbf{r}_1^H] \tag{4.11}$$

In the above equation $\mathbf{r}_1$ is only correlated with first k_1 impinging signals and is uncorrelated with the remaining signals and noise.

The law of the iterated logarithm [76] gives the upper limit on the fluctuations in the mean value estimated using data of finite sample size. It states that if X_i is independent and identically distributed random variables with mean μ and finite variance σ^2. Then

$$\lim_{N\to\infty}\left[\frac{\sum_{i=1}^{N}(X_i-\mu)}{(2\sigma^2\log\log N)^{\frac{1}{2}}}\right]=1 \; \textit{with probability } 1 \tag{4.12}$$

The law implies that the bracketed quantity in Eqn.(4.12) would approach 1 with probability 1(wp 1). This implies that the sampled average of the quantity X_i given by $\frac{\sum_{i=1}^{N}X_i}{N}$ would be equal to $\mu+O(N^{-1/2})$. Thus the law of iterated algorithm imposes upper limit on the extreme fluctuations.

In the proposed algorithm, estimated mean value of the correlated quantities is based on finite sample size. Hence we can apply the law of iterated algorithm here.

By applying law of iterated logarithm, it can be proven that

$$\hat{\mathbf{g}}_i = \mathbf{A}_1\mathbf{D}^{i-1}\begin{bmatrix}\alpha_1+O(N^{-1/2})\\ \vdots \\ \alpha_{k_1}+O(N^{-1/2})\\ O(N^{-1/2})\\ \vdots \\ O(N^{-1/2})\end{bmatrix}+\begin{bmatrix}O(N^{-1/2})\\ \vdots \\ O(N^{-1/2})\\ O(N^{-1/2})\\ \vdots \\ O(N^{-1/2})\end{bmatrix} \tag{4.13}$$

$$\hat{\mathbf{g}}_i = \mathbf{A}_1\mathbf{D}_{\alpha 1}\begin{bmatrix} \phi_{1i} \\ \vdots \\ \phi_{k_1 i} \\ \phi_{(k_1+1)i} \\ \vdots \\ \phi_{pi} \end{bmatrix} + \begin{bmatrix} O(N^{-1/2}) \\ \vdots \\ O(N^{-1/2}) \\ O(N^{-1/2}) \\ \vdots \\ O(N^{-1/2}) \end{bmatrix} \tag{4.14}$$

where $\mathbf{D}_{\alpha 1}$ is a p^{th} order diagonal matrix defined by Eqn.(4.15)

$$\mathbf{D}_{\alpha 1} = \begin{bmatrix} \mathbf{D}_1 & 0 \\ 0 & \mathbf{D}_2 \end{bmatrix} \tag{4.15}$$

$\mathbf{D}_1$ and $\mathbf{D}_2$ are k_1^{th} and $(p - k_1^{th})$ order diagonal matrices defined as:

$$\mathbf{D}_1 = \begin{bmatrix} \alpha_1 + O(N^{-1/2}) & 0 & 0 \\ \vdots & \ddots & 0 \\ 0 & 0 & \alpha_{k_1} + O(N^{-1/2}) \end{bmatrix} \tag{4.16}$$

$$\mathbf{D}_2 = \begin{bmatrix} O(N^{-1/2}) & 0 & 0 \\ 0 & \ddots & 0 \\ 0 & 0 & O(N^{-1/2}) \end{bmatrix} \tag{4.17}$$

$\phi_{k_1 i}$ is defined as $e^{-j2\pi\frac{d}{\lambda}(i-1)\sin\theta_{k_1}}$.

If we take $\bar{\mathbf{A}}_1$ as the direction vector matrix of first k_1 paths and $\mathbf{A}_1^{'}$ as the matrix comprising of the remaining direction vectors in $\mathbf{A}_1$

$$\hat{\mathbf{g}}_i = \bar{\mathbf{A}}_1\mathbf{D}_1\begin{bmatrix}\phi_{1i}\\ \vdots \\ \phi_{k_1 i}\end{bmatrix} + \mathbf{A}_1^{'}\mathbf{D}_2\begin{bmatrix}\phi_{(k_1+1)i}\\ \vdots \\ \phi_{pi}\end{bmatrix} + \begin{bmatrix}O(N^{-1/2})\\ \vdots \\ O(N^{-1/2})\end{bmatrix} \tag{4.18}$$

$$= \bar{\mathbf{A}}_1\mathbf{D}_\alpha\begin{bmatrix}\phi_{1i}\\ \vdots \\ \phi_{k_1 i}\end{bmatrix} + \mathbf{A}_1\mathbf{D}_0\begin{bmatrix}\phi_{1i}\\ \vdots \\ \phi_{k_1 i}\\ \phi_{(k_1+1)i}\\ \vdots \\ \phi_{pi}\end{bmatrix} + \begin{bmatrix}O(N^{-1/2})\\ \vdots \\ O(N^{-1/2})\end{bmatrix} \tag{4.19}$$

Here $\mathbf{D}_0$ is a diagonal matrix consisting of terms of $O(N^{-1/2})$ as diagonal elements. For $N \gg p$, this can be approximated as

$$\hat{\mathbf{g}}_i = \bar{\mathbf{A}}_1\mathbf{D}_\alpha\begin{bmatrix}\phi_{1i}\\ \vdots \\ \phi_{k_1 i}\end{bmatrix} + O(N^{-1/2}) \tag{4.20}$$

This can be extended to the matrix $\mathbf{G}$ defined in Chapter 3. $\mathbf{G}$ is formed by concatenating $\hat{\mathbf{g}}_i$'s from different arrays. Instead of expectation, we use the

sample average and the new sample average based $\hat{\mathbf{G}}$ is defined as follows,

$$\hat{\mathbf{G}} = [\hat{\mathbf{g}}_1 \cdots \hat{\mathbf{g}}_M] \tag{4.21}$$

$$= \bar{\mathbf{A}}_1 \mathbf{D}_\alpha \begin{bmatrix} 1 & e^{-j2\pi\frac{d}{\lambda}\sin\theta_1} & \cdots & e^{-j2\pi\frac{d}{\lambda}(M-1)\sin\theta_1} \\ \vdots & \vdots & \ddots & \vdots \\ 1 & e^{-j2\pi\frac{d}{\lambda}\sin\theta_{k_1}} & \cdots & e^{-j2\pi\frac{d}{\lambda}(M-1)\sin\theta_{k_1}} \end{bmatrix} + O(N^{-1/2}) \tag{4.22}$$

$$= \bar{\mathbf{A}}_1 \mathbf{D}_\alpha \mathbf{B} + O(N^{-1/2}) \tag{4.23}$$

$$= \mathbf{G} + O(N^{-1/2}) \tag{4.24}$$

The $O(N^{-1/2})$ term consists of the random contributions from the uncorrelated sources, input noise and the fluctuations in sample correlation. The elements of this matrix can be assumed to be a Gaussian random variable of $O(N^{-1/2})$. □

According to theorem 3.3.1, the matrix $\mathbf{G}$ would span the same subspace as column vectors of $\bar{\mathbf{A}}_1$. Hence eigenvectors of $\mathbf{G}\mathbf{G}^H$ would span the same subspace as the direction vectors.

Theorem 4.3.2. *The fluctuation in eigenvectors of $\hat{\mathbf{G}}\hat{\mathbf{G}}^H$ would be of order $O(N^{-1})$*

Proof. In conventional subspace processing, (for example [74]) one estimates the sample covariance matrix $\hat{\mathbf{R}}_x$ of the array as shown in Eqn.(4.25)

$$\hat{\mathbf{R}}_x = \frac{1}{N}\sum_{i=1}^{N} \mathbf{X}_i \mathbf{X}_i^H \tag{4.25}$$

The estimated covariance matrix is related to true covariance matrix by the relation [30]

$$\hat{\mathbf{R}}_x = \mathbf{R}_x + \rho\mathbf{Q} \tag{4.26}$$

In Eqn.(4.26), $\mathbf{Q}$ is a random perturbation matrix and ρ is equal to $N^{-1/2}$.

Similarly, one can express $\hat{\mathbf{G}}\hat{\mathbf{G}}^H$ as

$$\hat{\mathbf{G}}\hat{\mathbf{G}}^H = \mathbf{G}\mathbf{G}^H + \rho_1\mathbf{Q}_1 \tag{4.27}$$

Here, $\mathbf{Q}_1$ is a random perturbation matrix and ρ_1 is equal to N^{-1}.

By using the perturbation analysis given in [100], one can show that the eigenvectors $\hat{\mathbf{e}}_i$ of $\hat{\mathbf{R}}_x$ is related to the true eigenvectors $\mathbf{e}_i$ of actual $\mathbf{R}_x$ by the Eqn.(4.28)

$$\hat{\mathbf{e}}_i = \mathbf{e}_i + O(N^{-1/2}) \tag{4.28}$$

Similarly, the eigenvectors $\hat{\mathbf{v}}_i$ of $\hat{\mathbf{G}}\hat{\mathbf{G}}^H$ is related to the true eigenvectors $\mathbf{v}_i$ of $\mathbf{G}\mathbf{G}^H$ by the Eqn.(4.29)

$$\hat{\mathbf{v}}_i = \mathbf{v}_i + O(N^{-1}) \tag{4.29}$$

□

Comparing Eqn.(4.28) and Eqn.(4.29), one can see that the perturbations in eigenvectors in the proposed algorithm is smaller compared to the conventional systems and hence it provides more accurate results for single frequency case.

4.4 Comparison with spatial smoothing

The proposed algorithm's performance can be compared with spatial smoothing scheme for the determining the DOA of coherent sources. In spatial smoothing scheme, subarrays are formed as in the proposed algorithm. Let $\mathbf{X}_i \triangleq [\mathbf{x}_i(n)\ \mathbf{x}_i(n+1) \cdots \mathbf{x}_i(n+N)]$ be the matrix formed by concatenating the i^{th} subarray output vectors at during the symbols n to n+N. It can be shown that

$$\mathbf{X}_i = \mathbf{A}_1 \mathbf{D}^{i-1} \mathbf{S} + \mathbf{Z}_i \quad i = 1, \cdots, M \tag{4.30}$$

Where M is the number of subarrays. Covariance of individual subarrays are calculated and averaged. The averaged covariance is given by Eqn.(4.31)

$$\hat{\mathbf{R}}_x^f = \frac{1}{M} \sum_{i=1}^{M} \mathbf{X}_i \mathbf{X}_i^H \tag{4.31}$$

$$\hat{\mathbf{R}}_x^f = \frac{1}{M} (\mathbf{X}_1 \mathbf{X}_1^H + \mathbf{X}_2 \mathbf{X}_2^H + \cdots + \mathbf{X}_M \mathbf{X}_M^H) \tag{4.32}$$

By substituting the values of $\mathbf{X}_1, \mathbf{X}_2, \cdots, \mathbf{X}_3$ in the above equation,

$$\begin{aligned} \hat{\mathbf{R}}_x^f = \frac{1}{M} (&\mathbf{A}_1 \mathbf{S}\mathbf{S}^H \mathbf{A}_1^H + \mathbf{Z}_1 \mathbf{Z}_1^H + \mathbf{A}_1 \mathbf{D}\mathbf{S}\mathbf{S}^H \mathbf{D}^H \mathbf{A}_1^H + \mathbf{Z}_2 \mathbf{Z}_2^H + \cdots + \\ &\mathbf{A}_1 \mathbf{D}^{M-1} \mathbf{S}\mathbf{S}^H (\mathbf{D}^{M-1})^H \mathbf{A}_1^H + \mathbf{Z}_M \mathbf{Z}_M^H) \end{aligned} \tag{4.33}$$

$$\hat{\mathbf{R}}_x^f = \frac{\mathbf{A}_1 [\mathbf{S}\mathbf{S}^H + \mathbf{D}\mathbf{S}\mathbf{S}^H \mathbf{D}^H + \cdots + \mathbf{D}^{M-1} \mathbf{S}\mathbf{S}^H (\mathbf{D}^{M-1})^H] \mathbf{A}_1^H + \sum_{i=1}^{M} \mathbf{Z}_i \mathbf{Z}_i^H}{M} \tag{4.34}$$

Similarly,

$$Mean(\hat{\mathbf{G}} \hat{\mathbf{G}}^H) = \frac{1}{M} \sum_{i=1}^{M} \hat{\mathbf{g}}_i \hat{\mathbf{g}}_i^H$$

$$Mean(\hat{\mathbf{G}}\hat{\mathbf{G}}^H) = \frac{1}{M}(\mathbf{A}_1[\mathbf{S}_1\mathbf{S}_1^H + \mathbf{D}\mathbf{S}_1\mathbf{S}_1^H\mathbf{D}^H + \cdots + \mathbf{D}^{M-1}\mathbf{S}_1\mathbf{S}_1^H(\mathbf{D}^{M-1})^H]\mathbf{A}_1^H) + \frac{1}{M}(\sum_{i=1}^{M}\mathbf{Z}_{1i}\mathbf{Z}_{1i}^H) \quad (4.35)$$

Here,

$$\mathbf{S}_1 = \frac{1}{N}\mathbf{S}\mathbf{r}_1^H \quad (4.36)$$

$$\mathbf{Z}_{1i} = \frac{1}{N}\mathbf{Z}_i\mathbf{r}_1^H \quad (4.37)$$

Comparing Eqn.(4.34) and Eqn.(4.35), one can see that $\hat{\mathbf{R}}_x^f$ and mean value of $(\hat{\mathbf{G}}\hat{\mathbf{G}}^H)$ are similar. Mean $(\hat{\mathbf{G}}\hat{\mathbf{G}}^H)$ can be substituted for $\hat{\mathbf{R}}_x^f$ into the results of Pillai [67] and Kwon [51] on the performance of the spatial smoothing scheme. The performance of new scheme would be better owing to the reduced perturbations in $\mathbf{S}_1$ and $\mathbf{Z}_{1i}$. Besides, the new scheme would also be able to detect the DOA of coherent paths even in the presence of larger inband interferers.

4.5 Performance of UWB

In the case of UWB systems, the objective is to combine the subspaces at different frequency bins to improve the SNR. Since the subspaces at different frequencies are different, they will have to be aligned. Otherwise they will be spanning the entire space. Focussing was proposed for aligning the subspaces. Schemes proposed by Wang [92] and Hung [38] makes use of coarse estimation of angles for estimating the focussing matrices. The focussing also makes the averaged source covariance matrix nonsingular in most of the situations. Another well known problem with focussing is

related to the bias introduced by focussing [27]. The focussing operation basically minimizes Frobenius norm of the difference between the array matrix at focussing frequency and the focussed array matrix corresponding to another frequency. The proposed focussing matrices introduces a deterministic error based on coarse estimated DOA, actual DOA and the frequencies. This would be multiplied by a factor depending on the initial delay. This error components would combine to produce bias and large fluctuations in estimated DOA. In typical short range environments, where initial path delays are very close, the averaged covariance matrix is close to singular and as a result fails to resolve closely spaced paths. Even though it resolves multipaths, performance degrades with variation in multipath power. In the presence of inband interferers with higher power, the performance degrades significantly.

4.6 New Focussing Scheme

In previous section, it was shown that the conventional focussing scheme results in significant bias in the final estimate. This bias is a function of the error in coarse estimation as well as the focussing frequency. The bias also increases when the signal bandwidth increases [49], [86], [27].

To avoid any ambiguity in DOA estimation, the interelement spacing of the arrays is taken to be equal to the half wave length of the highest frequency component. Simulation showed that the bias and failure due to closely spaced delays are reduced when focussing frequency is chosen nearer

to the array centre frequency. Hung and Kaveh [38] proposed a class of focussing matrices with unitary characteristics. Still the performance suffers in typical environments with very small delay spreads between closely spaced paths.

In some UWB operations, one may encounter only few narrowband interferers. In some other operations, two nets would be operating at shorter distances apart. The objective of this work is to explore new schemes to combine the subspaces to reduce the estimation bias under such circumstances.

Most of the algorithms proposed after Wang and Kaveh proposed coherent signal subspace processing [92], were exploring means for reducing the bias due to coarse estimation. [37] proposes an algorithm for estimating focusing matrices without coarse estimation of DOA. The drawback of the algorithm is the computational complexity.

Valaee and Kabal [89,90] studied the optimum focusing subspace for coherent signal subspace processing and on selection of focussing frequency. They propose suboptimum methods based on maximizing the singular values of array matrix under certain constraints. The scheme is computationally complex and of limited value as this is also highly depended on the coarse DOA estimation.

Hung and Mao [39] had proposed choosing the focussing matrix based on minimizing the error between the transformed source representation space (defined as $\mathbf{A}(\boldsymbol{\theta}, \omega_j)\mathbf{A}^H(\boldsymbol{\theta}, \omega_j)$) at the given frequency and at focussing

frquency. The source representation space is a better approximation to the array manifold around the estimated DOA. They provided better performance and less sensitivity to variations in coarse DOA estimates.

Sellone [75] proposes an iterative method for focussing without prior estimation of coarse DOA. An initial focussing matrix is designed by minimizing the Frobenius norm of the difference between array vectors at the chosen frequency and the focussing frequency over the entire observation space. This is used to focus the observed data and the data is used as in conventional CSSM to estimate the DOA. This DOA is used in further iteration for calculating the focussing matrix and the interval of focussing is reduced in each iteration concentrating on minimizing the error around the DOA estimated in previous iteration. Computational complexity of the system is main drawback of the proposed method.

The above works all point to differing algorithms aims at reducing the bias in the DOA estimation due to focussing. As mentioned earlier most of the algorithms are computationally complex and will have to be done in real time. In the earlier chapter also, the proposed algorithm using conventional focussing introduced irreducible bias. Besides, the algorithm's sensitivity towards the closer delays between paths at closer angles of arrival is also very high. Hence, the next section look at new focussing scheme targeted at reducing this sensitivity.

4.7 Data Model

In this work, we use the same system model used in Chapter 3. The system consists of multiple UWB sources conforming to the WiMedia UWB standard [88]. Consider p UWB signals $\{s_1(n), s_2(n), \cdots, s_p(n)\}$ impinging on a q element uniform linear array (ULA) from different directions $\{\theta_1, \theta_2, \cdots, \theta_p\}$. Out of this p sources, k_1 belongs to the target source and remaining are uncorrelated interfering signals coming from another net at a lower power level.

4.8 Proposed Scheme

In the proposed schemes in previous chapter, the q elements of uniform linear array is divided into M overlapping subarrays of size $l \triangleq (q-M+1)$ with sensors $\{1, \cdots, l\}$ forming the first subarray, sensors $\{2, \cdots, l+1\}$ forming the second subarray and so on. The i^{th} subarray output is an $l \times 1$ vector obtained by taking the i^{th} to $(i+l-1)^{th}$ entries out of $\mathbf{x}$(n). Since transmit data is known only for pilot carrier frequencies, we form subarrays for pilot carriers corresponding to each hopping carrier frequency. Let $\mathbf{X}_i \triangleq [\mathbf{x}_i(n)\ \mathbf{x}_i(n+1) \cdots \mathbf{x}_i(n+N)]$ be the matrix formed by concatenating the i^{th} subarray output vectors at different symbols for carrier frequency ω_c and subcarrier frequency ω_j. One can define $\mathbf{r}_1$ as $\mathbf{r}_1 \triangleq [r_1(n)\ r_1(n+1)\ \cdots\ r_1(n+N)]^H$ as the frequency domain pilot data corresponding to the chosen subcarrier and main carrier at the chosen symbol periods. Let $\mathbf{g}_i \triangleq \mathbf{E}[\mathbf{X}_i \mathbf{r}_1]$. One can define a new matrix $\mathbf{G} = [\mathbf{g}_1 \cdots \mathbf{g}_M]$

by concatenating the $\mathbf{g}_i's$ corresponding to the different subarrays for each pilot carrier. According to theorem 3.3.1, matrix $\mathbf{G}$ will span the column space of matrix formed by the subarray vectors corresponding to the DOA of multipaths of the desired UWB signal. Similarly one can calculate the matrix $\mathbf{G}$ for the other pilot frequencies as well. It is to be noted that these matrices would span the subspaces corresponding to the direction of arrival at the respective pilot frequency-carrier frequency combination. The algorithm combines these subspaces after aligning those by premultiplying it with focussing matrices.

Hung and Kaveh [38] proposed rotational signal subspace focussing matrix by minimizing the Frobenius norm of the difference matrix obtained by subtracting the focussed array matrix at frequency ω_j from the array matrix at focussing frequency ω_0. It was also proven in [38] that the focussing matrix $\mathbf{T}(\omega_j)$ is given by $\mathbf{V}\mathbf{U}^H$, where $\mathbf{U}$ and $\mathbf{V}$ are left and right singular vectors of the matrix product $\mathbf{A}(\omega_j, \boldsymbol{\alpha})\mathbf{A}^H(\omega_0, \boldsymbol{\alpha})$. Here $\boldsymbol{\alpha}$ represents a set of preselected angles derived from the preliminary estimated angles. This preliminary coarse estimation is done by conventional beamforming and this results in estimation errors and thus introduces error in final estimation as well.

Let $\omega_{c,j}$ represents the actual frequency $\omega_c + \omega_j$. According to theorem 3.3.1, $\mathbf{G}(\omega_{c,j})$ spans the same subspace as $\mathbf{A}(\omega_{c,j})$. The basic principle of the new scheme is that one can align $\mathbf{G}$ matrices at different frequencies to a common frequency instead of aligning the array direction matrices $\mathbf{A}$.

Thus by using **G** matrices, one can eliminate the need for coarse angle estimation and its associated errors. To align G matrices, a new focussing matrix $\mathbf{T}(\omega_{c,j})$ given by $\mathbf{V}\mathbf{U}^H$, where **U** and **V** are left and right singular vectors of the matrix product $\mathbf{G}(\omega_{c,j})\mathbf{G}^H(\omega_{0,i})$ based on the focussing principle in [38] by minimizing the Frobenius norm of the difference of the two G matrices at two different frequencies. Here $\omega_{0,i}$ is the focussing frequency. To minimize the overall error, frequency nearer to the array centre frequency was chosen as the focussing frequency. Hence the direction of arrival can be determined using the conventional MUSIC analysis at the focusing frequency for the focussed correlation matrix.

Algorithm 4.1

1. Sample the outputs from array elements at the defined sampling rate. The samples corresponding to the selected carrier frequencies are grouped (based on the hopping sequences) and converted into frequency domain.

2. Form subarray 1 data $\mathbf{X}_1$ by picking the output of first l array elements, subarray 2 data $\mathbf{X}_2$ by picking the output of 2^{nd} to l+1 array elements for each subcarrier - carrier frequency combination and so on.... The i^{th} subarray data is the output of the i^{th} to $(i+l-1)^{th}$ array elements.

3. Calculate $\mathbf{g}_i = E(\mathbf{X}_i\mathbf{r}_1^H)$ for each subcarrier - carrier frequency combination. Here, $\mathbf{r}_1^H$ is column vector consisting of the conjugate

of known frequency domain pilot data of source 1 for the selected subcarrier- carrier frequency combination. In practice, one would be estimating expected value based on finite data set. The estimated value $\hat{\mathbf{g}}_i$ given by the expression $\hat{\mathbf{g}}_i = \frac{1}{N}[\mathbf{X}_i \mathbf{r}_1^H]$ would be used in place of $\mathbf{g}_i$

4. Calculate $\mathbf{G}(\omega_{c,j}) = [\mathbf{g}_1(\omega_{c,j}) \cdots \mathbf{g}_M(\omega_{c,j})]$ for each carrier frequency ω_c and pilot frequency ω_j.

5. Pick one of the $\mathbf{G}(\omega_{c,j})$ near the centre as $\mathbf{G}(\omega_{0,i})$

6. $\mathbf{T}(\omega_{c,j}) \triangleq \mathbf{V}\mathbf{U}^H$, where $\mathbf{U}$ and $\mathbf{V}$ are left and right singular vectors of the matrix product $\mathbf{G}(\omega_{c,j})\mathbf{G}^H(\omega_{0,i})$.

7. $\mathbf{G}(\omega_{c,j})$ at each subcarrier ω_j is translated to a common focussing frequency $\omega_{0,i}$ by pre-multiplying it with corresponding focussing matrix $\mathbf{T}(\omega_{c,j})$.

8. Find noise subspace of the average of $\mathbf{T}(\omega_{c,j})\mathbf{G}(\omega_{c,j})\mathbf{G}^H(\omega_{c,j})\mathbf{T}^H(\omega_{c,j})$ over all ω_c and ω_j.

9. Estimate DOA using conventional MUSIC techniques using the noise subspace estimated in previous step.

4.9 Computer Experiments

In the experiment, UWB system operating at 200 Mbits/sec is chosen. Four multipath signals arriving from $-40°$, $-30°$, $10°$, $20°$ was generated with

equal amplitude and phase, thus creating the scenario of highly correlated multipaths. Three uncorrelated UWB signals arriving from -10° , 0°, 40° were added as interferers. The desired signals were modeled as arriving with exponentially distributed delay and interferers were assumed to be arriving with random delays at the array. The SNR is defined as the ratio between the power in each multipath component reaching an antenna element and the noise in the element. In the current simulation, all multipath components are assumed to be having equal SNR. The signal to interference ratio for each interferer was fixed at 15dB. Packet size was chosen as 12000bytes. As explained in Chapter 3, the receiver achieves synchronization by making use of the preamble transmitted at the beginning of the transmission. This synchronization would determine the starting point of the OFDM symbol boundary. The array signal was processed as explained in Chapter 3. The pilot carrier location data for each symbol was separated and were correlated with the respective pilot data. The matrix $\mathbf{G}$ defined in algorithm 4.1 was formed for each pilot frequency. The system was evaluated for focussing frequencies of 3.980625GHz, 4.508625GHz and 4.714875GHz. The focussing matrix was calculated as explained in algorithm 4.1. Focused $\mathbf{G}\mathbf{G}^H$ was calculated for each translated pilot frequency and their average was found to calculate the final focussed average $\mathbf{G}\mathbf{G}^H$. This was analyzed using conventional MUSIC techniques to find DOA.

To compare the performance, the same system was evaluated with original focussing matrix as proposed by Hung [38] for 15dB signal to inter-

ference ratio as explained in algorithm 3.1. The system was evaluated for 5dB to 25dB SNR at 5dB increments. 100 Monte Carlo runs were carried out for each SNR for both the cases.

The new focussing scheme was evaluated for its suitability for narrow-band interferences. For this, an interferer was created at same angle for one of the pilot subcarrier frequencies for each main carrier with power 5dB more than the desired multipath power. The focussing scheme was evaluated for data sizes of 12000 bytes and 32000bytes.

4.10 Discussions

Both the new focussing scheme as well as the conventional scheme was able to estimate the direction of arrival. In this case, one is trying to align subspaces corresponding to frequencies spanning from approximately 3.1GHz to 4.8 GHz. Hence, the approximation error would be minimum when the subspaces corresponding to frequencies nearer to the centre of the band is chosen as focussing subspace. It is known that the spacing between the steering vectors would be larger for frequencies closer to array centre frequency. Hence, the frequencies in the upper band would be better as focussing frequency. This was validated in the computer experiments. The focussing frequencies of 3.980625GHz and 4.508625GHz performed better than 4.714875GHz, thus confirming our empirical observation. Focussing at 4.508GHz provided the best performance under random delay to the reference element. The conventional scheme performs better when the dif-

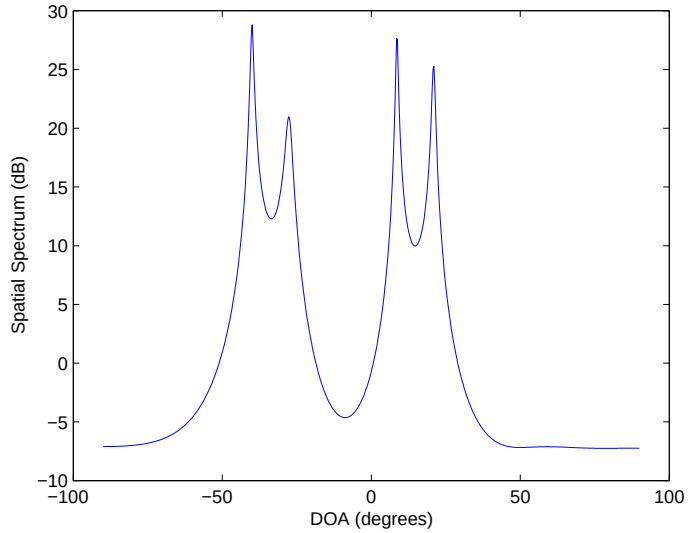

(a) Spatial spectrum old

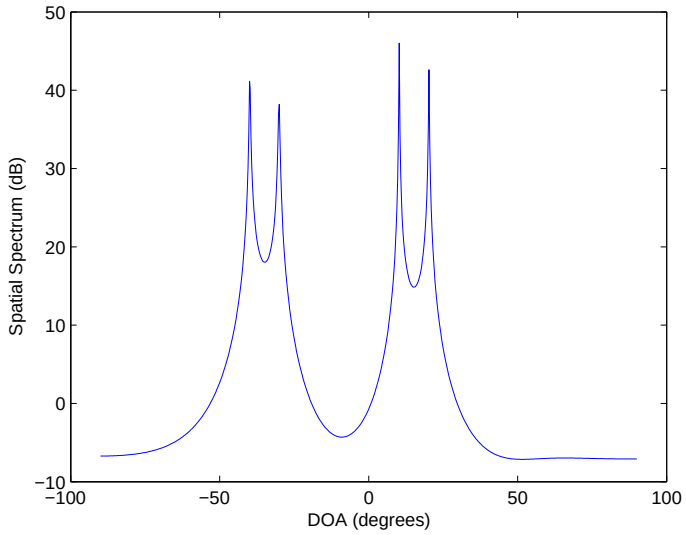

(b) Spatial spectrum new

Figure 4.1: Spatial spectrum of estimated direction of arrival of the two focussing methods for angles of arrival of $-40°$, $-30°, 10°$, $20°$ with low level interferers.

ference in steering vectors are maximum. Hence focussing frequency of 4.714875GHz was used for the conventional case. The spatial spectrum for both cases are shown in Figure 4.1. Figures 4.2 and 4.3 shows the mean and variances of the estimated DOAs by using the new focussing scheme.

The Tables 4.1 and 4.2 lists the mean and variances of DOA estimation using the new focussing matrix. As seen from the figures and the table, the new focussing scheme provides almost bias free estimation of DOA with very low variance. The scheme is also less sensitive to the random delay to the reference element.

Table 4.1: Mean DOA

SNR \ DOA	-40	-30	10	20
5	-39.94	-30.11	9.95	19.95
10	-39.97	-30.03	10	19.97
15	-40	-30.03	10.06	20.03
20	-40.06	-30.04	10	20.04
25	-40.01	-29.99	10	20.03

The system was evaluated for narrowband interference with 5 dB more power than the desired multipath. The new focussing scheme could not separate the sources with 12000 bytes. With increased sample size of 32000bytes, it was able to resolve the multipath DOAs under stronger interference. The higher power interference would increase the difference

Table 4.2: Variance of DOA

SNR \ DOA	-40	-30	10	20
5	0.24	0.25	0.12	0.16
10	0.14	0.14	0.10	0.11
15	0.11	0.13	0.10	0.1
20	0.09	0.13	0.09	0.09
25	0.09	0.10	0.07	0.07

Table 4.3: Mean DOA under narrowband interference

SNR \ DOA	-40	-30	10	20
5	-40.14	-30.06	10.06	19.96
10	-40.02	-30.07	10.02	20
15	-40	-29.93	10.08	20.02
20	-39.97	-30.08	10.05	19.99
25	-40.04	-30.05	10.02	20.02

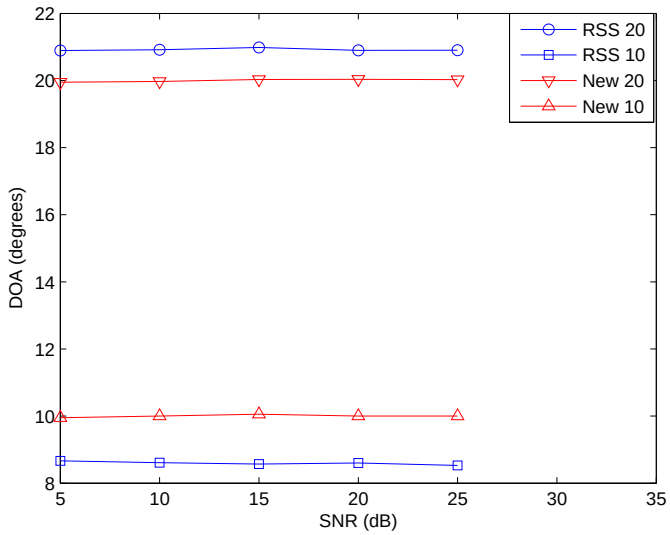

(a) 10°, 20°

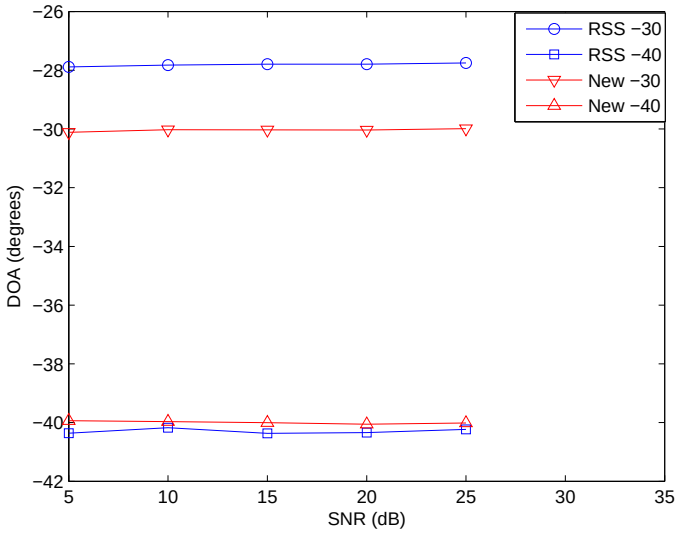

(b) −40°, −30°

Figure 4.2: Mean of estimated direction of arrival of different focussing for angles of arrival of −40°, −30°, 10°, 20° and interferers at DOA −10°, 0°, 40°.

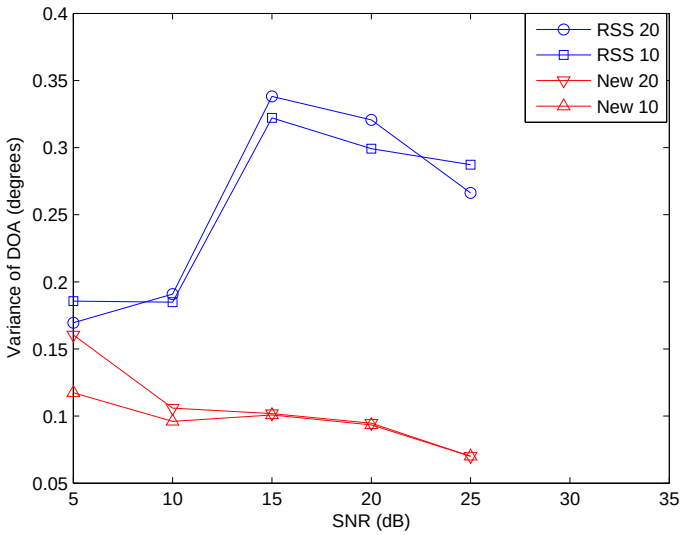

(a) 10°, 20°

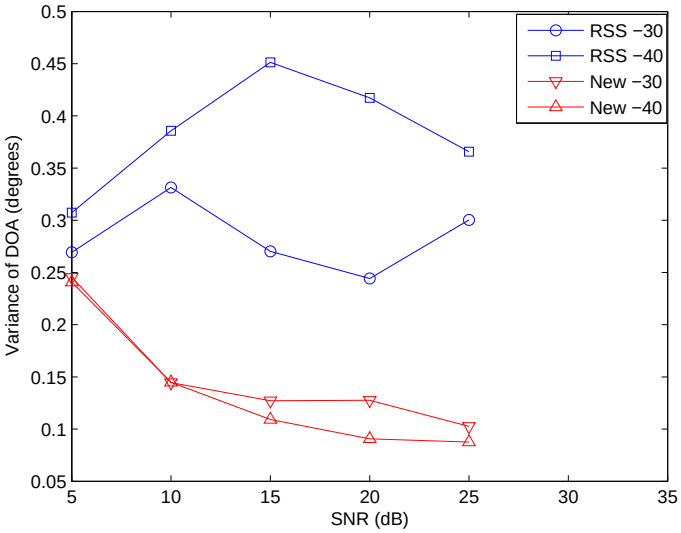

(b) −40°, −30°

Figure 4.3: Variance of estimated direction of arrival of different methods for angles of arrival of −40°, −30°, 10°, 20° and interferers at DOA −10°, 0°, 40°.

between signal subspace and the matrix **G** . This results in failure of the focussing scheme for lower data size. By increasing data size, one would be reducing the error by correlating over larger sample size. This results in closer approximation of the signal subspace by the matrix **G**. This explains the better result with larger data size. This also shows that one would be able to increase the data size and achieve accurate DOA estimation of UWB signals using the new focussing scheme. The results are summarized in Tables 4.3 and 4.4

Table 4.4: Variance of DOA under narrowband interference

SNR \ DOA	-40	-30	10	20
5	0.44	0.64	0.23	0.12
10	0.27	0.33	0.10	0.07
15	0.24	0.37	0.2	0.10
20	0.36	0.49	0.21	0.12
25	0.27	0.4	0.15	0.08

4.11 Summary

In this chapter, it is proven that the proposed algorithm provide more accurate estimation than conventional schemes. As shown in the previous paragraphs, the new algorithm performs better than other algorithms owing to the smaller fluctuations in the eigenvectors of the newly formed

matrix **G**, whose column space represent the signal subspace. Besides, the proposed algorithm also perform well in the presence of inband interferers.

One of the main limitation of the conventional focussing schemes like proposed in [38] were the bias introduced by the coarse estimation of DOA. The performance of this algorithms also degraded in the case of closely spaced delays for closely spaced sources. A new focussing scheme was proposed in this thesis to overcome these limitations. The strength of the proposed focussing scheme are fourfold. Firstly, the new focussing scheme eliminates the need for the preliminary coarse estimation of the DOA. This will reduce the processing requirements for the initial coarse estimation of DOA. Secondly, any error in coarse estimation translates to bias in final estimation. This error increases when sources are having different power and wide bandwidth. Even though this bias can be eliminated through an iterative process, the computational complexity of those methods are excessive. In fact, Sellone [75] has proposed such a technique. The main drawback of the system was the computational complexity. When focussing is used to exploit the wideband data to improve the detection threshold, these iterations involved computation of focussed data iteratively. One can't be sure about the number of iterations required to achieve this. On the other hand, the proposed focussing scheme achieves this in a single step, saving lot of computations. The proposed method eliminates the bias in final estimate with lesser computational complexity. Thirdly, conventional focussing methods fails to resolve sources when closely spaced sources arrives

with narrow delay spreads seen in typical short range environments. The proposed scheme doesn't suffer from this drawback. And finally, the effect of strong interferers is also reduced. The new focussing scheme can handle both narrowband as well as broadband interference scenarios. The new focussing scheme can also be employed in environments with no interference. This would be similar to the the low interference case and the new focussing scheme would achieve negligible bias and low variance in estimated DOA.

The proposed scheme can be implemented directly using DSP based processors or FPGAs. The complexity of the proposed algorithm is less than the complexity of large FFT blocks used in DAB like systems. Besides, matrix inversion operation used in the proposed scheme also handles relatively smaller matrices, and hence can be implemented using existing processors/ FPGAs. Since these devices are operating in slow changing environments, the estimation of direction of arrival needs to be done only at long intervals. Hence the processing may be done in commercial DSPs in such systems.

One of the weakness of most of the array processing schemes is the complexity of the hardware implementation of the scheme. One would require as many receiver as the number of array elements. This research work would look at a simplified processing scheme which would reduce the number of required antenna elements in the next chapter.

Chapter 5

Hardware Efficient Enhancement for the Algorithm

5.1 Introduction

The algorithm proposed in Chapter 3 is able to resolve the DOA of multipath components coming from UWB sources in the presence of inband interfering signals. Conventional DOA estimation implementations require simultaneous sampling of the output signals of all the sensor elements. This means that the implementation of the algorithm in its present form require 10 receivers. The receiver of a WiMedia UWB system is very complex compared to conventional radio receiver owing to the need for frequency hopping from symbol to symbol and the ultrawide bandwidth of

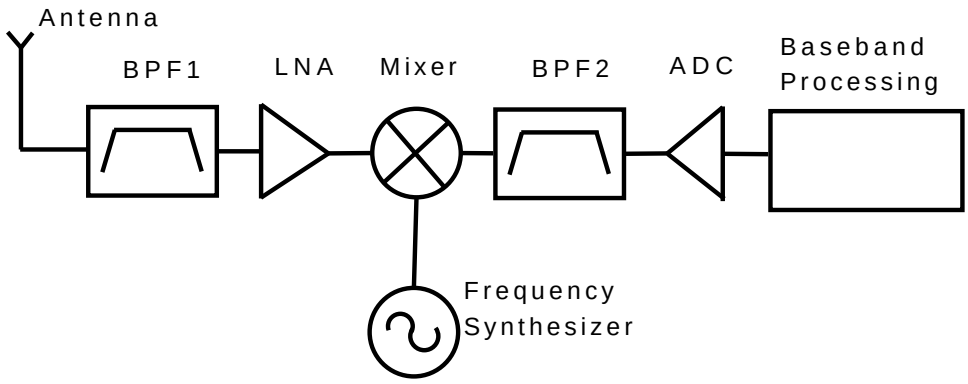

Figure 5.1: UWB Receiver block diagram

the system. This necessitates fast frequency synthesizers covering a wide bandwidth. Besides, the circuits need to operate at very high bandwidth and this will increase the cost and power consumption of the front end. The presence of potential interferers necessitates RF front end with high dynamic range. Besides, the complexity of the OFDM baseband receiver required also would be very high. Since the bandwidth is very high one will have to operate the circuits at very high clock frequencies (528MHz clock frequency) and this would result in significant power consumption. The block diagram of a typical UWB receiver is shown in Figure 5.1. One would have to build 10 such parallel receiver for the implementation of the algorithm. This results in a very expensive hardware system for the implementation of the proposed algorithm. Besides, the total power consumption also would be high. Hence, it would be of great interest to reduce the implementation complexity. This research looks at ways to reduce the implementation complexity of the proposed scheme.

5.2 Problem Definition

Consider p signals $\{s_1(n), s_2(n), \cdots, s_p(n)\}$ impinging on a q element uniform linear array (ULA) from different directions $\{\theta_1, \theta_2, \cdots, \theta_p\}$.

The input spectrum can be split into individual components and the array output at any frequency ω_j at a sampling instant n is a $q \times 1$ vector and is given by

$$\mathbf{x}(\omega_j, n) \triangleq [x_1(\omega_j, n)\ x_2(\omega_j, n)\ \cdots\ x_q(\omega_j, n)]^T \tag{5.1}$$

$$= \mathbf{A}\mathbf{s}(\omega_j, n) + \mathbf{z}(\omega_j, n) \tag{5.2}$$

where $\mathbf{A} \triangleq [\mathbf{a}(\theta_1)\ \cdots\ \mathbf{a}(\theta_p)]$ is a $q \times p$ matrix consisting of p steering vectors defined by

$$\mathbf{a}(\theta_i) \triangleq [1\ e^{-j(\omega_j)d\sin\theta_i}\ \cdots\ e^{-j(\omega_j)(q-1)\sin\theta_i}]^T \tag{5.3}$$

where $\mathbf{z}(\omega_j, n)$ denotes $q \times 1$ additive noise vector and $\mathbf{s}(\omega_j, n)$ is the signal vector and are defined below.

$$\mathbf{z}(\omega_j, n) \triangleq [z_1(\omega_j, n)\ z_2(\omega_j, n)\ \cdots\ z_q(\omega_j, n)]^T \tag{5.4}$$

$$\mathbf{s}(\omega_j, n) \triangleq [s_1(\omega_j, n)\ s_2(\omega_j, n)\ \cdots\ s_p(\omega_j, n)]^T \tag{5.5}$$

In conventional array processing, one will concatenate the array output vector from time instant n to $n+N$ to form the input data matrix $\mathbf{X}$. It can be easily proved that

$$\mathbf{X}(\omega_j) = \mathbf{A}\mathbf{S}(\omega_j) + \mathbf{Z}(\omega_j) \tag{5.6}$$

In Eqn.(5.6), $\mathbf{S}$ and $\mathbf{Z}$ represent the concatenation of signal samples and noise samples at the chosen time instants.

5.3 Hardware Efficient Enhancement of the Algorithm

Each column of array output matrix $\mathbf{X}$ represents the linear combination of the source direction vectors with signal value at the particular instant as the weighing factor for the directional vectors. As can be seen from Eqn.(5.3), each element of the array vector represents the phase shift encountered by the source signal at the corresponding element. The array output contribution from any source is a column vector whose elements represent the source signal phase shifted in the corresponding array element. As a result, one need to sample the sensors at the same instant. Otherwise, any variation in the original signal value between the sampling instants would be interpreted as a phase shift at the array element and subspace estimation based on the sample covariance matrix of this data would estimate the wrong subspace and hence DOA estimation also would be in error. Hence, one will have to use as many receivers as the number of sensors. The proposed algorithm is having a different structure for estimating the signal subspace which would allow it to simplify the hardware requirements. Since the analysis of UWB signals is an extension of the narrowband case, let us first look into the narrow band case.

In the algorithm proposed in Chapter 3, l element subarrays were formed from the main array. The i^{th} subarray was formed by picking the

elements from i to $i+l-1$. The subarray vectors can be expressed as

$$\mathbf{X}_1 = \mathbf{A}_1\mathbf{S} + \mathbf{Z}_1 \tag{5.7}$$

$$\mathbf{X}_2 = \mathbf{A}_2\mathbf{S} + \mathbf{Z}_2 \tag{5.8}$$

and so on. In general,

$$\mathbf{X}_i = \mathbf{A}_i\mathbf{S} + \mathbf{Z}_i \tag{5.9}$$

In the Eqn.(5.9), $\mathbf{X}_i$ represents the output signal matrix of the subarray and $\mathbf{Z}_i$ represents the output noise matrix of the subarray. $\mathbf{A}_i$ represent the matrix formed by picking the l rows of the array matrix $\mathbf{A}$, starting from the i^{th} row.

Theorem 5.3.1. *Matrix* $\mathbf{G}$ *can be generated by time multiplexed sampling of array outputs instead of simultaneous sampling.*

Proof. As explained earlier, the contribution from source in the array output is the steering vector, multiplied by the instantaneous value of the source signal. In this case, all the elements of the steering vector must be weighed by the same term. In the proposed algorithm, instead of $\mathbf{X}_i$, a new matrix $\mathbf{G}$ is used. $\mathbf{G}$ is made up of column vectors $\mathbf{g}_i$ obtained by correlating the subarray output signal with known pilot wave form $\mathbf{r}_1$.

$$\mathbf{g}_i = E(\mathbf{X}_i\mathbf{r}_1^H) \tag{5.10}$$

$$= E(\mathbf{A}_i\mathbf{S}\mathbf{r}_1^H) + E(\mathbf{Z}_i\mathbf{r}_1^H) \tag{5.11}$$

$$= \mathbf{A}_i E(\mathbf{S}\mathbf{r}_1^H) + E(\mathbf{Z}_i\mathbf{r}_1^H) \tag{5.12}$$

$$\mathbf{g}_i = \mathbf{A}_i \begin{bmatrix} \alpha_1 \\ \vdots \\ \alpha_{k_1} \\ 0 \\ \vdots \\ 0 \end{bmatrix} \tag{5.13}$$

In Eqn.(5.13), $\mathbf{g}_i$ is the weighted sum of the column vectors of $\mathbf{A}_i$, with weighing factor equal to the correlation value of the source signal with the known waveform. All the elements of the steering vectors are multiplied by the correlation value.

Since the source signals are stationary ergodic signals, the correlation of the subarray output with known waveform (expected value of $\mathbf{X}_i\mathbf{r}_1^H$) is equal to the time average of the product of $\mathbf{X}_i\mathbf{r}_1^H$, i.e.,

$$E(\mathbf{X}_i\mathbf{r}_1^H) = \frac{1}{N}\boldsymbol{X}_i\mathbf{r}_1^H \tag{5.14}$$

In Eqn.(5.14), $\mathbf{X}_i$ is a $l \times N$ matrix and $\mathbf{r}_1$ is $1 \times N$ row vector.

When N is sufficiently large, there is no significant variation in the time averages taken at different time instants. If one take $E[\mathbf{X}_i\mathbf{r}_1^H]$, it can be seen that the expected value will not change if we drop some samples from the expectation calculation as long as sample size is large. This opens the possibility of time multiplexing the receivers and thus gives opportunity for reducing the number of receivers.

$\mathbf{g}_i$ can be written as

$$\mathbf{g}_i = \begin{bmatrix} a_{i\ 1} & a_{i\ 2} & \cdots & a_{i\ k_1} \\ a_{i+1\ 1} & a_{i+1\ 2} & \cdots & a_{i+1\ k_1} \\ \vdots & \vdots & \ddots & \vdots \\ a_{i+l-1\ 1} & a_{i+l-1\ 2} & \cdots & a_{i+l-1\ k_1} \end{bmatrix} \begin{bmatrix} \alpha_1 \\ \alpha_2 \\ \vdots \\ \alpha_{k_1} \end{bmatrix} \tag{5.15}$$

The two matrices on the right hand side of the Eqn.(5.15) represents $\mathbf{A}_i$ and a column vector consisting of elements corresponding to the correlation of the multipath with known waveform. The array vector corresponding to the first source is weighed by α_1 in the product. This can be written as

$$\alpha_1 \begin{bmatrix} a_{i\ 1} \\ a_{i+1\ 1} \\ \vdots \\ a_{i+l-1\ 1} \end{bmatrix} = \alpha_1 \begin{bmatrix} a_{i1} \\ 0 \\ \vdots \\ 0 \end{bmatrix} + \alpha_1 \begin{bmatrix} 0 \\ a_{i+1\ 1} \\ \vdots \\ 0 \end{bmatrix} + \cdots + \alpha_1 \begin{bmatrix} 0 \\ 0 \\ \vdots \\ a_{i+l-1\ 1} \end{bmatrix} \tag{5.16}$$

Looking at the Eqn.(5.16), one can see that time multiplexing would not produce any error as long as they are weighed by the same constant factor corresponding to the correlation of the source signal with known waveform. One can trade off the number of receivers and total sampling duration.

In Eqn.(5.13), $\mathbf{A}_i$ can be expressed as

$$\mathbf{A}_i = \mathbf{A}_1 \mathbf{D}^{i-1} \tag{5.17}$$

where $\mathbf{D}$ is defined as

$$\mathbf{D} = \begin{bmatrix} e^{-j2\pi\frac{d}{\lambda}\sin\theta_1} & 0 & \cdots & 0 \\ 0 & e^{-j2\pi\frac{d}{\lambda}\sin\theta_2} & \cdots & 0 \\ \vdots & \vdots & \ddots & \vdots \\ 0 & \cdots & 0 & e^{-j2\pi\frac{d}{\lambda}\sin\theta_{k_1}} \end{bmatrix} \tag{5.18}$$

Hence $\mathbf{g}_i$ can be expressed as

$$\mathbf{g}_i = \bar{\boldsymbol{A}}_1 \mathbf{D}^{i-1} \begin{bmatrix} \alpha_1 \\ \vdots \\ \alpha_{k_1} \end{bmatrix} \tag{5.19}$$

Here, $\bar{\boldsymbol{A}}_1$ represents the first k_1 columns of A_1.

It is proven in above analysis that the multiplexing of receivers is not going to affect the value of $\mathbf{g}_i$ as long as we take sufficient number of samples so that time average is very close to the statistical mean. Matrix $\mathbf{G}$ is formed by concatenating $\mathbf{g}_1, \mathbf{g}_2, \cdots, \mathbf{g}_M$. Hence the properties of $\mathbf{G}$ remains the same. □

For illustration, the array output of a 4 element array with one receiver for 4 antenna elements is given in Eqn.(5.20).

$$\mathbf{X}_1 = \begin{bmatrix} x_1(n) & 0 & 0 & 0 & \cdots & 0 \\ 0 & x_2(n+1) & 0 & 0 & \cdots & 0 \\ 0 & 0 & x_3(n+2) & 0 & \cdots & 0 \\ 0 & 0 & 0 & x_4(n+3) & \cdots & x_4(n+N) \end{bmatrix} \tag{5.20}$$

In the proposed scheme, we will be grouping the sensors into different groups. We will be allocating one receiver each for elements in a group and

thus the total number of the receivers would be decided by the number of elements in the group. For example, in a 12 element array, one can group the sensors 1,5,9 into the first group, sensors 2,6,10 into second group, sensors 3,7,11 into the third group and sensors 4,8,12 into the fourth group and so on. The elements in a group are sampled simultaneously. After sampling the elements in the group for a predetermined time, the receiver would be switched to the antenna elements in the next group and so on. After completing the last group, the cycle repeats for the total duration. In the above example, one need only 3 receivers instead of original 12.

In the case of narrow band signals, the sampling period can be chosen arbitrarily. In the case of wideband and ultra wideband systems, the processing is done in frequency domain. Hence, one need to acquire sufficient number of samples required for the chosen frequency resolution. In the case of OFDM based systems like WiMedia UWB, the appropriate duration before sampling would be equal to the symbol period. Since the WiMedia UWB processing involves addition of samples from zero padding period to include the delayed energy from multipath signals, it would be appropriate to include this period as well in the time the receiver samples from one antenna element. During the zero padding duration at the end of the symbol, one can synchronously switch the receiver circuitry without loss of any information. This switching would be possible only for synchronous systems using OFDM like processing and having a guard interval, which is discarded in frequency domain processing. This concept can be exploited

to reduce the number of receivers used in the system and hence significant reduction in complexity for implementing the algorithm can be achieved by using multiplexed receivers.

As explained in Chapter 3, the array outputs corresponding to different frequency components were translated to a common focussing frequency before calculating the correlation with the the known waveform. Since this involves only the translation of the array matrix at one frequency, this operation doesn't effect the new multiplexing scheme. Since the proposed algorithm makes use of the correlation with known waveform of pilot subcarrier, the new multiplexing scheme is applicable only for pilot subcarriers.

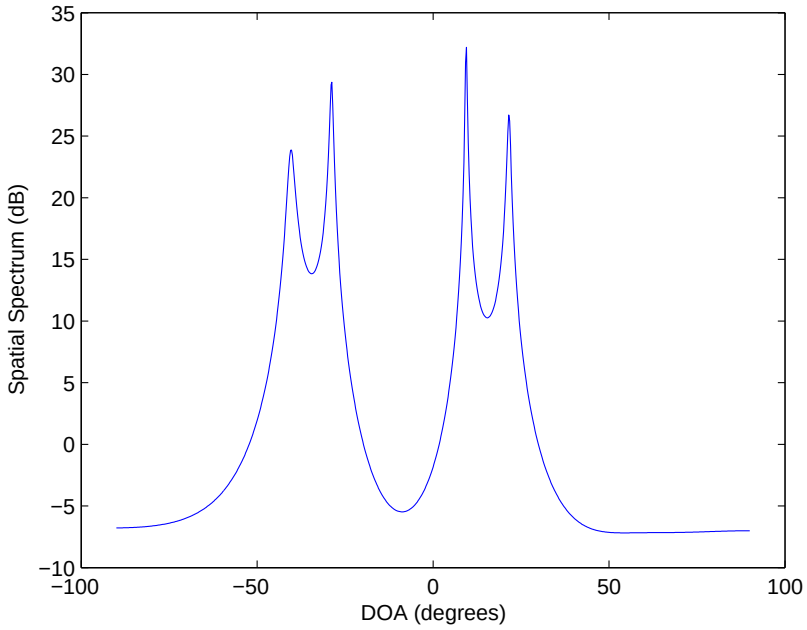

Figure 5.2: Spatial spectrum of the signals using multiplexed receiver

5.4 Computer Experiments

In this experiment, UWB system operating at 200 Mbits/sec is chosen. The same set up as in the Chapter 3 involving 4 desired multipaths and 3 intefering signal was chosen. The sampling frequency was fixed at 528 Msamples/sec. The desired multipath were assumed to be having exponentially distributed delay less than 32 sample periods. In the receiver side, perfect synchronization was assumed. This can be achieved by using the conventional processing of preamble data. The subarrays were formed as described in the algorithm section. The system was evaluated for focussing frequencies of 4.714875 GHz and 4.508625 GHz. The focused data corresponding to different pilot carrier frequencies were correlated with the respective pilot data. The matrix $\mathbf{G}$ defined in Section 5.3 was formed for each pilot frequency. $\mathbf{G}\mathbf{G}^H$ was calculated for each translated pilot frequency and the average correlation matrix was calculated. The correlation matrix was analyzed using conventional MUSIC techniques to find DOA.

The system was evaluated for 5dB to 25dB SNR at 5dB increments. 100 Monte Carlo runs were carried out for each SNR. The initial DOA was estimated using conventional frequency domain beamforming using an array size of 10 elements. The system was evaluated using the algorithm proposed in Chapter 3 with subarray size of 6.

The same data set of multipaths and interferer was repeated for the sampled scheme. 12 antenna elements were used in this experiment. The sensors were split into 4 groups of 3 sensors each as explained in the example

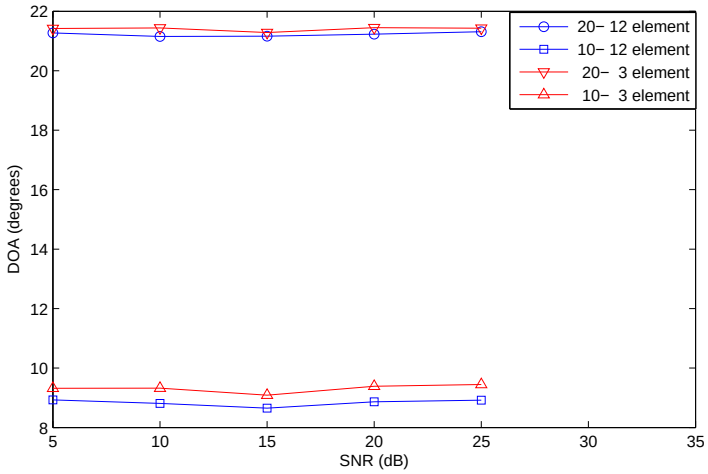

(a) 10°, 20°

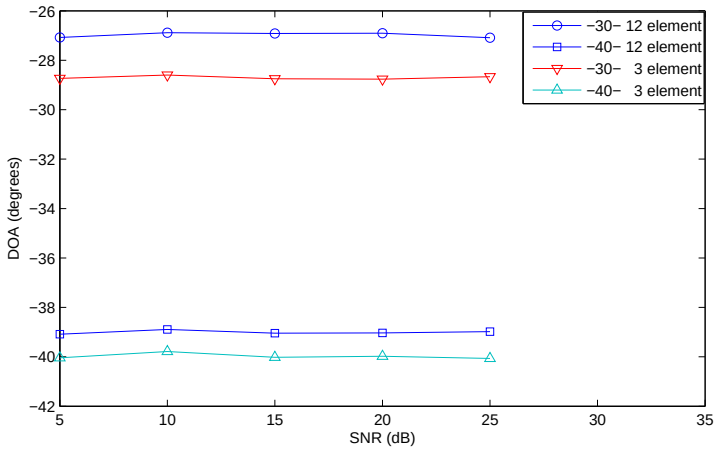

(b) −40°, −30°

Figure 5.3: Mean of estimated direction of arrival of different focussing for angles of arrival of −40°, −30°, 10°, 20° and interferers at DOA −10°, 0°, 40°.

in Section 5.3. Instead of 12 receivers, 3 receivers were used. Signals from each antenna element was picked for one OFDM symbol duration + 32 sampling periods for every four transmitted symbols (165 sample periods

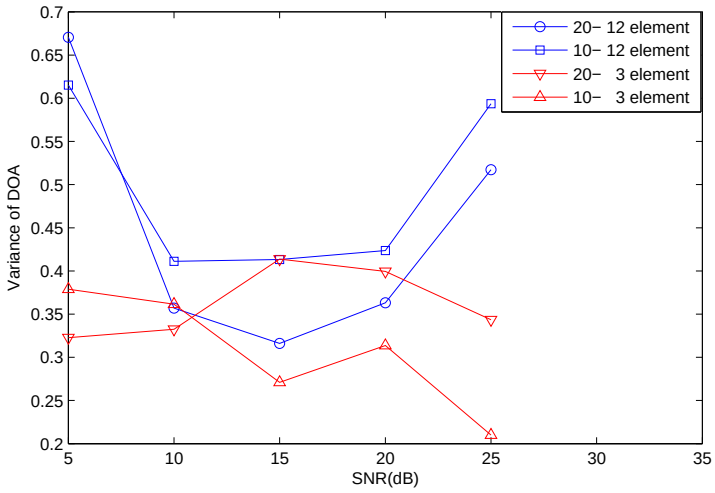

(a) 10°, 20°

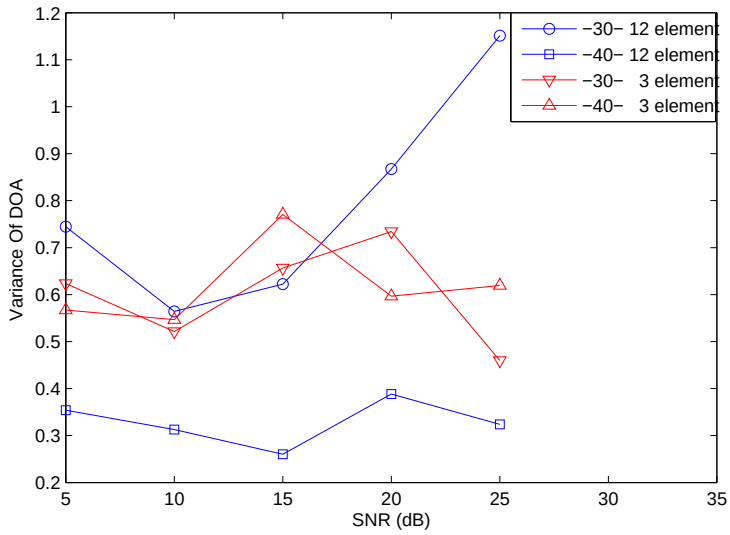

(b) −40°, −30°

Figure 5.4: Variance of estimated direction of arrival of different methods for angles of arrival of −40°, −30°, 10°, 20° and interferers at DOA −10°, 0°, 40°.

duration). The receiver was switched to the next group in the remaining period of 5 sample points of transmit symbol. This was repeated for the

total transmitting duration. This sampled data was converted to frequency domain and correlated with the pilot data for the respective symbol and processed like the original algorithm. Zeros were substituted for the missing samples. DOA was estimated using conventional techniques.

5.5 Discussion

The proposed enhancement using multiplexing was successful in resolving the direction of arrival of all multipaths. The spatial spectrum using multiplexed receiver at focussing frequency of 4.714875 GHz is shown in Figure 5.2. As explained in Chapter 3, the original algorithm with 10 elements failed to resolve the closely spaced signals in around 3% of cases. On the other hand, the new enhancement using multiplexed receivers was able to resolve the DOA in all trials. This can be attributed to the better resolution ability of 12 element antenna array. Besides, the performance of the system did not show any notable variation between the two focussing frequencies. The mean and variance against different SNR values for the original algorithm and simplified architecture employing multiplexed receiver are shown in Figures 5.3 and 5.4.

As can be seen from the figures, 12 element array produces better result in terms of estimation bias as well as the variance of the estimates than 10 element array. This can be attributed to the better resolution properties of the 12 element array. The main advantage of the new enhancement is the ability to use 12 element array with 75% reduction in hardware

complexity. This performance enhancement was achievable because of the use of expected value of the correlation with the known waveform as the weighing factor for steering vectors instead of the instantaneous source signal value in the new algorithm.

5.6 Summary

As can be seen from the figures, the multiplexed receiver system works equally well like the conventional receivers. The use of expected value instead of instantaneous value during the OFDM symbol period allows us to use the multiplexed receiver. The potential drawback may be the requirement for more number of samples. This will have to be studied further as the effect of using lesser samples against the dropping of error term in focussing will have to be investigated. In the experiments conducted during the research, there was no significant degradation in performance even when the number of samples in calculating the expected values were only 25% of the number of samples used in the simulation experiments in Chapter 3. As seen from the figures, in some cases multiplexed receiver gives less bias. Overall, this scheme provide an excellent means for reducing the number of receivers significantly with the addition of extra two antennas. In the frequency of operation of UWB systems, the extra antennas will not be a big issue for the access points. Thus the proposed enhancement achieved a simplified receiver architecture with less hardware resources and lower power consumption than the algorithm using conventional receiver

architecture.

The major contribution of this Chapter is the simple receiver architecture which will save significant hardware. There is no performance improvement in this case. In the illustrated example in the thesis, hardware saving is of the order of 75% excluding the switches for multiplexing. One will have to ensure that sufficient samples are captured so that the approximation of expected value by sample average is accurate. Apart from this, there are no specific constraints on this architecture. One will be able to adapt the architecture to suit his needs easily.

In the previous chapters, the number of multipaths was assumed to be known. Conventional source enumeration schemes made use of multiplicity of the nearly equal value of the noise subspace eigenvalues to determine the number of sources. In the next chapter, we will look at the performance of these algorithms for the multipath scenario studied in this research. Besides, the suitability of the source enumeration algorithms for the proposed algorithms in this research would be studied and new schemes suitable for the algorithms proposed in this chapter would be developed.

Chapter 6

Estimation of the Number of Multipaths

6.1 Introduction

The algorithm proposed in Chapter 3 is able to resolve the DOA of multipath components coming from UWB sources. The number of sources was assumed to be known in Chapter 3. One will have to identify the number of the multipaths to separate the subspace into signal subspace and its orthogonal compliment. Signal enumeration itself is a vast topic and a detailed research into signal enumeration is beyond the scope of this study. This study mostly looks at the adaptation of the known algorithms for determining the number of multipaths while using the algorithms proposed in this research. Different methods have been proposed in the literature for the narrowband enumeration. On the other hand, there has not been much research related to source enumeration in wideband case using focussing.

In this chapter, estimation of number of multipaths using the proposed algorithm for UWB case will be explored. Computer experiments would be carried out to validate the performance of the proposed method.

6.2 State of the Art

If p UWB signals $\{s_1(n), s_2(n), \cdots, s_p(n)\}$ are impinging on a q element uniform linear array (ULA) from different directions $\{\theta_1, \theta_2, \cdots, \theta_p\}$, the sampled array output vectors can be expressed as

$$\mathbf{x}(\omega_j, n) \triangleq [x_1(\omega_j, n)\ x_2(\omega_j, n)\ \cdots\ x_q(\omega_j, n)]^T \tag{6.1}$$

$$= \mathbf{A}\mathbf{s}(\omega_j, n) + \mathbf{z}(\omega_j, n) \tag{6.2}$$

Here the $\mathbf{A}$, $\mathbf{s}$, $\mathbf{z}$ are as defined in Chapter 3 and this equation is valid for any of the frequency components of input UWB signal. The smallest eigenvalues of the covariance matrix of array output vectors would be equal and the multiplicity of these smallest eigenvalues is taken as the dimension of the noise subspace. q - dimension of noise subspace would give the number of the sources. In practice, one takes n samples of $\mathbf{x}$ and concatenate the array output vector from time instant n to $n+N$ and to form the input data matrix $\mathbf{X}$. The sample covariance matrix of the data is defined as $\mathbf{X}\mathbf{X}^H/N$. The sample covariance matrix is estimated and the eigenvalues would be calculated. Because of the finite observation window, the smallest eigenvalues will be different and would be scattered around an average value. Hence estimation based on multiplicity will not provide accurate

result. This would be especially true in lower SNR case. Besides, the lower eigenvalues corresponding to the signal space eigenvectors also can be closer to this scattered set. Different criteria are used to estimate the order of this clustered values.

Wax and Kailath [98] proposed the detection based on the information theoretic criteria. Here, the array output vectors are assumed to be independent complex Gaussian random vectors with zero mean. Their joint probability density function is given by [98]

$$f(\mathbf{x}(n), \cdots, \mathbf{x}(n+N)/\theta^{(k)}) = \prod_{n=n}^{n+N} \frac{1}{\pi^p \ det \ \mathbf{R}^{(k)}} exp(-\mathbf{x}(n)^H [\mathbf{R}^{(k)}]^{-1} \mathbf{x}(n)) \tag{6.3}$$

Under the assumption of this pdf, they calculated the log likelihood function and estimated $\theta^{(k)}$ by maximizing it. They applied this in adapting the Akaike's method [1] and Rissanen's MDL [72] for determining the number of sources. Here, they related the joint pdf of the observation vectors to the eigenvalues and eigenvectors of the covariance matrix of the sampled data to estimate the number of signals.

The number of sources is determined by minimizing the cost function for either of the methods. The cost function of the Akaike criteria and MDL criteria are given in Eqn.(6.4) and Eqn.(6.5) [98] respectively.

$$AIC(k) = -2 \log \left(\frac{\prod_{i=k+1}^{q} l_i^{1/(q-k)}}{\frac{1}{(q-k)} \sum_{i=k+1}^{q} l_i} \right)^{(q-k)N} + 2k(2q-k) \tag{6.4}$$

$$MDL(k) = -2 \log \left(\frac{\prod_{i=k+1}^{q} l_i^{1/(q-k)}}{\frac{1}{(q-k)} \sum_{i=k+1}^{q} l_i} \right)^{(q-k)N} + 0.5k(2q-k) \log N \tag{6.5}$$

In the above equations l_i represents the i^{th} eigenvalue of covariance matrix. Since the smaller eigenvalues of the focussed matrix tend to zero for large sample size, the methods proposed by Wax and Kailath fail in determining the number of sources in the proposed method in this research.

A. Di [26] proposed a scheme not requiring the eigen decomposition of the covariance matrix. In the scheme, a new submatrix $R^{(l)}$ is formed by taking p rows from the covariance matrix starting from the l^{th} row. He proved that if one formed new matrices by concatenating the $R^{(l)}$ matrices, with l starting from 1 , the rank of the newly formed concatenated matrix would reach an upper limit and this upper limit would be equal to the number of sources. This is applicable in the case of narrowband sources. This is mostly applicable in high SNR conditions. Its computational complexity would be very high for wideband case as one will have to do this for each frequency component.

Wax [99] developed the MDL algorithm to include the estimation of the number of the coherent sources including multipaths. Here the observed array vector was partitioned into noise space and signal subspace components. The code length required to encode the signal space and noise space components was minimized to find the number of sources. The complexity of multidimensional minimization was a major disadvantage of the algorithm in the narrowband case itself.

Wu and Fuhrmann [101] proposed parametric approach for determining the number of sources. The method was based on maximizing the likelihood

function for the parameters. It was proven that this was equal to minimizing the squared norm of the projection of the observed array output vector to noise subspace. The computational complexity of this method was also too high even in narrowband case. Nezafat, Kaveh and Xu [64] explored the possibility of using eigenvectors for the estimation of the number of sources to reduce the sensitivity to the model perturbations. The method is based on the eigen decomposition of the array covariance matrix. Different subspaces were defined by excluding the first k eigenvectors. If all k eigenvectors spanning the the signal subspace are excluded, the projection of the steering vectors corresponding to the actual direction of arrival would be having a negligible component in the subspace defined by excluding the signal subspace eigenvectors. This component would not vary significantly by the deletion of any more eigenvectors. This fact is used in the new technique. A new metric for evaluating this equality was proposed in the paper. One will have to calculate this metric for all potential angles of arrival and this was a serious disadvantage of this scheme. In [65], Nezafat and Kaveh reduced the computational complexity by making use of prior coarse estimation of DOA. Chen, Wu and Yang [22] makes a comparative study of the model selection criteria for the estimation of signals. The performance of AIC, MDL and some of their derivatives are compared. Basically all these criteria consists of a likelihood function and a penalty term for over fitting the model. The likelihood function is same for all criteria and is equal to the first term of the RHS of Eqn.(6.4). The penalty term is different and

this results in different performance under varying conditions of sample size, number of sources and number of array elements. Since the smallest eigenvalue is nearly zero in the algorithm proposed in this research, all the mentioned schemes fail in determining the number of sources.

Yang and Li [103] proposed a new method for estimating the number of harmonics in coloured noise. Basically this scheme is based on the eigenvalues of an enhanced matrix. This matrix is formed by taking L samples $x(0), x(1), \cdots x(L-1)$ of the noisy data as the first column and $x(1), x(2), \cdots x(L)$ as the second column and so on. $L \times (N-L)$ matrix $\mathbf{Y}(L)$ is formed and eigenvalues of the covariance of matrix $\mathbf{Y}(L)$ is calculated. This is repeated for different values of L. Based on the spectral property of eigenvalues, one would be able to express the k^{th} eigenvalue as $\lambda_k(L)$ $\lambda_k(L) = a_k L + b_k$. The value of a_k should be above a threshold. It is proven that this is true for largest P eigenvalues, where P is the number of harmonics. The computational complexity was a major disadvantage for this method as one will have to do the eigen decomposition of each $\mathbf{Y}(L)$.

Shah and Tufts [78] proposed a threshold based approach relying on the fluctuations singular values of the array output matrix. The sum of the squares of noise subspace singular values is calculated. The statistical distribution of these singular values is used to determine a threshold. As long as the sum includes only the squares of the noise subspace singular values, this would be dominated by noise and hence the sum would be below the threshold. Once a signal subspace singular value is included, this

sum would include contributions from signal sources and hence it would be above the threshold. The focussing operation for arbitrary angles of arrival for wideband signal is complex function of angle of arrival, focussing frequency and signal bandwidth. In the case of multipath signals, this would also depend on the initial delay to the reference element. It is mathematically too complex to model and hence difficult to calculate a statistical distribution for the noise/ error terms introduced by focussing. Hence the results of [78] couldn't be directly applied to calculate the number of sources in our case. Chen, Wong and Reilly [23] provided threshold calculation for detection of the number of signals in the narrowband case. Their focus was on the fluctuations caused by element noise alone and their result was based on the fluctuations in eigenvalues under such conditions. The results couldn't be directly applied to wideband case due to difficulty of modeling the error introduced by focussing.

Wang and Kaveh looked into the problem of detecting the number of wideband sources in their classical paper on focussing [92]. They proposed coherent Minimum Akaike Information Criteria Estimate (MAICE) for wideband sources.

$$MAICE(k) = (q-k)N \log \left(\frac{\frac{1}{(q-k)} \sum_{i=k+1}^{q} l_i}{\prod_{i=k+1}^{q} l_i^{1/(q-k)}} \right) + k(2q-k) \qquad (6.6)$$

This was modified by Wang and Kaveh [95] by treating the different frequency components as independent. They applied both AIC and MDL for the estimation of the number of sources by minimising the metric given

by Eqn.(6.7)

$$MAICE(k) = J(q-k)N \log \left(\frac{\frac{1}{(q-k)} \sum_{i=k+1}^{q} l_i}{\prod_{i=k+1}^{q} l_i^{1/(q-k)}} \right) + p(d,N) \tag{6.7}$$

In Eqn.(6.7), J represents the number of frequency components and $p(d,N)$ represents the penalty function. The penalty function for AIC is given by

$$p(d,N) = d(2q-d) \tag{6.8}$$

and that for MDL is given by

$$p(d,N) = \frac{1}{2} d(2q-d) \log JK \tag{6.9}$$

From the above equations, it can be seen that the criteria can't be applied in our case since the lowest eigenvalue approaches zero. The other work related to source enumeration [16] is an adaptation of Wang and Kaveh's result for their algorithm and hence can't be applied in our case.

6.3 Detection of the number of multipaths under low/ no inband interference

The proposed algorithm is trying to estimate the direction of arrival of the k_1 multipaths corresponding to the desired source. For this, subarrays were formed and the array output vector was correlated with the known signal from the desired sources as explained in Chapter 3. A new subarray vector $\mathbf{g}_i$ was defined for each subarray, where m^{th} element of this vector was the correlation between the output signal of the m^{th} element of the subarray

and the desired waveform. It was shown that

$$\mathbf{g}_i = E[\mathbf{X}_i \mathbf{r}_1] \tag{6.10}$$

$$= \bar{\mathbf{A}}_1 \mathbf{D}_\alpha \mathbf{c}_i \tag{6.11}$$

for $i = 1, \cdots, M$. $\bar{\mathbf{A}}_1$ and $\mathbf{D}_\alpha$ are defined as in Chapter 3. $\mathbf{c}_i$ is a column vector for the i^{th} subarray and is given by

$$\mathbf{c}_i = [e^{-j2\pi \frac{d}{\lambda}(i-1)\sin\theta_1}, \cdots, e^{-j2\pi \frac{d}{\lambda}(i-1)\sin\theta_{k_1}}]^T \tag{6.12}$$

The vectors $\mathbf{g}_i$ of different subarrays are concatenated to form $\mathbf{G}$. It can be shown that $\mathbf{G}$ is given by

$$\mathbf{G} = \begin{bmatrix} u_1 & u_2 & \cdots & u_{q-l+1} \\ u_2 & u_3 & \cdots & u_{q-l+2} \\ \vdots & \vdots & \cdots & \vdots \\ u_l & u_{l+1} & \cdots & u_q \end{bmatrix} \tag{6.13}$$

Here $u_m = E[\mathbf{x}_m \mathbf{r}_1^H]$, where $\mathbf{x}_m$ is the output of the m^{th} element of the array. It can be seen from Eqn.(6.13) that the columns of $\mathbf{G}$ are related and as such the algorithms derived on the assumption of independence of columns would not be applicable here. Besides, the sample average of $\mathbf{G}\mathbf{G}^H$ approaches its asymptotical value faster than that of sample average of covariance matrix of raw data. As a result, estimated noise subspace eigenvalues would be very small. This results in poor performance of the conventional schemes.

6.4 Proposed algorithm

In practice, $\mathbf{G}$ is estimated from a finite data set. Let the estimated value of $\mathbf{G}$ be $\hat{\mathbf{G}}$. In $\hat{\mathbf{G}}$, each element $\hat{u}_m$ is calculated by the following expression

$$\hat{u}_m = \frac{1}{N}\sum_{i=1}^{N} x_m(i) r_1^*(i) \tag{6.14}$$

Here, $x_m(i)$ is the output of the m^{th} array element at the i^{th} instant. It can be shown that

$$\hat{u}_m = \hat{\mathbf{A}}_{mk_1}\begin{bmatrix} \alpha_1 \\ \vdots \\ \alpha_{k_1 i} \end{bmatrix} + \hat{\mathbf{A}}_m \begin{bmatrix} \hat{\alpha}_1 \\ \vdots \\ \hat{\alpha}_{k_1} \\ \alpha_{(k_1+1)} \\ \vdots \\ \alpha_p \end{bmatrix} + [\hat{z}] \tag{6.15}$$

Here $\hat{\mathbf{A}}_{mk_1}$ and $\hat{\mathbf{A}}_m$ represents the m^{th} row of the first k_1 columns of $\mathbf{A}$ and the m^{th} row of $\mathbf{A}$ respectively. The first term on the right hand side of Eqn.(6.15) represents the mean value u_m. The elements of the column vector in second term have asymptotical mean zero. The $\hat{z}$ represents the correlation of noise with the known waveform and its asymptotical mean is also zero.

Using the above result one can write $\hat{\mathbf{G}}$ as

$$\hat{\mathbf{G}} = \bar{\mathbf{G}} + \tilde{\mathbf{G}} \tag{6.16}$$

Here $\bar{\mathbf{G}}$ and $\tilde{\mathbf{G}}$ represents the mean value and perturbations of $\hat{\mathbf{G}}$ respectively. It may be noted that $\bar{\mathbf{G}}$ would be equal to $\mathbf{G}$. Similarly we can

write the focussed $\hat{\mathbf{G}}_f$ as

$$\hat{\mathbf{G}}_f = \bar{\mathbf{G}}_f + \tilde{\mathbf{G}}_f \tag{6.17}$$

Let $\hat{u}_{mf}$, $\bar{u}_{mf}$ and $\tilde{u}_{mf}$ represent the corresponding elements of $\hat{\mathbf{G}}$, $\bar{\mathbf{G}}_f$ and $\tilde{\mathbf{G}}_f$ respectively. By the central limit theorem, $\hat{u}_m$ tends to its mean value. The law of the iterated logarithm (LIL) [76] specifies the extreme perturbations in these averages. According to LIL, the extreme perturbations $\breve{e}_i$ in each element in the column vectors of the second term on the right hand side of Eqn.(6.15) is given by the Eqn.(6.18).

$$\breve{e}_i = \frac{\sigma_i (2loglog(N))^{1/2}}{N^{1/2}} \tag{6.18}$$

Here, σ_i represents the variance of the i^{th} element in the column vector and it is a function of the power in the i^{th} path. Similar expression holds true for the perturbations in $\hat{z}$ also. The sum of these perturbations would give the extreme perturbations in each element. Since the variance of each elements are unknown, one will have to make some approximations about them.

The maximum perturbations in $\hat{u}_m$ is given by

$$\breve{u}_m = \rho_m (2loglog(p))^{1/2} p^{1/2} \frac{(2loglog(N))^{1/2}}{N^{1/2}} \tag{6.19}$$

Here ρ_m represents effect of the combined variance and is a function of the powers of the desired multipaths and interfering sources power. This is an unknown quantity. The perturbations given by Eqn.(6.19) would be the maximum value. For large values of N, the perturbations can be taken as half of this value.

In the proposed new focussing scheme, one translates matrix $\mathbf{G}$ at different frequency to a common focussing frequency. It is noted that the column space of $\mathbf{G}$ spans signal subspace corresponding to each pilot frequency asymptotically. In implementing algorithm, one will have to use $\hat{\mathbf{G}}$ in the place of $\mathbf{G}$. When one align the column space of $\hat{\mathbf{G}}$ at different frequency by focussing and takes the average of matrix product $\hat{\mathbf{G}}\hat{\mathbf{G}}^H$, the random component in the original matrix $\hat{\mathbf{G}}$ and the random error introduced in focussing are being averaged. If there are N_c carrier frequencies and N_p pilot frequencies, the total carriers in the averaging process would be $N_{cp} = N_c N_p$. This combining process would translate into multiplication by another factor equal to $\frac{(0.5\ loglog(N_{cp}))^{1/4}}{\mathrm{N}_{cp}^{1/4}}$ for the random component in elements of matrix $\hat{\mathbf{G}}$. As result, the peak perturbations in the focussed case using new focussing scheme can be approximated as

$$\breve{u}_{mf} = \rho_m (2loglog(p))^{1/2} p^{1/2} \frac{0.5(2loglog(N_s))^{1/2}}{N_s^{1/2}} \frac{(0.5\ loglog(N_{cp}))^{1/4}}{N_{cp}^{1/4}} \tag{6.20}$$

In the above Eqn.(6.20), the term $\rho_m (2loglog(p))^{1/2} p^{1/2}$ is an unknown quantity depending on the number of signals and the power of each signal. It is well known that the largest eigenvalue would be directly related to this quantity and we can use a factor proportional to the largest eigenvalue of $\hat{\mathbf{G}}\hat{\mathbf{G}}^H$ in the calculation of the threshold. Hence the upper bound of perturbations can be approximated as

$$\breve{u}_{mf} = \beta \frac{0.5\ (2loglog(N_s))^{1/2}}{N_s^{1/2}} \frac{(0.5\ loglog(N_{cp}))^{1/4}}{N_{cp}^{1/4}} \tag{6.21}$$

Here β is an adjustment factor to account for the variance, which is related

to power of the individual signals, which is unknown. Let us define η as

$$\eta = \frac{0.5\ (2loglog(N_s))^{1/2}}{N_s^{1/2}} \frac{(0.5\ loglog(N_{cp}))^{1/4}}{N_{cp}^{1/4}} \tag{6.22}$$

Hence $\breve{u}_{mf}$ can be written as

$$\breve{u}_{mf} = \beta\eta \tag{6.23}$$

Eqn.(6.23) gives the upper limit of the elements of $\tilde{\mathbf{G}}_f$ in Eqn.(6.17)

Theorem 2 in [47] gives the upper limit for the difference in the singular values of a matrix and its perturbed version.Theorem 2 is summarized below.

Theorem 2: Let **A**, **B** and **E** are $m \times n$ real valued matrices with **B** = **A** + **E**. Denote their respective singular values by α_i, β_i and ϵ_i with $i = 1, 2, \cdots, k, \quad k \leq \min(m, n)$. Each set is labeled in decreasing order. Then

$$|\beta_i - \alpha_i| \leq \epsilon_i \tag{6.24}$$

$$= \parallel \mathbf{E} \parallel_2 \quad i = 1, 2, \cdots, k \tag{6.25}$$

By making use of this theorem, one can find the upper limit for the absolute value of the difference between the singular values of two matrices, one of which is the perturbed version of the other. In this case, $\hat{\mathbf{G}}_f$ is the perturbed version of the $\bar{\mathbf{G}}_f$. It is proven in Chapter 3 that the rank of $\bar{\mathbf{G}}_f$ (equal to $\mathbf{G}_f$) is equal to the number of multipaths k_1. Hence $(k_1 + 1)^{st}$ singular value of $\bar{\mathbf{G}}_f$ is equal to zero. According to theorem 2 in [47], the difference between the $(k_1 + 1)^{st}$ singular values of $\hat{\mathbf{G}}_f$ and $\bar{\mathbf{G}}_f$ is equal to

the $\|\tilde{\mathbf{G}}_f\|_2$. The order of $\hat{\mathbf{G}}_f$ is l $\times$ (q - $l+1$) and hence the upper bound of the $\|\tilde{\mathbf{G}}_f\|_2$ is equal to $\sqrt{l(q-l+1)}$ $\mid \breve{u}_{mf} \mid$

The smallest eigenvalues of $\bar{\mathbf{G}}_f \bar{\mathbf{G}}_f{}^H$ should be zero. It is known result [18] that the eigenvalues of $\hat{\mathbf{G}}_f \hat{\mathbf{G}}_f{}^H$ is equal to the square of the singular values of $\hat{\mathbf{G}}_f$. Hence the $(k_1+1)^{st}$ eigenvalue of $\hat{\mathbf{G}}_f \hat{\mathbf{G}}_f{}^H$ is bounded by $l(q\ -l+1)(\mid \breve{u}_{mf} \mid)^2$.

By substituting the value of $(\mid \breve{u}_{mf} \mid)^2$, upper limit for the noise space eigenvalues can be calculated. This can be set as the threshold for determining the noise space eigenvalue and is given by

$$thres = l(q-l+1)\beta^2\eta^2 \tag{6.26}$$

In the presence of signal, largest eigenvalue would be a function of the number of elements in the subarray and the total power of the signals. Hence an appropriate value for β^2 would be λ_1 for l element subarray. Here, λ_1 is the largest eigenvalue of $\hat{\mathbf{G}}\hat{\mathbf{G}}^H$.

In the absence of desired multipaths, the fluctuations in eigenvalues are higher. Besides, the largest eigenvalue in this case would be small. The threshold in this case is set as 100 times the normal threshold with β equal to one. This is the minimum value of the largest eigenvalue for signal conditions. The new threshold for the largest eigenvalue under no signal condition is given by Eqn.(6.27).

$$Threshold = 100(l(q-l+1))\eta^2 \tag{6.27}$$

In actual operation, largest eigenvalue is checked for no signal condition. If signal is detected, the eigenvalues are compared with threshold given in

Eqn.6.26. The number of eigenvalues exceeding the threshold would be equal to the number of multipaths.

6.5 Computer Experiments

In this experiment, UWB system operating at 200 Mbits/sec is chosen. The array noise was fixed at 1. SNR of the sources and interfering signals were defined as the ratio between their power and the unit array noise power. The interfering signals power was fixed at 15 dB below the chosen desired source SNR. Up to four multipath signals arriving from -40° , -30°, 10°, 20° were generated with equal amplitude. The multipath components were assumed to be reaching the antenna array with different exponentially distributed propagation delays. Three uncorrelated UWB signals arriving from -10° , 0°, 40° were added as interferers. To generate the no signal scenario, all the multipath signals were turned off while retaining the interfering signals. These baseband data were subjected to phase shift corresponding to the appropriate carrier frequency as defined in the standard for each symbol. Packet size was chosen as 12000 bytes (corresponding to 1542 symbols). The pilot carrier location data for each symbol was separated and subarrays were formed as explained in Chapter 3. Matrix $\mathbf{G}$ was calculated as explained earlier for each pilot carrier frequency. The matrix $\mathbf{G}$ at different frequencies were focussed as explained in Chapter 4 to focussing frequency 4.508625 GHz and average $\mathbf{G}\mathbf{G}^H$ was calculated. Eigendecomposition of the $\mathbf{G}\mathbf{G}^H$ was carried out for scenarios correspond-

ing to different number of sources.The performance of the algorithm was evaluated for SNR values ranging from -10 to 25dB at 5dB increments.

The estimated eigen values for no source, two sources, 4 sources at different SNR values are given in the Tables 6.1, 6.2 and 6.3 respectively. The number of the multipaths were detected using the proposed algorithm. The frequency of detected multipaths at -10, 0 and 25dB for different number of actual multipaths in 100 trials are given in Tables 6.4, 6.5 and 6.6 respectively.

Table 6.1: Calculated Eigenvalues with no desired multipath signal

Eigenvalue / SNR	1	2	3	4	5	6
-10	0.000	0.010	0.013	0.015	0.017	0.019
-5	0.000	0.010	0.013	0.015	0.017	0.020
0	0.000	0.011	0.014	0.016	0.019	0.022
5	0.000	0.011	0.015	0.017	0.023	0.032
10	0.000	0.012	0.015	0.019	0.037	0.066
15	0.000	0.012	0.016	0.025	0.086	0.173
20	0.000	0.012	0.016	0.043	0.24	0.505
25	0.000	0.012	0.016	0.103	0.756	1.652

Table 6.2: Calculated Eigenvalues with 2 desired multipath signal

SNR \ Eigenvalue	1	2	3	4	5	6
-10	0.000	0.011	0.014	0.017	0.321	5.676
-5	0.000	0.011	0.014	0.018	1.066	17.36
0	0.000	0.012	0.015	0.020	3.168	53.81
5	0.000	0.013	0.019	0.028	10.10	178.2
10	0.000	0.013	0.03	0.054	32.93	548.7
15	0.000	0.015	0.061	0.127	101	1741
20	0.000	0.018	0.177	0.401	351	5367
25	0.000	0.023	0.509	1.22	1024	16876

6.6 Discussion

As seen from the above results, new detection scheme is accurate above 0dB SNR under 15dB SIR. The detection performance suffers at lower SNR below -5dB when number of sources are small. The detection performance improves when the there are large number of multipaths. This is quite understandable because the fluctuations from noise and other interfering signals would be more prominent under such circumstances since the signal components which will stabilize the eigenvalues are quite small. It can also be seen that the performance can be improved by taking more symbols as this would reduce the effect of undesired interferers. The proposed scheme

Table 6.3: Calculated Eigenvalues with 4 desired multipath signal

Eigenvalue / SNR	1	2	3	4	5	6
-10	0.000	0.0121	0.195	0.500	4.405	6.384
-5	0.000	0.012	0.602	1.555	14.28	20.65
0	0.000	0.012	1.802	5.031	44.08	65.03
5	0.000	0.013	5.712	15.21	138.5	204.25
10	0.000	0.016	17.6	49.21	433.3	647.24
15	0.000	0.023	54.33	152.9	1405	2003
20	0.000	0.046	177.9	480	4428	6401
25	0.000	0.118	569	1507	13953	20470

Table 6.4: Frequency of detection at -10dB SNR

Detected multipaths / No of multipaths	1	2	3	4	5
1	66	33	1	0	0
2	0	100	0	0	0
3	0	0	100	0	0
4	0	0	0	100	0

Table 6.5: Frequency of detection at 0dB SNR

Detected multipaths / No of multipaths	1	2	3	4	5
1	100	0	0	0	0
2	0	100	0	0	0
3	0	0	100	0	0
4	0	0	0	100	0

Table 6.6: Frequency of detection at 25dB SNR

Detected multipaths / No of multipaths	1	2	3	4	5
1	100	0	0	0	0
2	0	100	0	0	0
3	0	0	100	0	0
4	0	0	0	100	0

provides a reliable and robust scheme for the estimation of the number of multipaths for the proposed algorithm.

6.7 Detection of the number of multipaths under high inband interference

In the case of higher inband interference, the new focussing scheme requires more samples compared to conventional focussing scheme. This is required to ensure that $\mathbf{G}$ is a good approximation to the array direction vector in terms of its column space. If one can't ensure this, conventional focussing as explained in [38] would be the better choice. As explained earlier in this chapter, the columns of $\mathbf{G}$ are not independent and smallest eigenvalues tends to zero and as such the conventional detection schemes won't be effective. This is especially true when the number of multipaths are closer to the number of elements in the array. The proposed threshold based scheme can be adapted here to address the case using conventional focussing scheme.

In the proposed new focussing scheme, one translates the $\mathbf{G}$ at different frequency to a common focussing frequency. In practical implementation, one would be estimating matrix $\mathbf{G}$ based on finite data. Let $\hat{\mathbf{G}}$ be the estimated $\mathbf{G}$. When one align the column space of $\hat{\mathbf{G}}$ at different frequency and takes the average, the random component in the original $\hat{\mathbf{G}}$ and the random error introduced in focussing are being averaged. On the other hand, in the

case of conventional focussing scheme, one align the array matrix at different frequency. When RSS matrices are used for focussing, this introduces a deterministic error element which does not cancel out through averaging. Hence the term related to the averaging effect of different pilot carrier frequencies are not applicable here. As result, the extreme fluctuations in the focussed case using conventional focussing scheme can be approximated as

$$\breve{u}_{mf} = \rho_m (2loglog(p))^{1/2} p^{1/2} \frac{0.5(2loglog(N_s))^{1/2}}{N_s^{1/2}} \tag{6.28}$$

Since it is difficult to analytically model the combined effect of focussing errors for array matrix at each frequency, rest of the situation can be assumed to be similar to the new focussing scheme. Following the arguments in the previous section, one can set the threshold for the conventional focussing scheme as

$$Threshold = \rho l(q - l + 1)\lambda_1 \eta_1^2 \tag{6.29}$$

where η_1 is given by

$$\eta_1 = \frac{0.5(2loglog(N_s))^{1/2}}{N_s^{1/2}} \tag{6.30}$$

The ρ term in the Eqn.(6.29) is a correction factor to account for the combined effect of focussing errors and the averaging introduced in calculating average $\hat{\mathbf{G}}_f \hat{\mathbf{G}}_f^{H}$. The system was simulated to evaluate its performance.

6.8 Computer Experiments

In this experiment, UWB system operating at 200 Mbits/sec is chosen. The same set up as in the previous case for low interference was used. Instead of 15dB below the chosen desired SNR, the interfering signal's SNR was fixed at 10 dB above the chosen desired source SNR. Coarse estimation of the DOA was done using conventional frequency domain beamforming. The array data was focussed and matrix $\mathbf{G}$ was calculated as explained earlier for each pilot carrier frequency. The focussing frequency was 4.714875 GHz and average $\mathbf{GG}^H$ was calculated. Eigendecomposition of $\mathbf{GG}^H$ was carried out for scenarios corresponding to different number of sources.The performance of the algorithm was evaluated for SNR values ranging from -10 to 25dB at 5dB increments. ρ was chosen as 1.2. The estimated mean eigenvalues for two sources, four sources at different SNR values are given in the Tables 6.7 and 6.8 respectively. The number of the multipaths were detected using the proposed algorithm. The frequency of detected multipaths at -10, 0 and 25dB for different number of actual multipaths in 100 trials are given in Tables 6.9, 6.10 and 6.11 respectively.

6.9 Summary

As can be seen from the Tables 6.1,6.2 and 6.3 , the smallest eigenvalue of $\mathbf{GG}^H$ tends to zero. As a result, both AIC and MDL based detection schemes fail as this value tends to dominate the decision metric. The

Table 6.7: Calculated mean Eigenvalues with 2 desired multipath signal

Eigenvalue / SNR	1	2	3	4	5	6
-10	0.018	0.039	0.115	0.176	0.754	5.412
-5	0.032	0.099	0.312	0.539	2.39	17.59
0	0.078	0.287	1.053	1.746	7.622	54.48
5	0.213	0.895	3.306	5.468	23.75	171.8
10	0.665	2.753	10.03	17.30	75.95	561.0
15	2	8.536	32.58	52.06	236.1	1754
20	6.709	27.21	102	165.2	777.9	5390
25	20.48	87.34	335.4	539.2	2400	17889

Table 6.8: Calculated mean Eigenvalues with 4 desired multipath signal

Eigenvalue / SNR	1	2	3	4	5	6
-10	0.038	0.199	0.577	1.386	4.557	6.212
-5	0.096	0.613	1.818	4.393	14.81	19.57
0	0.269	1.896	5.689	13.85	44.73	60.59
5	0.834	5.857	17.66	42.34	143.8	196.2
10	2.625	18.81	56.42	135.9	443.1	594.8
15	8.006	58.49	173.3	420.4	1417	1946
20	26.38	188.8	580.9	1393	4632	6128
25	81.39	589.4	1750	4318	14399	19626

Table 6.9: Frequency of detection at -10dB SNR

No of multipaths \ Detected multipaths	1	2	3	4	5
1	0	0	0	0	0
2	4	5	0	0	0
3	0	6	10	0	0
4	0	0	12	14	0

Table 6.10: Frequency of detection at 0dB SNR

No of multipaths \ Detected multipaths	1	2	3	4	5
1	78	21	1	0	0
2	1	94	5	0	0
3	0	4	96	0	0
4	0	0	3	97	0

Table 6.11: Frequency of detection at 25dB SNR

No of multipaths \ Detected multipaths	1	2	3	4	5
1	87	12	1	0	0
2	3	94	2	1	0
3	0	5	93	2	0
4	0	0	10	90	0

proposed threshold based scheme produce a good estimate of the source consistently above -10 dB SNR. Since the perturbation limit become more accurate asymptotically and as a result the performance of the algorithm becomes more consistent with larger number of samples. Since the perturbations in eigenvalues are of the order of $O(N^{-1})$ against the $O(N^{-1/2})$ order perturbations in eigenvectors, it was found that the detection scheme was able to produce accurate estimation of the number of multipaths with fewer number of samples than those required for the estimation of the DOA of multipaths. Besides, the threshold is decided based on the eigenvalue at that run of simulation.

On the other hand, the performance of the detector using conventional focussing scheme suffers and correct estimation occurs only in 80 to 90 % cases. It completely fails below 0dB to detect the number of sources accurately. The proposed correction factor ρ may have to be explored further or it may have to be combined with other schemes to estimate the number accurately.

The proposed detection algorithm is used in conjunction with proposed DOA estimator elucidated in Chapter 3. The conventional detection methods fails to detect the number of multipaths while using the proposed scheme due to the very small (near zero) value of the eigenvalues of matrix $\mathbf{G}$. Extensive Investigation has to be carried out in order to establish the efficiency of the proposed detection algorithm to other DOA techniques.

Chapter 7

Conclusions and Future Work

The research work presented in this report looks at ways of estimating the direction of arrival of multipaths in WiMedia UWB systems. Even though the problem addressed and the simulations were based on the WiMedia UWB, the model used is a generic OFDM system and as such, all the schemes and algorithms are applicable for any OFDM systems using pilots carrying known data. OFDM based systems carry known data for channel estimation and frequency offset estimation. Hence, these schemes can be adapted for any OFDM system and would be applicable for both fixed pilot or moving pilot locations. As long as system is operating as a synchronous system, one would be able to recover the pilot data and correlate with known waveform.

A new algorithm for the estimation of direction of arrival of multipath components is proposed in Chapter 3. The algorithm makes use of the knowledge of pilot data to remove the effect of inband interfering signals and sensor noise. The performance of the algorithm in estimating direc-

tion of arrival of multipath is demonstrated through computer simulation experiments.

The multipath signals coming from closer angles of arrival, are generally having closer delays while reaching the reference element. The difference in the delays would result in a small phase difference in the signals reaching the reference element and this effect would be equivalent to bringing the direction vectors closer. This, when combined with error/noise created by focussing operation, can effect the re-solvability of the signal. To the best of my knowledge, there is no previous work looking into this scenario of having inband interferences and closely spaced delays between multipaths for ultrawideband systems. This is the first work looking into the performance of direction of arrival estimation under such environments. Detailed research needs to be done in this area. The high fluctuations in the variance of DOA can also be attributed to this and this requires a detailed study. When the resolvability reaches its limit, the resolved DOA deviates significantly and this also need to be investigated further. The array central frequency is chosen based on the highest frequency component in the signal spectrum to eliminate ambiguity in the direction of arrival. Focussing is used for combining the signal information from different frequency components. Selection of focussing frequency was done based on maximizing the vectorial difference between the closely spaced direction vectors. These choices resulted in smaller differences in direction vectors for lower frequency components. These two selections need to be further studied and the trade

off involved in optimum selection of these two frequencies for estimation of direction of arrival of multipath components need to be analyzed. One starting point for focussing frequency would be around the midpoint of the upper half of the spectrum. This may be an optimum choice as around 75% of the frequency components would be having unambiguous detection and should be able to compensate for the ambiguity coming from the remaining components. At the same time, this would introduce a larger difference between direction vectors at lower frequency components. Besides, the effect of including all the frequency components also needs to be investigated. It may be better to exclude some of the lowest frequency components in the focussing operation to eliminate the larger errors introduced by them. This would require detailed investigation to validate these assumptions.

The superiority of the proposed scheme was established in Chapter 4. Besides, a new focussing scheme was introduced in Chapter 4. The conventional focussing scheme introduces significant bias as demonstrated by the simulations presented here as well as those shown in all past literature on this topic. The bias is related to the bandwidth and coarse estimation of the DOA. The new focussing scheme introduced here eliminates the problem by aligning the matrix $\mathbf{G}$ whose column span is same as the signal subspace. Simulations have validated the superiority of the scheme for both low interference scenario as well as narrowband interference. In typical environments, where the ultra wideband systems are used, the environment is not expected to change fast and this allow the possibility of

using more symbols for DOA estimation. The performance of the new focussing scheme improves significantly with large number of symbols. Since the proposed scheme uses the correlation of sensor data with the known waveforms, which are defined by some simple polynomial / combination of some repeating patterns, one can calculate intermediate results as new sensor data arrives and this relaxes the storage requirement significantly. The focussing scheme also doesn't require coarse DOA estimation and this also simplifies the overall receiver. Selection of focussing frequency needs further investigation. Here also, the array central frequency / focussing frequency selection has to be jointly investigated. The smaller vector difference between direction vectors seems to effect the focussing operation when chosen frequency is in the lower half of the spectrum. This is especially true at the case of closely spaced delays for closer angle of arrivals of multipaths. The best performance is obtained at the middle of upper half of the spectrum. More studies are required for optimum selection of focussing frequency / array centre frequency trade off.

One of the main drawback of array processing schemes are the requirement for larger number of receivers. The small wavelength of the UWB scheme can be used for designing repeatable linear arrays of reasonable size. The correlation based scheme uses the mean value of the correlation as the weighing factor for elements of array direction vectors in forming the array output. This weighing factor is independent of time and this is the basic principle used in the simplified receiver architecture proposed in

Chapter 5. This allows the possibility of taking sensor samples at different time instants and calculating mean value based on samples collected at different times. This simplifies the receiver hardware complexity. This result is quite generic and it can be employed in narrowband cases as well. This would result in significant reduction in the complexity of array processing receivers in narrowband schemes as well.

For accurate estimation of DOA, one need to estimate the number of multipaths. This is a challenging job especially in the case of coherent scenario. The conventional source enumeration schemes depend on metrics based on the eigenvalues of covariance matrices. In the proposed scheme, the array output vectors are correlated with known waveform. In the ideal scenario, correlation with sensor noise would be zero and as a result, the lowest eigenvalue would be zero. As a result, the conventional schemes fail to determine the number of multipaths as the metric used for determining the number of multipaths would be dominated by the lowest eigenvalue. A new threshold based scheme is proposed in Chapter 6. The threshold is calculated based on the statistical properties of the extreme fluctuations of the mean of independent random variables. This is a fairly accurate assumption in the case of the proposed new focussing scheme. As expected, the proposed detection scheme using threshold provided excellent results in simulations for the scenario using new focussing scheme. The threshold is derived from known system parameters and hence is not subjective. Due to the complex nature of the relationship between the eigenvalues and signal

parameters in focussing operation, probability of correct/ false decision could not be calculated. This is also another potential area for future research.

The detection for the case of conventional focussing need further study as the success rate is only around 80%. This may be attributed to the error in assumption of the randomness of the errors introduced in focussing and the residual error in correlation values. This is also influenced by the initial delay and the angle of arrival. The complex interactions among these parameters in forming eigenvalues need to studied in detail to fix an appropriate threshold under the conventional focussing scheme. The possibility of taking a weighted average of higher eigenvalues instead of the largest eigenvalue in determining the threshold needs to be investigated. Besides, the possibility of excluding the lowest frequency components also needs to be analyzed.

Overall, the research carried out in this project has come out with a detailed scheme for estimating the direction of arrival of multipaths for OFDM based wideband systems with a new practical implementation architecture.

Bibliography

[1] H. Akaike, "A new look at the statistical model identification", *IEEE Trans. on Automatic Control*, vol. AC-19, no.6 , pp. 716-723, Dec. 1974.

[2] T.W. Anderson, *An introduction to Multivariate Statistical Analysis*, 3rd Edition, John Wiley & Sons(Asia) Pte. Ltd, 2003.

[3] T.W. Anderson, "Asymptotic theory for principal component analysis", *The Annals of Mathematical Statistics*, vol. 34, no.1, pp. 122-148, Mar. 1963.

[4] L.N. Atallah and S. Marcos, "DOA estimation and association of coherent multipaths using reference signals", *Signal Processing*, vol. 84, issue. 6, pp. 981-996, Jun. 2004.

[5] W.P. Ballance and A.G. Jaffer, "Direction finding in the presence of fully correlated specular multipath", *in Proc. of IEEE International Conference on Acoustics, Speech, and Signal Processing*, vol. 5, pp. 2849-2852, Apr. 1988.

[6] A. Barabell, "Improving the resolution performance of eigenstructure-based direction-finding algorithms", *in Proc. of IEEE International*

Conference on Acoustics, Speech, and Signal Processing, vol. 8, pp. 336-339, Boston, US, 14-16, Apr. 1983.

[7] M.G.D. Benedetto and G. Giancola, *Understanding Ultra Wide Band Radio Fundamentals*, 1st Edition, Pearson Education Inc., 2004.

[8] V. Bharadwaj and R.M. Buehrer, "An interference suppression scheme for UWB signals using multiple receive antennas", *IEEE communications letters*, Vol.9, No.6, pp. 529-531, June 2005.

[9] G. Bienvenu and L. Kopp, "Optimality of high resolution array processing using the eigensystem approach", *IEEE Trans. on Acoustics, Speech, and Signal Processing*, vol. ASSP-31, no. 5, pp. 1235 -1248, Oct. 1983,

[10] G. Bienvenu, "Influence of the spatial coherence of the background noise on high resolution passive methods", *in Proc. of IEEE International Conference on Acoustics, Speech, and Signal Processing*, vol. 4, pp. 306-309, Washington, US, 2-4, Apr. 1979.

[11] G. Bienvenu, "Eigensystem properties of the sampled space correlation matrix", *in Proc. of IEEE International Conference on Acoustics, Speech, and Signal Processing*, vol. 8, pp. 332-335, Boston, US, 14-16, Apr. 1983.

[12] G. Bienvenu, P. Fuerxer, G. Vezzosi, L. Kopp and F. Florin "Coherent wide band high resolution processing for linear array", *in Proc. of IEEE*

International Conference on Acoustics, Speech, and Signal Processing, vol. 4, pp. 2799-2802, Glasgow, Scotland 22-25, May 1989.

[13] D.H. Brandwood, "A complex gradient operator and its application in adaptive array theory", *IEE Proceedings (F and H) on Radar and Signal Processing*, vol. 130, no. 1, pp. 11-16, Feb. 1983

[14] D.R. Brillinger, *Time Series Data Analysis and Theory*, Expanded Edition, Holden-Day Inc, 1981.

[15] T.P. Bronez and J.A. Cadzow, "An algebraic approach to superresolution array processing", *IEEE Trans. on Aerospace and Electronic Systems*, vol. AES-19, no. 1, pp. 123-133, Jan. 1983.

[16] K.M. Buckley and L.J. Griffiths "Broad-band signal-subspace spatial-spectrum (BASS-ALE) estimation", *IEEE Trans. on Acoustics, Speech, and Signal Processing*, vol. 36, no. 7, pp. 953-964, Jul. 1988.

[17] J.A. Cadzow, "A high resolution direction- of-arrival algorithm for narrow-band coherent and incoherent sources", *IEEE Trans. on Acoustics, Speech, and Signal Processing*, vol. 36, no. 7, pp. 965-979, Jul. 1988.

[18] J.A. Cadzow, "Least squares, modelling and signal processing", *Digital Signal Processing*, vol. 4, no. 1, pp. 2-20, Jan. 1994.

[19] M. Cedervall, and R.L. Moses, "Efficient maximum likelihood DOA estimation for signals with known waveforms in the presence of multi-

path", *IEEE Trans. on Signal Processing*, vol. 45, no. 3, pp. 808- 812, Mar. 1997.

[20] S. Chandran(ed), *Advances in Direction of Arrival Estimation*, 1st Edition, Artech House Inc., 2006.

[21] Y.H. Chen and R.H. Chen, "Directions-of-Arrival estimations of multiple coherent broadband signals", *IEEE Trans. on Aerospace and Electronic Systems*, vol. 29, no. 3, pp. 1035-1043, Jul. 1993.

[22] P. Chen, T.J. Wu and J. Yang, "A comparative study of model selection criteria for the number of signals" , *IET Radar, Sonar and Navigation*, vol. 2, no. 3, pp. 180-188, Jun 2008.

[23] W. Chen and K.M. Wong and J.P. Reilly, "Detection of the number of signals: a predicted eigen-threshold approach", *IEEE Trans. on Signal Processing*, vol. 39, no. 5, pp. 1088-1098, May 1993.

[24] K.B. Datta, *Matrix and Linear Algebra*, 1st Edition, Prentice Hall of India Private Ltd., 2003.

[25] J.P. Delmas and Y. Meurisse, "Robustness of narrowband DOA algorithms with respect to signal bandwidth", *Signal Processing*, vol. 83, no. 3, pp. 493-510, Mar. 2003.

[26] A. Di, "Multiple source location - a matrix decomposition approach", *IEEE Trans. on Acoustics, Speech, and Signal Processing*, vol. ASSP-33, no. 4, pp. 1086-1091, Oct. 1985.

[27] M.A. Doron and A.J. Weiss, "On focusing matrices for wide-band array processing", *IEEE Trans. on Signal Processing*, vol. 40, no. 6, pp. 1295-1302, Jun. 1992.

[28] M.A. Doron, E. Doron and A.J. Weiss, "Coherent wide-band procesing for arbitrary array geometry", *IEEE Trans. on Signal Processing*, vol. 41, no. 1, pp. 414- 417, Jan. 1993.

[29] V.T. Ermolaev and A.B. Gershman, "Eigenvalue analysis of spatial covariance matrices for correlated signals", *IEE Electronic Letters*, vol. 28, no. 12, pp. 1114-1115, 4th Jun. 1992.

[30] D.R. Farrier, D.R. Jeffries and R. Mardani, "Theoretical performance prediction of the MUSIC algorithm", *IEE Proceedings (F) on Radar and Signal Processing*, vol. 135, no. 3, pp. 216-222, Jun. 1988

[31] D.R. Farrier, D.R. Jeffries and R. Mardani, "Perturbation analysis of the MUSIC algorithm", *in Proc. of IEEE International Conference on Acoustics, Speech, and Signal Processing*, vol. 5, pp 2873-2876, New York, US, 11-14, Apr. 1988.

[32] B. Friedlander and A.J. Weiss, "Direction finding for wideband signals using interpolated array", *IEEE Trans. on Signal Processing*, vol. 41, no. 4, pp. 1618-1634, Apr. 1993.

[33] M. Frikel and S. Bourennane, "Statistical Analysis to wideband array processing", *in Proc. of IEEE TENCON. on Digital Signal Processing Applications*, vol. 1, pp. 435-439, Perth, Australia, 26-29, Nov. 1996.

[34] J. Foerster, "Channel modeling sub-committee report final", IEEE P802.15 Working Group for Wireless Personal Area Networks, Feb. 2003.

[35] G.H. Golub and C.F. Van Loan, *Matrix Computations*, 3rd Edition, The John Hopkins University Press, 1996.

[36] H. Hashemi, T.S. Chu and J. Roderick, "Integrated true-time-delay-based ultra-wideband array processing", *IEEE Communications Magazine*, vol. 46, no. 9, pp. 162-172, Sept. 2008.

[37] W. Hong and A.H. Tewfik, "Focusing matrices for wideband array processing with no a priori angle estimates", *in Proc. of IEEE International Conference on Acoustics, Speech, and Signal Processing*, vol. 2, pp 493-496, Sanfrancisco, US, 23-26, March 1992.

[38] H. Hung and M. Kaveh, "Focussing matrices for coherent signal-subspace processing", *IEEE Trans. on Acoustics, Speech, and Signal Processing*, vol. 36, no. 8, pp. 1272-1281, Aug. 1988.

[39] H.S. Hung and C.Y. Mao, "Robust coherent signal subspace processing for directions of arrival estimation of wideband sources", *IEE Proceedings on Radar, Sonar and Navigation*, vol. 141, no. 5, pp. 256-262, Oct. 1994.

[40] D.J. Jeffries and D.R. Farrier, "Asymptotic results for eigenvector methods", *IEE Proceedings (F) on Radar and Signal Processing*, vol. 132, no. 7, pp. 589-594, Dec. 1985.

[41] S.S. Jeng and C.W. Tsung, "Multipath direction finding with frequency allocation subspace smoothing for an OFDM wireless communication system", *in Proceedings of IEEE 16th International Symposium on Personal, Indoor and Mobile Radio Communications*, vol. 4, pp. 2471-2475, Berlin, Germany, 11-14,Sep. 2005.

[42] S.S. Jeng, H.P. Lin, G. Okamoto, G. Xu and W.J. Vogel, "Multipath direction finding with subspace smoothing", *in Proceedings of IEEE International Conference on Acoustics, Speech, and Signal Processing*, vol. 5, pp. 3485-3488, Munich, Germany, 21-24, Apr. 1997.

[43] D.H. Johnson and S.R. Degraaph, "Improving the resolution of bearing in passive sonar arrays by eigenvalue analysis", *IEEE Trans. on Acoustics, Speech, and Signal Processing*, vol. ASSP-30, no. 4, pp. 638-647, Aug. 1982.

[44] T. Kaiser and B.T. Sieskul, "An introduction to multiple antennas for UWB communication and localization ", *in Proc. of 40th Annual Conference on Information Sciences and Systems*, pp 638-643, Princeton, US, 22-24, March 2006.

[45] M. Kaveh and A.J. Barabell, "The statistical performance of the MUSIC and the Minimum- Norm algorithms in resolving plane waves in noise", *IEEE Trans. on Acoustics, Speech, and Signal Processing*, vol. ASSP-34, no. 2, pp. 331-341, Apr. 1986.

[46] M. Kaveh and A.J. Barabell, "Corrections to the statistical performance of the MUSIC and the Minimum- Norm algorithms in resolving plane waves in noise", *IEEE Trans. on Acoustics, Speech, and Signal Processing*, vol. ASSP-34, no. 3, pp. 633, Jun. 1986.

[47] K. Konstantinides and K. Yao, "Statistical analysis of effective singular values in matrix rank determination", *IEEE Trans. on Acoustics, Speech, and Signal Processing*, vol. 36, no. 5, pp. 757-763, May. 1988.

[48] H. Krim and M Viberg, "Two decades of array signal processing research", *IEEE Signal Processing Magazine*, vol. 13, issue. 4, pp. 67-94, Jul. 1996.

[49] J. Krolik and D. Swingler, "Multiple broad-band source location using steered covariance matrices", *IEEE Trans. on Accoustics, Speech, and Signal Processing*, vol. 37, no. 10, pp. 1481-1494, Oct. 1989.

[50] R. Kumaresan and D.W. Tufts, "Estimating the angles of arrival of multiple plane waves", *IEEE Trans. on Aerospace and Electronic Systems*, vol. AES-19, no. 1, pp. 134-139, Jan. 1983.

[51] B.H. Kwon and S.U. Pillai, "A self inversive array processing scheme for angle of arrival estimation", *Signal Processing*, vol. 17, issue. 3, pp. 259-277, Jul. 1989.

[52] H.B. Lee and M.S. Wengrovitz, "Resolution threshold of beamspace MUSIC for two closely spaced emitters", *IEEE Trans. on Accoustics, Speech, and Signal Processing*, vol. 38, no. 9, pp. 1545-1559, Sep. 1990.

[53] H.B. Lee, "Eigenvalues and eigenvectors of covariance matrices for signals closely spaced in frequency", *IEEE Trans. on Signal Processing*, vol. 40, no. 10, pp. 2518- 2535, Oct. 1992.

[54] T.S. Lee, "Efficient broadband source localization using beamforming invariance technique", *IEEE Trans. on Signal Processing*, vol. 42, no.6, pp. 1376-1387, Jun. 1994.

[55] J. Li, and R.T. Compton, "Maximum likelihood angle estimation for signals with known waveforms", *IEEE Trans. on Signal Processing*, vol. 41, no. 9, pp. 2850-2862, Sep. 1993.

[56] J. Li, B. Halder, P. Stoica and M. Viberg, "Computationally efficient angle estimation for signals with known waveforms", *IEEE Trans. on Signal Processing*, vol. 43, no. 9, pp. 2154-2163, Sep. 1995.

[57] J.C. Liberti and T.S. Rappaport, *Smart Antennas for Wireless Communications IS-95 and Third Generation CDMA Applications*, 1st Edition, Prentice Hall PTR, 1999.

[58] D. Madurasinghe, "Direction finding in a multipath environment", *IEE Electronic Letters*, vol. 27, no. 1, pp. 61-62, 3rd Jan. 1991.

[59] H. Messer, "The use of spectral information in optimal detection of a source in the presence of directional interference", *IEEE Journal of Oceanic Engineering*, vol.19, no.3, pp. 422-430, Jul. 1994.

[60] H. Messer, "The potential performance gain in using spectral information in passive detection/ localisation of wideband sources", *IEEE Trans. on Signal Processing*, vol. 43, no. 12, pp. 2964-2974, Dec. 1995.

[61] A. Moghaddamjoo and T.C. Chang, "Signal enhancement of spatial smoothing algorithm", *IEEE Trans. on Signal Processing*, vol. 39, no. 8, pp. 1907-1911, Aug. 1991.

[62] A. Moghaddamjoo, "Spatial filtering approach to the direction of arrival estimationin a multipath environment", *in Proc. of IEEE International Conference on Acoustics, Speech, and Signal Processing*, vol. 4, pp. 2752-2755, Glasgow, UK, May 1989.

[63] T.K. Moon and W.C. Stirling, *Mathematical Methods and Algorithms for Signal Processing*, 1st Edition, Pearson Education, 2000.

[64] M. Nezafat, M. Kaveh and W. Xu, "Estimation of the number of sources based on the eigenvectors of the covariance matrix", *in Proceedings of IEEE Sensor Array and Multichannel Signal Processing Workshop, 2004*, pp. 465-469, Sitges, Spain, 18-21, Jul. 2004.

[65] M. Nezafat and M. Kaveh "Estimation of the number of sources with DOA priors", *in Proceedings of 13th IEEE /SP Workshop on Statistical Signal Processing, 2005*, pp. 603-608, Bordeaux, France, 17-20, Jul. 2005.

[66] D. Pal, "A temporal averaging technique for direction of arrival estimationin a multipath environment", *in Proceedings of IEEE International*

Symposium on Circuits and Systems, vol. 2, pp. 617-620, London, UK, 30 May -2 Jun. 1994.

[67] S.U. Pillai and B.H. Kwon, "Performance analysis of MUSIC-type high resolution estimators for direction finding in correlated and coherent scenes", *IEEE Trans. on Acoustics, Speech, and Signal Processing*, vol. 37, no. 8, pp. 1176-1189, Aug. 1989.

[68] S.U. Pillai and B.H. Kwon, "Forward/backward spatial smoothing techniques for coherent signal identification", *IEEE Trans. on Acoustics, Speech, and Signal Processing*, vol. 37, no. 1, pp. 8-15, Jan. 1989.

[69] S.U. Pillai, "Signal resolution using generalized eigenvalues for coherent sources", *in Proceedings of Fourth IEEE Region 10 International Conference*, pp. 284-288, Bombay, India, Nov. 1989.

[70] A.D. Poularikas, *The Handbook of Formulas and Tables for Signal Processing*, 1st Edition, CRC Press, 1998.

[71] S.S. Reddi, "Multiple source location- a digital approach", *IEEE Trans. on Aerospace and Electronic Systems*, vol. AES-15, no. 1, pp. 95-105, Jan. 1979.

[72] J. Rissanen, "Modelling by shortest data description", *Automatica*, vol. 14, pp. 465-471, 1978.

[73] R. Roy and T. Kailath, "ESPRIT- estimation of signal parameters via rotational invariance techniques", *IEEE Trans. on Acoustics, Speech, and Signal Processing*, vol. 37, no. 7, pp. 984-994, Jul. 1989.

[74] R.O. Schmidt, "Multiple emitter location and signal parameter estimation", *IEEE Trans. on Antennas and Propagation*, vol. AP-34, no. 3, pp. 276-280, Mar. 1986.

[75] F. Sellone, "Robust autofocusing wideband DOA estimation", *Signal Processing*, vol. 86, no. 1, pp. 17-37, Jan. 2006.

[76] R.J. Serfling, *Approximation Theorems of Mathematical Statistics*, 1st Edition, John Wiley & Sons Inc, 1980.

[77] A. Seyedi, V. Gaddam and D. Birru, "Performance of multi-band OFDM UWB system with multiple receive antennas ", *in Proc. of IEEE Wireless Communications and Networking Conference, WCNC 2006*, Vol.2, pp 792-797, Las Vegas, US, 3-6, April 2006.

[78] A.A. Shah and D.W. Tufts, "Determination of the dimension of a signal subspace from short data records", *IEEE Trans. on Signal Processing*, vol. 42, no. 9, pp. 2531-2535, Sept. 1994.

[79] T.J. Shan, M. Wax and T. Kailath, "On spatial smoothing for direction of arrival estimation of coherent signals", *IEEE Trans. on Acoustics, Speech, and Signal Processing*, vol. ASSP-33, no. 4, pp. 806-811, Aug. 1985.

[80] K.C. Sharman and T.S. Durrani, "Resolving power of signal subspace methods for finite data lengths", *in Proc. of IEEE International Conference on Acoustics, Speech, and Signal Processing*, vol. 10, pp. 1501-1504, Tampa, US, 26-29 Mar. 1985.

[81] K.C. Sharman and T.S. Durrani, "A comparative study of modern eigenstructure methods for bearing estimation - a new high performance approach", *in Proc. of IEEE Conference on Decision and Control*, vol. 25, pp. 1737-1742, Athens, Greece, 10- 12, Dec. 1986.

[82] G.E. Shilov, *Linear Algebra*, 1st Edition, Dover Publications, 1977.

[83] J. Sorelius, R.L. Moses, T. Soderstrom and A.L. Swindlehurst, "Effect of nonzero bandwidth on direction of arrival estimators in array signal processing", *IEE Proceedings on Radar, Sonar and Navigation*, vol. 145, no. 6, pp. 317-323, Dec. 1998.

[84] H. Stark and J.W. Woods, *Probability and Random Processes with Applications to Signal Processing*, 3rd Edition, Pearson Education Asia, 2002.

[85] P. Stoica and A. Nehorai, "MUSIC, Maximum Likelihood, and Cramer-Rao bound", *IEEE Trans. on Acoustics, Speech, and Signal Processing*, vol. 37, no. 5, pp. 720-741, May 1989.

[86] D.N. Swingler and J. Krolik, "Source location bias in the coherently focused high resolution broadband beamformer", *IEEE Trans. on Acoustics, Speech, and Signal processing,* vol. 37, no. 1, pp. 143-145, Jan. 1989.

[87] P. Totarong and A.E. Jaroudi, "Robust high-resolution direction of arrival via signal eigenvector domain", *IEEE Journal on Oceanic Engineering*, vol. 18, no. 4, pp. 491-499, Oct. 1993.

[88] "High Rate Ultra Wideband PHY and MAC Standard", ECMA- 368, ECMA International, December 2005.

[89] S. Valaee and P. Kabal, "Selection of focusing frequency in wideband array processing - MUSIC and ESPRIT", *in Proc. of 16th Biennial Symposium on Communications*, pp. 410-414 , Kingston, Canada, 27 - 29, May 1992.

[90] S. Valaee and P. Kabal, "The optimal focusing subspace for coherent signal subspace processing", *IEEE Trans. on Signal processing*, vol. 44, no. 3, pp. 752-756, Mar. 1996.

[91] S. Valaee and P. Kabal, "Wideband array procesing using a two sided correlation transformation", *IEEE Trans. on Signal Processing*, vol. 43, no. 1, pp. 160-172, Jan. 1995.

[92] H. Wang and M. Kaveh, "Coherent signal-subspace processing for the detection and estimation of angles of arrival of multiple wide-band sources", *IEEE Trans. on Acoustics, Speech, and Signal Processing,* vol. ASSP-33, no. 4, pp. 823-831, Aug. 1985.

[93] N. Wang, P. Agathoklis and A. Antoniou, "A new DOA estimation technique based on subarray beamforming", *IEEE Trans. on Signal Processing*, vol. 54, no. 9, pp. 3279-3290, Sep. 2006.

[94] H. Wang and M. Kaveh, "On the performance of signal-subspace processing- part I: narrow-band systems," *IEEE Trans. on Acoustics,*

Speech, and Signal Processing, vol. ASSP-34, no. 5, pp. 1201-1209 , Oct. 1986.

[95] H. Wang and M. Kaveh, "On the performance of signal-subspace processing- part II: coherent wide-band systems", *IEEE Trans. on Acoustics, Speech, and Signal Processing*, vol. ASSP-35, no. 11, pp. 1583-1591, Nov. 1987.

[96] D.B. Ward, Z. Ding and R.A. Kennedy, "Broadband DOA estimation using frequency invariant beamforming", *IEEE Trans. on Signal Processing*, vol. 46, no. 5, pp. 1463-1469, May 1998.

[97] M. Wax, T.J. Shan, and T. Kailath, "Spatio-temporal spectral analysis By eigen structure methods", *IEEE Trans. on Acoustics, Speech, and Signal Processing,* vol. ASSP-32, no. 4, pp. 817-827, Aug. 1984.

[98] M. Wax and T. Kailath, "Detection of signals by information theoretic criteria", *IEEE Trans. on Accoustics, Speech, and Signal Processing*, vol. ASSP-33, no. 2, pp. 387-392, Apr. 1985.

[99] M. Wax and I. Ziskind, "Detection of the coherent signals by the MDL Principle", *IEEE Trans. on Accoustics, Speech, and Signal Processing*, vol. 37, no. 8, pp. 1190-1196, Aug. 1989.

[100] J.H. Wilkinson, *The Algebraic Eigenvalue Problem*, 1st Edition, Oxford Science Publications, 1988.

[101] Q. Wu and D.R. Fuhrmann, "A parametric method for determining the number of signals in narrowband direction finding", *IEEE Trans. on Signal Processing*, vol. 39, no. 8, pp. 1848-1857, Aug. 1991.

[102] J. Yang, A. Seyedi, D. Birru and D. Wong "Design and Performance of multi-band OFDM UWB system with multiple receive antennas ", *in Proc. of* 18^{th} *IEEE International Symposium on Personal, Indoor and Mobile Radio Communications, PIMRC 2007*, pp 1-5, Athens, Greece, 3-7 Sept. 2007.

[103] S. Yang and H. Li, "Estimating the number of harmonics using enahnced matrix", *IEEE Signal Processing Letters*, vol. 14, no.2, pp. 137-140, Feb. 2007.

[104] Y.S. Yoon, L.M. Kaplan and J.H. McCellan, "New signal subspace direction-of-arrival estimator for wideband sources", *in Proc. of IEEE International Conference on Acoustics, Speech, and Signal Processing*, vol. 5, pp. 225-228, Hong Kong, 6-10, Apr. 2003.

[105] Y.S. Yoon, L.M. Kaplan and J.H. McCellan, "TOPS: new DOA estimator for wideband signals", *IEEE Trans. on Signal Processing*, vol. 54, no. 6, pp. 1977-1989, Jun. 2006.

[106] M. Zatman, "How narrow is narrowband" , *IEE Proceedings on Radar, Sonar and Navigation*, vol. 145, no. 2, pp. 85-91, Apr. 1998.

[107] M. Zoltowski, "A vector space approach to direction finding in a coherent multipath environment", *IEEE Trans. on Antennas and Propagation*, vol. AP-34, no. 9, pp. 1069-1079, Sep. 1986.

Author's Publications

[1] A.K. Marath, A.R. Leyman and H.K. Garg, "New Focussing Scheme for DOA Estimation of Multipath Clusters in WiMedia UWB Systems," IEEE Communications Letters, Vol. 14, No.2, pp 102-104, Feb 2010.

[2] A.K. Marath, A.R. Leyman and H.K. Garg, "DOA estimation of Multipath Clusters in Wimedia UWB systems," in Proc. *The fifth IEEE Sensor Array and Multichannel Signal processing Workshop, SAM 2008, Darmstadt, Germany, July 2008*

[3] A.K. Marath, A.R. Leyman and H.K. Garg, "Efficient Scheme for DOA Estimation of Multipath Clusters in WiMedia UWB systems," in Proc. *3rd International Conference on Cognitive Radio Oriented Wireless Networks and Communications, CrownCom 2008, Singapore, May 2008*

[4] A.K. Marath, A.R. Leyman and H.K. Garg, "Estimation of the number of Multipath Clusters in WiMedia UWB Systems," under preparation